UNIVERSIDADE FEDERAL DO RIO GRANDE DO SUL
FACULDADE DE FARMÁCIA
PROGRAMA DE PÓS-GRADUAÇÃO EM CIÊNCIAS FARMACÊUTICAS

Relevância dos alcaloides oxindólicos em *Uncaria tomentosa* (Willd.) DC. (Unha-de-gato): adulteração, quimiotipos e isomerização

SAMUEL KAISER

PORTO ALEGRE, 2016

UNIVERSIDADE FEDERAL DO RIO GRANDE DO SUL
FACULDADE DE FARMÁCIA
PROGRAMA DE PÓS-GRADUAÇÃO EM CIÊNCIAS FARMACÊUTICAS

Relevância dos alcaloides oxindólicos em *Uncaria tomentosa* (Willd.) DC. (Unha-de-gato): adulteração, quimiotipos e isomerização

Tese apresentada por **SAMUEL KAISER** para obtenção do TÍTULO DE DOUTOR em Ciências Farmacêuticas**.**

Orientador: Prof. Dr. George González Ortega

PORTO ALEGRE, 2016

Tese apresentada ao Programa de Pós-Graduação em Ciências Farmacêuticas, em nível de Doutorado Acadêmico da Faculdade de Farmácia da Universidade Federal do Rio Grande do Sul e aprovada em 18.07.2016, pela Banca Examinadora constituída por:

Prof. Dr. Eloir Paulo Schenkel
Universidade Federal de Santa Catarina

Prof. Dr. Marco Flôres Ferrão
Universidade Federal do Rio Grande do Sul

Profa. Dr. Valquíria Linck Bassani
Universidade Federal do Rio Grande do Sul

CIP - Catalogação na Publicação

Kaiser, Samuel
Relevância dos alcaloides oxindólicos em Uncaria tomentosa (Willd.) DC. (Unha-de-gato): adulteração, quimiotipos e isomerização / Samuel Kaiser. -- 2016.
180 f.

Orientador: George González Ortega.

Tese (Doutorado) -- Universidade Federal do Rio Grande do Sul, Faculdade de Farmácia, Programa de Pós-Graduação em Ciências Farmacêuticas, Porto Alegre, BR-RS, 2016.

1. Uncaria tomentosa (Cat's claw). 2. Alcaloides Oxindólicos. 3. Adulteração. 4. Quimiotipos. 5. Isomerização. I. Ortega, George González , orient. II. Título.

Elaborada pelo Sistema de Geração Automática de Ficha Catalográfica da UFRGS com os dados fornecidos pelo(a) autor(a).

Este trabalho foi desenvolvido no Laboratório de Desenvolvimento Galênico (LDG). Análises complementares foram realizadas na Central Analítica do Programa de Pós-Graduação em Ciências Farmacêuticas, Laboratório de Imunologia Clínica e Toxicologia, Universidade Federal do Pampa (UNIPAMPA) e Laboratório de Enzimologia Aplicada do Departamento de Bioquímica desta universidade.

Dedico este trabalho a minha esposa,
Cinthia Patrícia Batista Garcia Kaiser;
Aos meus pais, Leoni Kaiser e Iara Maria Hatwig Kaiser,
e ao meu avô Afonso Guilherme Hatwig
Fontes eternas de inspiração e força.

AGRADECIMENTOS

Agradeço ao Professor Dr. George G. Ortega por esses 11 anos de convivência e ensinamentos que propiciaram meu desenvolvimento intelectual e pessoal e por compreender que a verdadeira orientação não se resume a cobrar resultados, e sim desenvolver o aluno para os novos desafios que surgirão. Ao meu eterno orientador meu muito obrigado de coração.

A Professora Dr. Ana Maria Oliveira Battastini e a Doutoranda Fabricia Dietrich do Departamento de Bioquímica desta universidade pela colaboração na avaliação da atividade citotóxica em linhagens de células tumorais.

Ao Professor Dr. Luis Flávio Souza de Oliveira e sua equipe do Laboratório de Imunologia Clínica e Toxicologia da Universidade Federal do Pampa (UNIPAMPA) pela colaboração na avaliação da atividade genotóxica e citotóxica em leucócitos.

A FAMÍLIA LDG, em especial aos meus colegas Vanessa Pittol, Ânderson Ramos Carvalho, Sara Elis Bianchi, Bruna Medeiros e Giovanni Zorzi, pela ajuda nesta caminhada e pela grata convivência diária que certamente vai deixar saudades e boas recordações.

Aos meus colegas do Laboratório de Química Aplicada (LQA)/Souza Cruz pelo incentivo e compreensão no decorrer desta jornada.

Aos meus irmãos Moacir e Suzana e a minha madrinha Lucia, a quem amo de coração, pela a força e por sempre acreditarem em minha capacidade.

A minha querida esposa e grande amor Cinthia pela paciência, compreesão e enorme incentivo para a superação desta etapa importante em minha formação.

Aos meus pais, Leoni e Iara, por tudo que me ensinaram e pelo amor incondicional que sempre tiveram por mim.

RESUMO

Uncaria tomentosa (Willd.) DC. (Rubiaceae), popularmente conhecida como *cat's claw* ou "unha-de-gato", é uma liana encontrada principalmente na região Amazônica assim como *Uncaria guianensis* (Aubl.) Gmel. (Rubiaceae), que é utilizada como substituinte ou adulterante em relação a *U. tomentosa* devido à sua maior abundância e menor valor comercial. A diferenciação de ambas pode ser realizada com base em aspectos morfoanatômicos, mas limita-se à composição química em derivados, como extratos fluidos e secos. As cascas do caule de *U. tomentosa* são compostas majoritariamente por derivados triterpênicos, polifenóis e alcaloides oxindólicos, aos quais são atribuídas as principais atividades biológicas da espécie. Contudo, o perfil de alcaloides oxindólicos é variável devido à ocorrência de quimiotipos e a elevada susceptibilidade dos mesmos à isomerização. Assim, a presente tese teve como objetivo avaliar a relevância dos alcaloides oxindólicos em *U. tomentosa* no que tange ao reconhecimento de adulteração na espécie, ocorrência de quimiotipos e isomerização desses compostos. Para isso, foram construídos modelos de classificação e regressão multivariada a partir das análises de CLAE-PDA, IV e UV destinados a diferenciação entre *U. tomentosa* e *U. guianensis* e ao reconhecimento de adulteração e determinação do percentual de adulterante em amostras de *U. tomentosa*. Os resultados obtidos demonstraram que os critérios farmacopéicos atualmente utilizados no controle de qualidade da matéria-prima vegetal e derivados de *U. tomentosa* baseados nos alcaloides oxindólicos são inefetivos em relação ao reconhecimento de adulteração. A avaliação da atividade citotóxica dos diferentes quimiotipos baseados no perfil de alcaloides oxindólicos em *U. tomentosa* frente a leucócitos humanos e as células tumorias de bexiga (T24) e glioblastoma (U-251-MG) humanos, demonstrou que a seletividade frente às células tumorais é depentente do quimiotipo. Adicionalmente, a complexação dos alcaloides oxindólicos com sulfobutil-éter-β-ciclodextrina (SBE-βCD) minimizou a velocidade de isomerização sob condições de incubação (pH = 7,4; 37 ºC), sem contudo inibir o processo de isomerização.

Palavras chave: *Uncaria tomentosa*, *Uncaria guianensis*, alcaloides oxindólicos, adulteração, quimiotipos, isomerização.

ABSTRACT

Relevance of oxindole alkaloids at *Uncaria tomentosa* (Willd.) DC. (cat's claw): adulteration recognition, chemotypes and isomerization

Uncaria tomentosa (Willd.) DC. (Rubiaceae), popularly known as cat's claw, is a liana found mainly in the Amazon rainforest as well as *Uncaria guianensis* (Aubl.) Gmel. (Rubiaceae) used as substituent or adulterant due to their higher wild population and lower market value. The differentiation among the raw material of both species can be performed from morphological and microscopic characteristics, but is limited in derivatives such as fluid and freeze-dried extracts. The stem bark from *U. tomentosa* is composed mainly by quinovic acid glycosides, polyphenols and oxindole alkaloids, to which have been assigned the major biological activities of the specie. However, the oxindole alkaloids profile in the *U. tomentosa* is variable due to chemotype occurrence and their susceptibility to isomerization. Thus, this study aimed to evaluate the relevance of oxindole alkaloids at *U. tomentosa* in relation to adulteration recognition, chemotype occurrence and oxindole alkaloids isomerization. Classification and multivariate regression models were built from HPLC-PDA, FT-IR and UV data to differentation between *U. tomentosa* e *U. guianensis*, as well as for adulteration recognition and determination of the adulterant level in the *U. tomentosa*. The current U.S. pharmacopeia monographs specifications for quality control of stem bark raw material from *U. tomentosa*, as well as for their derivatives, such as powdered dried extract, based on the oxindole alkaloids were ineffective for adulteration recognition. The cytotoxic activity evaluation of the different chemotypes, based on the oxindole alkaloid profile, against the human leukocytes and against human bladder cancer cell line (T24) and human glioblastoma cell line (U-251-MG) demonstrated that selectivity against the tumoral cells is dependent of the chemotype. In addition, the complexation of the oxindole alkaloids with Sulfobutyl ether β-cyclodextrin (SBE-βCD) minimize the isomerization rate under incubation conditions (pH = 7.4; 37 ºC) but without, however, inhibit the isomerization process.

Keywords: *Uncaria tomentosa, Uncaria guianensis,* oxindole alkaloids, adulteration recognition, chemotypes, isomerization.

LISTA DE TABELAS

LISTA DE FIGURAS

LISTA DE ABREVIATURAS

CAA – Caffeic acid

CCD – Cromatografia em Camada Delgada

CLAE-EM – Cromatografia Líquida de Alta Eficiência - Espectrômetro de Massas

CLAE-PDA – Cromatografia líquida de alta eficiência - Detector de arranjo de fotodiodos

COA – Chlorogenic acid

DSC – Differential scanning calorimetry

EM – Espectrômetro de massas

FA – Formic acid

HCA – Hierarchical Cluster Analysis

HP-βCD – Hidroxipropil-β-ciclodextrina

IC_{50} – Inhibitory Concentration 50%

ISMITR – Isomitraphylline

ISPTER – Isopteropodine

ISRHY – Isorhynchophylline

IV – Infravermelho

k-NN – *k*-nearest neighbors

Ks – Apparent stability constant

L – Leaf samples

MIT – Mitraphylline

MW_{POA} – Average molecular weight of pentacyclic oxindole alkaloids

MW_{TOA} – Average molecular weight of tetracyclic oxindole alkaloids

OAPF – Oxindole alkaloid purified fraction

PBS – Phosphate buffered saline

PCA – Principal component analysis

PCR – Principal component regression

PLS – Partial least squares

POA – Pentacyclic oxindole alkaloids

PPH – Polyphenols

PTER – Pteropodine

QAG – Quinovic acid glycosides

r – Regression coefficient

RHY – Rhynchophylline

RMSEC – Root mean square error of calibration

RMSECV – Root mean square error of cross validation

RMSEP – Root mean square error of prediction

RMSEV – Root mean square error of validation

RUT – Rutin

S – Stem bark samples

SBE-βCD – Sulfobutil-éter-β-ciclodextrina

SEM – Scanning electron microscopy

SI – Selectivity index

SIMCA – Soft independent modeling of class analogy

So – Intrinsic solubility

SPEC – Speciophylline

T24 – Linhagens de células tumorais de bexiga humano

TFA – Trifluoroacetic acid

TOA – Tetracyclic oxindole alkaloids

U-251-MG – Linhagens de células tumorais de glioblastoma humano

UG – *Uncaria guianensis*

UNCF – Uncarine F

UT – *Uncaria tomentosa*

UV – Ultravioleta

WMW – Weighted molecular weight

α-CD – α-ciclodextrina

βCD – β-ciclodextrina

γ-CD – γ-ciclodextrina

SUMÁRIO

APRESENTAÇÃO

A presente tese foi redigida na forma de capítulos, em conformidade com as normas vigentes no Regimento Interno do Programa de Pós-Graduação em Ciências Farmacêuticas, da Universidade Federal do Rio Grande do Sul, e encontra-se organizada da seguinte forma:

- Introdução e Relevância do Tema;
- Objetivos: Geral e Específicos;
- Referencial Teórico;
- Capítulos 1 a 3: artigos publicados ou a serem submetidos à publicação;
- Discussão Geral;
- Conclusões;
- Referências;
- Agradecimento a Bolsa de Estudos;

INTRODUÇÃO E RELEVÂNCIA DO TEMA

Uncaria tomentosa (Willd.) DC. (Rubiaceae), caracterizada botanicamente como uma liana, é popularmente conhecida como unha-de-gato ou *cat's claw* devido à presença dos tomentos utilizados para galgar espécies de maior porte propiciando o seu adequado desenvolvimento. Esta espécie é nativa da região Amazônica e outras regiões tropicais da América do Sul e Central, onde desempenha um importante papel socioeconômico, principalmente no Peru (VALENTE, 2006). Relatos etnofarmacológicos descrevem a utilização de decoctos das cascas para distintas finalidades, como tratamento de úlceras gástricas, artrite reumatóide, infecções bacterianas e virais, alergias, asma e até mesmo câncer (REINHARD, 1999; HEITZMAN *et al.*, 2005; VALENTE, 2006). Dentre as atividades relatadas atribuídas à espécie, algumas foram posteriormente comprovadas por estudos científicos, sobretudo as atividades antiviral, antiinflamatória e antitumoral (KAISER *et al.*, 2013c; CAON *et al.*, 2014; DIETRICH *et al.*, 2014; DIETRICH *et al.*, 2015).

Uncaria guianensis (Aubl.) Gmel. (Rubiaceae) assim como a *U. tomentosa* também é popularmente conhecida como unha-de-gato ou *cat's claw*. Dentre as 34 espécies pertencentes ao gênero *Uncaria* catalogadas até o momento, apenas *U. tomentosa* e *U. guianensis* são encontradas na região Amazônica, sendo a última mais abundante (GATTUSO *et al.*, 2004; LAUS, 2004; HEITZMAN *et al.*, 2005; ZHANG *et al.*, 2015). Contudo, o potencial terapêutico e toxicológico em *U. guianensis* foi pouco explorado se comparado a *U. tomentosa* até o momento. Como ambas as espécies são obtidas principalmente via extrativismo devido ao cultivo incipiente, equívocos durante a coleta podem ser comuns, embora as espécies possam ser botanicamente diferenciadas mediante avaliação de aspectos morfoanatômicos, principalmente em seu estado *in natura* (QUINTERA; DE UGAZ, 2003; GATTUSO *et al.*, 2004; VALENTE, 2006; POLLITO; TOMAZELLO, 2006). O menor valor comercial da *U. guianensis* em relação a *U. tomentosa* também pode contribuir para ocorrência de adulteração em *U. tomentosa* empregando *U. guianensis*. Contudo, o reconhecimento desta prática se limita exclusivamente a aspectos químicos em derivados de *U. tomentosa* como extratos secos e até mesmo comprimidos. Entretanto, métodos analíticos capazes de reconhecer esta prática não estão disponíveis em

monografias oficiais destinados ao controle de qualidade da matéria-prima vegetal e derivados de *U. tomentosa*.

Três frações bioativas majoritárias são encontradas em *U. tomentosa*, a saber, polifenóis, derivados triterpênicos e alcaloides (LAUS, 2004; HEITZMAN *et al.*, 2005; ZHANG *et al.*, 2015). Aos alcaloides oxindólicos pentacíclicos são atribuídas as atividades biológicas mais relevantes da espécie, principalmente a atividade antitumoral (HEITZMAN *et al.*, 2005). Evidências recentes indicam a ocorrência de três quiomiotipos específicos em *U. tomentosa* baseados no perfil de alcaloides oxindólicos encontrado na espécie (PEÑALOZA *et al.*, 2015). Contudo, a influência dos diferentes quimiotipos em relação às atividades reconhecidamente atribuídas aos alcaloides oxindólicos, bem como em relação a aspectos toxicológicos ainda é desconhecida. Além disso, em decorrência da elevada susceptibilidade dos alcaloides oxindólicos a isomerização tanto em processos tecnológicos de obtenção de extratos fluidos e secos (PAVEI *et al.*, 2011; KAISER *et al.*, 2013a), quanto durante a avaliação do potencial biológico *in vitro* dos mesmos (KAISER *et al.*, 2013c), avaliar o potencial individual dos alcaloides oxindólicos é um processo no mínimo desafiador. Portanto, o presente trabalho se insere em tópicos muitas vezes negligenciados em *U. tomentosa* e que tem como ponto de convergência os alcaloides oxindólicos e sua relevância em relação ao reconhecimento de adulteração em *U. tomentosa* empregando *U. guianensis*, aos diferentes quimiotipos e sua influência em relação à atividade antitumoral e a busca de soluções para minimizar a isomerização dos mesmos.

OBJETIVOS

Objetivo geral

Avaliar a relevância dos alcaloides oxindólicos em *Uncaria tomentosa* no que tange ao reconhecimento de adulteração na espécie, ocorrência de quimiotipos e isomerização desses compostos.

Objetivos específicos

i) Desenvolver modelos multivariados de classificação destinados à diferenciação entre *U. tomentosa* e *U. guianensis*, bem como ao reconhecimento de adulteração em *U. tomentosa* mediante análises de CLAE-PDA, IV e UV;

ii) Desenvolver modelos multivariados de quantificação destinados a determinação do percentual de adulterante em *U. tomentosa* mediante análises de CLAE-PDA, IV e UV;

iii) Avaliar a ocorrência de adulteração em amostras de *U. tomentosa*, adquiridas no mercado popular Peruano, mediante emprego dos modelos multivariados de classificação e quantificação;

iv) Obter frações purificadas em alcaloides oxindólicos representativas dos diferentes quimiotipos relatados em *U. tomentosa* mediante fracionamento empregando resina de troca iônica;

v) Avaliar *in vitro* a atividade genotóxica e citotóxica das frações purificadas em alcaloides oxindólicos em leucócitos humanos;

vi) Avaliar *in vitro* a atividade citotóxica das frações purificadas em alcaloides oxindólicos em linhagens de células tumorais de bexiga e glioblastoma humano (T24 e U-251-MG);

vii) Avaliar a complexação dos alcaloides oxindólicos com β-ciclodextrina (βCD) e seus derivados hidrofílicos, hidroxipropil-β-ciclodextrina (HP-βCD) e sulfobutil-éter-β-ciclodextrina (SBE-βCD), mediante emprego de diagramas de solubilidade;

viii) Caracterizar os complexos obtidos mediante emprego de calorimetria exploratória diferencial, IV e microscopia eletrônica de varredura;

ix) Avaliar a cinética de isomerização dos alcaloides oxindólicos complexados com SBE-βCD em condições experimentais comumente utilizadas em avaliações biológicas *in vitro*.

REFERENCIAL TEÓRICO

Aspectos agronônicos e botânicos

O gênero *Uncaria* pertencente à família Rubiaceae é composto por aproximadamente 34 espécies distribuídas, em sua maioria, na África e Ásia (LAUS, 2004; HEITZMAN *et al.*, 2005; ZHANG *et al.*, 2015). *Uncaria tomentosa* (Willdenow ex Roemer & Shultes) D.C. é originária de florestas tropicais da América do Sul e Central (Peru, Colômbia, Equador, Guiana, Venezuela, Trinidad-Tobago, Suriname, Guatemala, Costa Rica, Panamá e República Dominicana). No Brasil, a espécie *U. tomentosa* pode ser encontrada nos estados do Amapá, Amazonas, Pará e, principalmente, no Acre (POLLITO, 2004). Em estado silvestre se apresenta como uma liana de grande porte e crescimento vigoroso que pode atingir de 25 a 30 m de altura e 25 cm de diâmetro que apresenta em seu caule espinhos originados de pedúnculos abortivos denominados tomentos, utilizados para galgar a copa de espécies de maior porte, sendo por isso popularmente conhecida como unha-de-gato ou *cat's claw* (GATTUSO *et al.*, 2004; POLLITO; TOMAZELLO, 2006). Ocupa o mesmo habitat de *Uncaria guianensis* (Aubl.) Gmel., com a qual é confundida, propiciando adulterações da matéria-prima vegetal (QUINTERA; DE UGAZ, 2003; GATTUSO *et al.*, 2004; VALENTE, 2006). Além disso, a densidade populacional de *U. guianensis* é superior se comparada a de *U. tomentosa* (POLLITO; TOMAZELLO, 2006). Neste sentido, aspectos morfoanatômicos das folhas e caules de ambas as espécies, bem como suas características microscópicas, podem ser utilizadas para diferenciação e, consequentemente, para o reconhecimento de substituição ou adulteração da matéria-prima vegetal (Tabela 1a) (GATTUSO *et al.*, 2004; POLLITO; TOMAZELLO, 2006). De forma simplificada, as características morfoanatômicas dos tomentos de ambas as espécies podem ser utilizadas na diferenciação. Enquanto *U. tomentosa* apresenta tomentos com uma curvatura que varia de 30−90º, *U. guianensis* possui tomentos com uma curvatura superior a 180º (Figure 1a).

Tabela 1a. Principais características morfoanatômicas de diferenciação entre *Uncaria tomentosa* e *Uncaria guianensis* (Adaptado de GATTUSO *et al.*, 2004; POLLITO; TOMAZELLO, 2006).

Estrutura	*Uncaria tomentosa*	*Uncaria guianensis*
Tomentos	Opostos e pouco curvados (curvatura de 30−90º)	Alternados e curvos (curvatura > 180º)
Estrutura foliar	Ovalada a elíptica. Apresenta tricomas na superfície abaxial.	Elíptica a oblonga. Ausência de tricomas na superfície.
Cascas do caule	Fibras maiores (1500 a 2000 µm de comprimento) com a presença de microcristais de oxalato de cálcio.	Fibras menores (800 a 1500 µm de comprimento) com a presença de macrocristais de oxalato de cálcio (40 a 80 µm).
Inflorescências	Mesclas de amerelo e branco, cinco lobos.	Mesclas de laranja e vermelho, três lobos.
Sementes	Pequenas	Grandes
Dimensões da espécie	10 – 30 m de comprimento 5 – 40 cm de diâmetro	4 – 10 m de comprimento 4 – 15 cm de diâmetro

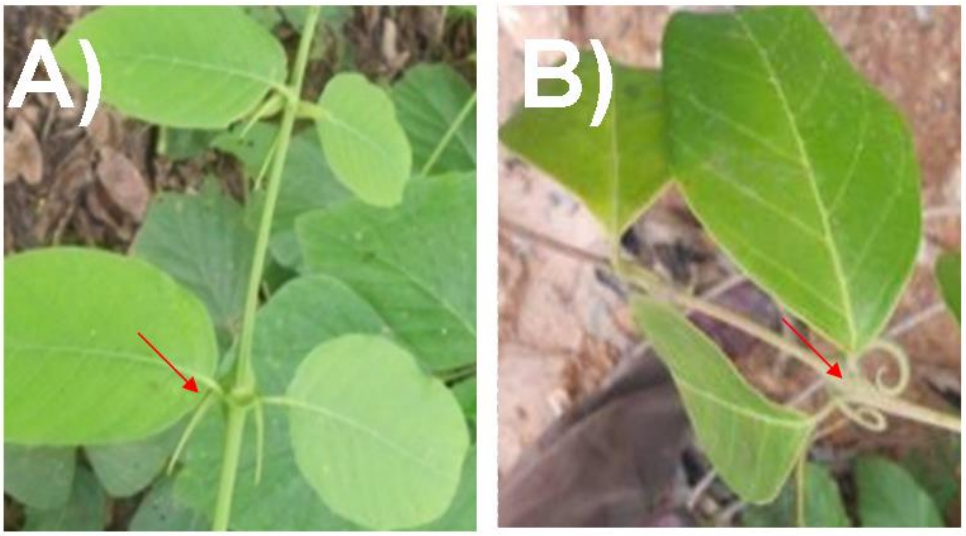

Figura 1a. Ramos de *Uncaria tomentosa* (**A**) e *Uncaria guianensis* (**B**) *in natura*. Em destaque as diferenças morfoanatômicas entre os tomentos das espécies.

Constituição química

Em relação a sua constituição química, *U. tomentosa* é composta majoritariamente por três frações bioativas, a saber, polifenóis, derivados triterpênicos e alcaloides, embora outras classes de compostos como fitoesteróis e coumarinas também tenham sido relatadas para a espécie (LAUS, 2004; HEITZMAN *et. al.*, 2005; ZHANG *et al.*, 2015).

Polifenóis

Ácidos fenólicos como ácido cafeico e ácido quínico, derivados cafeoilquinicos como o ácido clorogênico e alguns flavonóides como catequina, epicatequina e rutina além das antocianidinas são os principais constituintes da fração polifenólica em *U. tomentosa* (Figura 1b). Além disso, alguns polímeros como os taninos condensados que possuem elevada massa molecular podem perfazer até 20% da massa seca das cascas do caule em *U. tomentosa* (SANDOVAL *et al.*, 2000; GONÇALVES *et al.*, 2005; HEITZMAN *et al.*, 2005; ZHANG *et al.*, 2015).

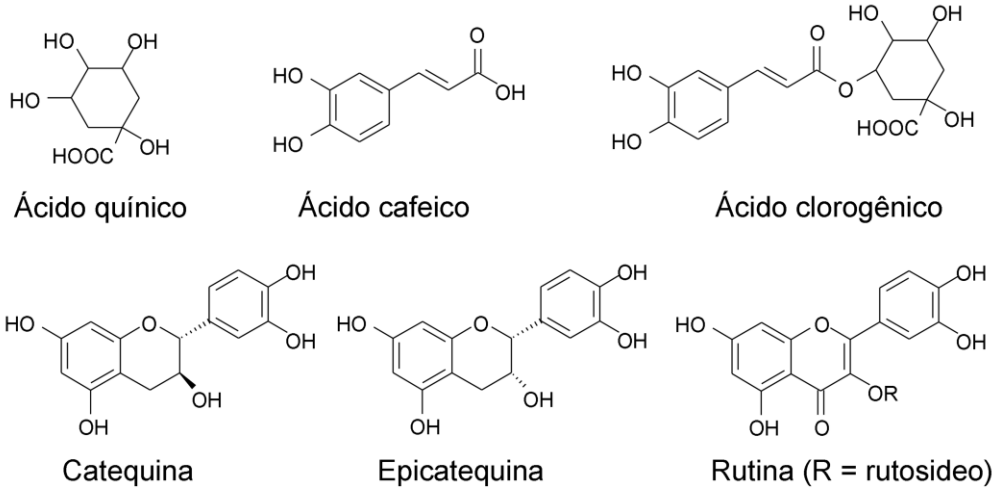

Figura 1b. Alguns constituintes da fração polifenólica de *Uncaria tomentosa*.

Compostos fenólicos como a rutina e canferitrina foram propostos como marcadores químicos de diferenciação entre *U. tomentosa* e *U. guianensis*. Assim, a

presença de rutina apenas em cascas de *U. guianensis* verificada via CCD foi sugerida como um marcador químico de diferenciação, visto que esse flavonóide estaria ausente em *U. guianensis* (VAN GINKEL, 1996). Contudo, trabalhos posteriores empregando análises de CLAE-UV de maior sensibilidade se comparada a CCD, revelaram a presença de rutina também em *U. tomentosa*, embora em menor concentração se comparada a *U. guianensis* (GRIEBELER, 2006; PAVEI *et al.*, 2010; PEÑALOZA *et al.*, 2015). Alternativamente, a canferitrina presente apenas nas folhas de *U. guianensis* conforme verificado via análises de CLAE-EM pode ser empregada como um marcador químico de diferenciação em relação a *U. tomentosa* (VALENTE *et al.*, 2009). No entanto, seu emprego em relação à diferenciação do caule, principal farmacógeno de ambas as espécies, é limitado devido à reduzida concentração de canferitrina neste, mesmo em *U. guianensis*.

Derivados triterpênicos

Heterosídeos derivados do ácido quinóvico, que podem ser mono- di- ou triglicosilados em função do número de açucares ligados ao núcleo triterpênico, são os componentes majoritários da fração triterpênica em *U. tomentosa* (Figura 1c) (CERRI *et al.*, 1988; AQUINO *et al.*, 1990; AQUINO *et al.*,1991; AQUINO *et al.*, 1997). Adicionalmente, derivados do ácido oleanólico, ursólico, 19α-hidróxi-ursólico e piroquinóvico também foram relatados como componentes minoritários desta fração (KITAJIMA *et al.*, 2000; KITAJIMA *et al.*, 2003).

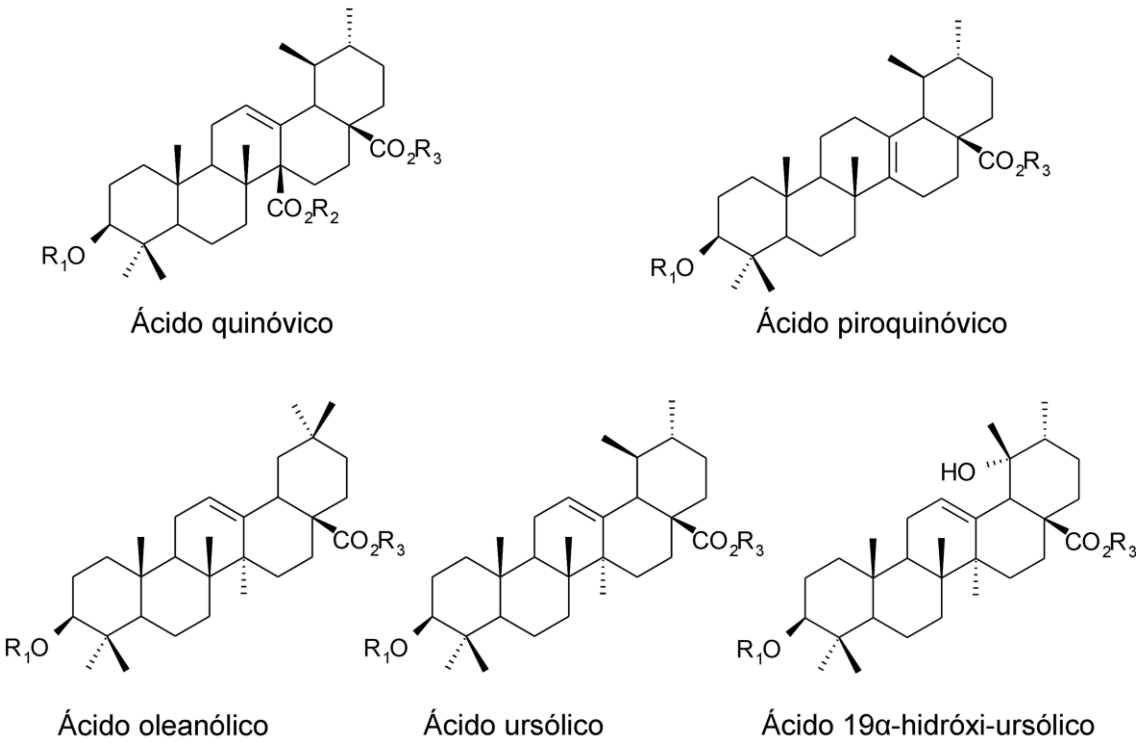

Figura 1c. Alguns constituintes da fração triterpênica de *Uncaria tomentosa*. Onde R_1, R_2, R_3 referem-se aos sítios de glicosilação dos heterosídeos derivados das agliconas.

Alcaloides

Dentre as frações bioativas verificadas em *U. tomentosa*, a fração alcaloídica exerce marcado protagonismo decorrente de sua abundância na espécie e, principalmente, devido às diversas e pronunciadas atividades biológicas atribuídas à mesma (REINHARD, 1999; LAUS, 2004; HEITZMAN *et al.*, 2005).

Estudos fitoquímicos pioneiros em *U. tomentosa* referem-se inicialmente ao isolamento dos alcaloides oxindólicos tetracíclicos, rincofilina, isorrincofilina, corinoxeina e isocorinoxeina (HEMINGWAY; PHILLIPSON, 1974) e, posteriormente, dos alcaloides oxindólicos pentacíclicos especiofilina, uncarina F, mitrafiliana, isomitrafilina, pteropodina e isopteropodina (WAGNER *et al.*, 1985). Tanto os alcaloides oxindólicos tetracíclicos quanto os pentacíclicos são diastereoisômeros diferindo-se pelas configurações de C-3, C-7, C-15 e C-20, e por isso apresentam distintas propriedades químicas, físicas e biológicas (IUPAC, 1976;

LIMA, 1997). Além destes, alcaloides indólicos penta- e tetracíclicos também foram relatados em *U. tomentosa*, a saber, acuamigina, angustina, angustolina, isoajmalicina, tetraidroalstonina, corinanteína, diidrocorinateína e seus N-óxidos e hirsuteina e seus N-óxidos (HEMINGWAY; PHILLIPSON,1974; MONTENEGRO DE MATTA *et al.*, 1976; WAGNER *et al.*, 1985).

O primeiro relato sobre da isomerização dos alcaloides oxindólicos de *U. tomentosa* se refere à interconversão de pteropodina em seus isômeros, especiofilina, uncarina F e isopteropodina em função do tempo de refluxo (LAUS; KEPLINGER, 1994). Posteriormente foi possível estabelecer a cinética e o mecanismo de isomerização dos alcaloides oxindólicos pentacíclicos e tetracíclicos, sendo a cinética dependente do tipo de solvente, pH e temperatura (LAUS *et al.*, 1996; LAUS, 1998).

O mecanismo de isomerização proposto para os alcaloides oxindólicos envolve reações de adição/eliminação reversíveis do tipo retro-Manich nos centros estereogênicos em C-3 e C-7 com a formação de um *zwitterion* intermediário (Figura 1d). Este intermediário pode ser facilmente estabilizado por solventes de elevada constante dielétrica o que diminui a energia de ativação e consequentemente favorece a isomerização. Assim, a velocidade isomerização é menor em solventes orgânicos quando comparada à água sendo diretamente proporcional a escala de polaridade de Dimroth-Reichardt. Modificações no pH revelaram que a velocidade de isomerização é menor em meio ácido do que em meio básico devido à protonação de N-4 em meio ácido que favorece a formação de ligação de hidrogênio com a carbonila lactâmica impedindo a formação do *zwitterion* intermediário. Já a temperatura exerce um efeito discreto sobre a velocidade de isomerização, havendo uma relação diretamente proporcional entre ambas variáveis (LAUS *et al.*, 1996; LAUS, 1998).

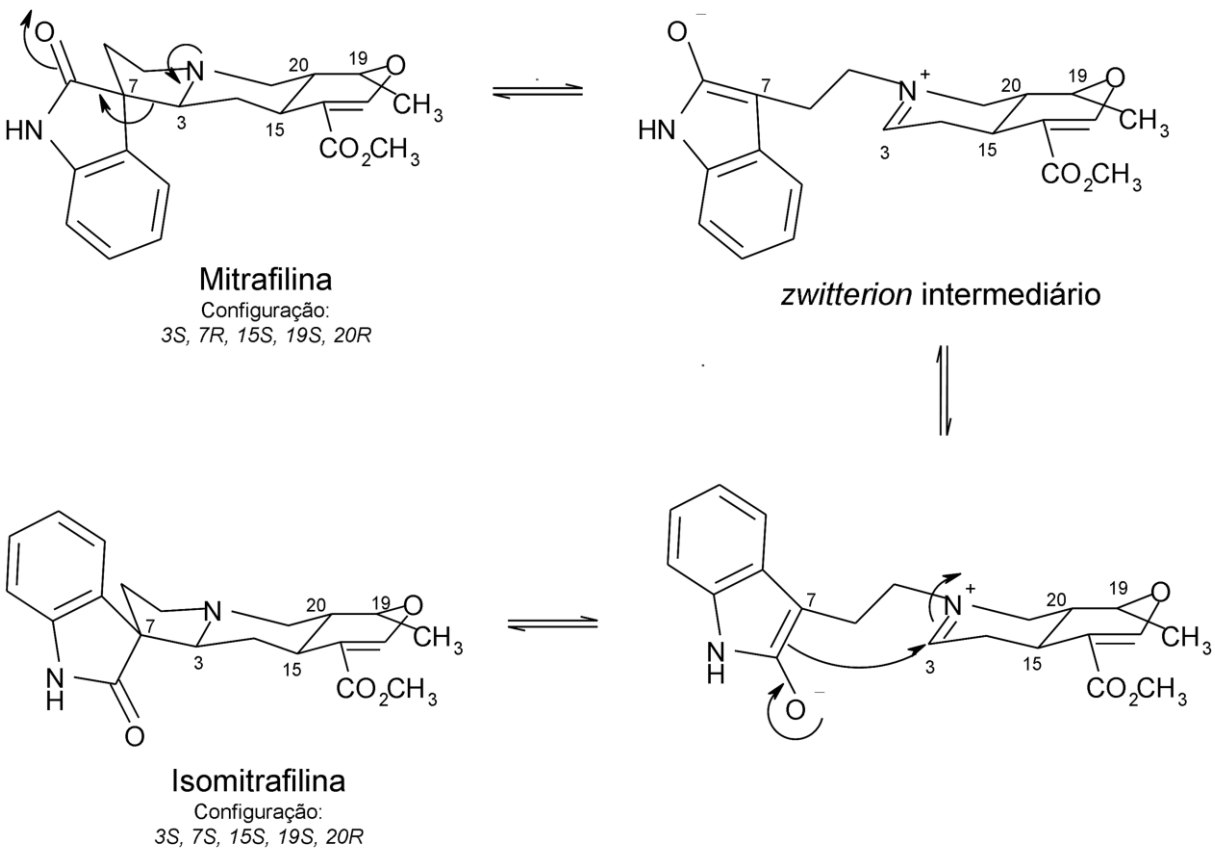

Figure 1d. Mecanismo de isomerização dos alcaloides oxindólicos e isomerização dos alcaloides oxindólicos pentacíclicos com junção dos anéis D/E em *trans* (Adaptado de LAUS *et al.*, 1996).

No caso dos alcaloides oxindólicos pentacíclicos, existem duas vias de isomerização determinadas, basicamente, pela conformação da junção dos anéis D/E (LAUS *et al.*, 1996). A conformação em *trans* determina a ocorrência de interconversão entre mitrafilina e isomitrafilina (Figura 1d). Já para a conformação em *cis* possibilita interconvesão mutua entre quatro formas isoméricas, a saber, pteropodina, isopteropodina, especiofilina e uncarina F (Figura 1e) (LAUS *et al.*, 1996). No caso dos alcaloides oxindólicos tetracíclicos, a presença dos grupamentos etila e vinila em C-19 determina a interconversão entre rincofilina/isorrincofilina ou corinoxeina/isocorinoxeina, respectivamente (Figura 1f) (LAUS, 1998).

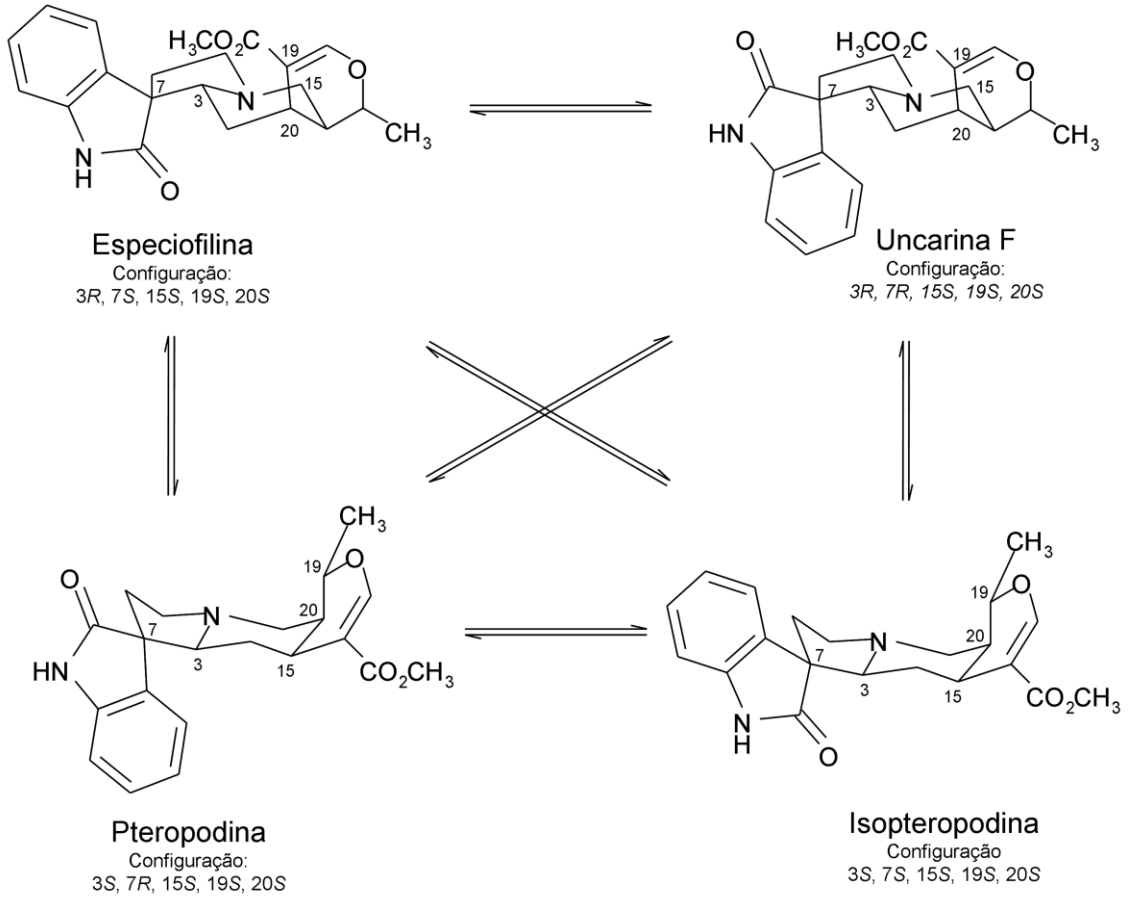

Figura 1e. Isomerização dos alcaloides oxindólicos pentacíclicos com junção D/E em *cis* (Adaptado de LAUS *et al.*, 1996).

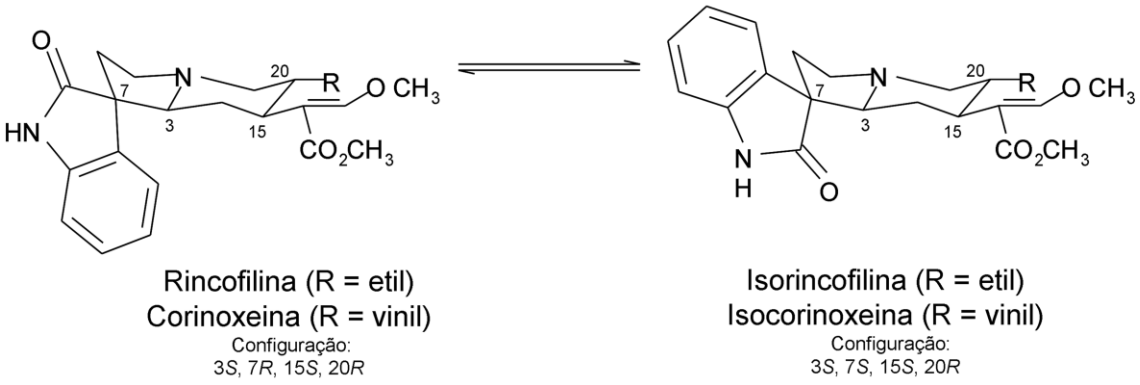

Figura 1f. Isomerização dos alcaloides oxindólicos tetracíclicos (Adaptado de LAUS, 1998).

As modificações induzidas no perfil de alcaloides oxindólicos decorrentes do processo de isomerização podem ocorrer em distintas etapas relacionadas tanto ao

processamento da matéria-prima vegetal, quanto em ensaios visando à avaliação do potencial terapêutico da espécie (KAISER *et al.*, 2013a; KAISER *et al.*, 2013b; KAISER *et al.*, 2013c). Processos extrativos como maceração estática em longo período, refluxo e turbo-extração ocasionaram modificações no perfil de alcaloides oxindólicos decorrentes da isomerização em virtude, principalmente, do tempo e temperatura (KAISER *et al.*, 2013a). Por outro lado, com o emprego de maceração dinâmica ou ultrassom é possível preservar o perfil de alcaloides oxindólicos em *U. tomentosa* (KAISER *et al.*, 2013a). Além disso, foi possível obter condições ótimas de extração via maceração dinâmica que propiciaram maximizar o rendimento de extração dos alcaloides oxindólicos preservando o perfil encontrado na matéria-prima vegetal (KAISER *et al.*, 2013b).

Recentemente foi demonstrada a ocorrência de isomerização durante o período de incubação em experimento simulando as condições habitualmente empregadas em culturas celulares (KAISER *et al.*, 2013c). As condições de incubação, como pH do meio (7,4) e temperatura (37 ºC), induziram a isomerização de especiofilina, uncarina F e pteropodina a isopteropodina (conformação dos anéis D/E em *cis*), de mitrafilina a isomitrafilina (conformação dos anéis D/E em *trans*) e rincofilina a isorrincofilina (tetracíclicos) (KAISER *et al.*, 2013c). Após 6 h de incubação, o perfil inicial de alcaloides oxindólicos foi alterado significativamente mantendo-se estável até as 24h de incubação.

Outro fator importante em *U. tomentosa* é a ocorrência de quimiotipos baseado em seu perfil de alcaloides oxindólicos. Inicialmente, STUPPNER *et al.* (1992a) verificaram que amostras distintas de caule e raiz apresentavam elevada variabilidade, tanto qualitativa quanto quantitativa, em relação à composição total de alcaloides oxindólicos. Posteriormente, constatou-se que o estágio de maturidade, épocas do ano, locais de coleta e distintas partes do vegetal contribuem para essa elevada variabilidade (LAUS *et al.*, 1997). A partir destes estudos, foi proposta a existência de dois quimiotipos em *U. tomentosa*, botanicamente indistinguíveis entre si, a saber, quimiotipo oxindólico *tetracíclico* e *pentacíclico* (LAUS *et al.*, 1997). Além disso, foi verificado que esses quimiotipos parecem exercer atividades biológicas antagônicas

(KEPLINGER *et al.*, 1999). Contudo, recentemente PEÑALOZA *et al.* (2015) verificaram a ocorrência de três quimiotipos mais específicos na espécie a partir da avaliação da composição química de folhas, galhos e cascas do caule de 22 indivíduos coletados em distintas regiões do Peru. Estes quimiotipos foram nominados de acordo com a composição química majoritária de alcaloides oxindólicos em: *quimiotipo I*, composto majoritariamente por alcaloides oxindólicos pentacíclicos com conformação dos anéis D/E em *cis* (especiofilina, uncarina F, pteropodina e isopteropodina); *quimiotipo II*, composto majoritariamente por alcaloides oxindólicos pentacíclicos com conformação dos anéis D/E em *trans* (mitrafilina e isomitrafilina); *quimiotipo III*, composto majoritariamente por alcaloides oxindólicos tetracíclicos (rincofilina e isorrincofilina). As folhas da espécie apresentam quimiotipos mais definidos quando comparado aos galhos e cascas do caule o que pode estar relacionado à biossíntese dos alcaloides que ocorre nas folhas e sua distribuição a partir destas para as demais partes do vegetal como galhos e caule possibilitando a bioconversão dos mesmos (LUNA-PALENCIA *et al.*, 2013; PEÑALOZA *et al.*, 2015).

Emprego etnofarmacológico e farmacológico

A medicina indígena Asháninka da região amazônica peruana utiliza decoctos e macerados das cascas e raízes de *U. tomentosa* há cerca de dois mil anos para o tratamento de úlceras gástricas, artrite reumatóide, infecções bacterianas e virais, alergias, asma e, até mesmo, câncer (REINHARD, 1999; HEITZMAN *et al.*, 2005; VALENTE, 2006). Diversos trabalhos científicos foram conduzidos com o intuito de comprovar o potencial terapêutico da espécie, sendo a maioria deles direcionados a fração alcaloídica de *U. tomentosa*. Um apanhado geral das atividades mais relevantes associadas ao emprego da espécie é apresentado a seguir.

Atividade anti-inflamatória

Diversos estudos realizados *in vitro* indicam que atividade anti-inflamatória de extratos obtidos das cascas de unha-de-gato está relacionada à prevenção da produção do fator transcriptacional NF-kβ a nível molecular inibindo assim a transcrição de genes associados ao processo inflamatório (SANDOVAL-CHACON *et al.*, 1998; SANDOVAL *et al.*, 2000; AKESSON *et al.*, 2003; ALLEN-HALL *et al.*, 2007; ALLEN-HALL *et al.*, 2010). O efeito anti-inflamatório da espécie foi também comprovado *in vivo* mediante redução de edema em pata de ratos após administração de extratos hidroetanólicos e decoctos das cascas de *U. tomentosa* (AQUINO *et al.*, 1991; AGUILAR *et al.*, 2002) e redução do dano celular em brônquios de ratos após inflamação pulmonar induzida por O_3 (CISNEROS *et al.*, 2005). Além disso, em ensaio clínico duplo-cego, randomizado, controlado por placebo, a administração de 20 mg de extrato enriquecido em alcaloides oxindólicos pentacíclicos foi capaz de reduzir os sintomas associados à artrite reumatóide (MUR *et al.*, 2002; SETTY; SIGAL, 2005). Por outro lado, alguns trabalhos associam o efeito anti-inflamatório dos extratos de *U. tomentosa* às propriedades antioxidantes dos polifenóis, sendo este independente da fração alcaloídica da espécie (SANDOVAL *et al.*, 2002; GONÇALVEZ *et al.*, 2005; PILARSKI *et al.*, 2006; AMARAL *et al.*, 2009; KRISHNAIAH *et al.*, 2011). Recentemente foi também demonstrado o efeito anti-inflamotório *in vivo* da fração purificada em derivados triterpênicos do ácido quinóvico em cistite hemorrágica induzida por ciclofosmamida (DIETRICH *et al.*, 2015).

Atividade imunoestimulante e imunomoduladora

A atividade imunoestimulante da espécie inicialmente verificada mediante aumento da fagocitose em granulócitos induzida pelos alcaloides oxindólicos tanto *in vitro* quanto *in vivo*, a exceção da mitrafilina e rincofilina (WAGNER *et al.*, 1985), posteriormente pôde ser comprovada mediante estimulação da secreção de citocinas (IL-1 e IL-6) em macrófagos alveolares após incubação com extratos aquosos de

cascas (LEMAIRE *et al.*, 1999). Extratos e frações enriquecidas em alcaloides oxindolicos pentacíclicos também foram capazes de estimular a proliferação de linfócitos T e B quando incubados inicialmente com células endoteliais, sendo este efeito inibido pelos alcaloides oxindólicos tetracíclicos denotando um efeito antagonista dos alcaloides oxindólicos tetracíclicos em relação aos pentacíclios (WURM *et al.*, 1998; KEPLINGER *et al.*, 1999). O extrato ácido das cascas de *U. tomentosa* enriquecido em alcaloides oxindólicos foi capaz de aumentar significativamente os níveis de linfócitos em pacientes portadores do HIV após cinco meses de uso (KEPLINGER *et al.*, 1999). Por outro lado, o extrato aquoso da cascas de *U. tomentosa* e a fração enriquecida em polifenóis obtida deste também foram capazes de estimular *in vitro* a produção de citocinas pró-inflamatórias TNF-α e IL-6 e reduzir os níveis de IL-1β em macrófagos, modulando assim sua atividade (LENZI *et al.*, 2013).

No entanto, extratos e frações de alcaloides oxindólicos também podem apresentar efeito imunológico depressor. Em células mononucleares periféricas foi observada diminuição dos níveis de neopterina e da relação quinurenina/triptofano (marcadores de reposta imune Th1 induzida por IFN-γ), efeito que se manteve após estimulação inicial com fitohemaglutinina e concavalina A (WINKLER *et al.*, 2004). De forma semelhante, o extrato hidroetanólico das cascas e a fração enriquecida em alcaloides oxindólicos inibiram a proliferação do vírus da dengue tipo 2 em monócitos humanos, com diminuição significativa dos níveis de citocinas pró-inflamatórias, TNF-α, IFN-γ e IL-10, associadas ao agravamento do quadro clínico (REIS *et al.*, 2008). Aumentos significativos na polpa branca do baço e timo e na produção *in vivo* de linfócitos T (principalmente $CD4^+$) e linfócitos B foram verificados após a administração do extrato de cascas de *U. tomentosa* a camundongos por 28 dias, não sendo evidenciado efeito imunotóxico nos animais tratados. O perfil de citocinas observado foi compatível com uma resposta Th2 mediada, devido ao aumento nos níveis de IL-4 e IL-5 e diminuição nos níveis de IL-2 e IFN-γ em células esplênicas, após estimulação com concavalina A (DOMINGUES *et al.*, 2011a). Também foi observado bloqueio da progressão do diabetes tipo 1 (imunomediada) em 95% dos

camundongos tratados com o extrato hidroetanólico das cascas, sendo o efeito relacionado à atividade imunomoduladora mediada por uma resposta Th2 (DOMINGUES *et al.*, 2011b). Além disso, a mitrafilina isolada das cascas de *U. tomentosa* foi capaz de modular a plasticidade dos monócitos e macrófagos humanos *in vitro* mediante inibição da produção de citocinas pró-inflamatórias TNF-α e IL-6 após estimulação prévia com lipopolissacarídeo (LPS) contribuindo assim para a atenuação da resposta imune (MONTSERRAT-DE LA PAZ *et al.*, 2015).

Atividade antitumoral e antiproliferativa

O potencial antitumoral e antiproliferativa da espécie foi demonstrado frente diversas linhagens celulares principalmente humanas, a saber: células leucêmicas (HL-60 e U-937) (STUPPNER *et al.,* 1993); células leucêmicas (K-562 e HL-60) e de linfoma (Raji) (SHENG *et al.*, 1998); células de melanoma (SK-MEL), carcinoma epidermóide (KB), carcinoma ductal (BT-549) e carcinoma de ovário (SK-OV-3) (MUHAMMAD *et al.,* 2001); carcinoma de mama (MCF7) (RIVA *et al.,* 2001); leucêmicas T linfoblásticas (CCRF-CEM-C7H2) (BACHER *et al.,* 2006); de osteossarcoma (SAOS), carcinoma de mama (MCF7) e carcinoma cervical (HeLa) (DE MARINO *et al.,* 2006); neuroblastoma (SKN-BE(2)) e glioma (GANG) (GARCÍA PRADO *et al.,* 2007); células leucêmicas (HL-60) (PILARSKI *et al.*, 2007; CHENG *et al.*, 2007; PILARSKI *et al.,* 2013); carcinoma medular de tireóide (MTC-SK) (RINNER *et al.,* 2009); sarcoma de Ewing (MHH-ES-1) e carcinoma de mama (MT-3) (GIMÉNEZ *et al.,* 2010); gliomas de rato (C6) e humanos (U138-MG) (PAVEI, 2010); adenocarcinoma de cólon (HT-29) adenocarcinoma colorretal (SW707), carcinoma cervical (KB), carcinoma de mama (MCF7), carcinoma de pulmão de células não-pequenas (A549), cistoadenocarcinoma ovariano (OAW-42), além de linhagens celulares de ratos, a saber, carcinoma pulmonar de Lewis (LLC LL/2) e melanoma (B16) (PILARSKI *et al.*,. 2010); modelo de carcinosarcoma Walker-256 (DREIFUSS *et al.,* 2010; DREIFUSS *et al.,* 2013); carcinoma colorretal (HCT116 e SW480) carcinoma cervical (HeLa) (GURROLA-DÍAZA *et al.,* 2011);

células tumorais de bexiga (T24 e RT4) (KAISER *et al.*, 2013a; DIETRICH *et al.*, 2014). Embora a atividade antitumoral em *U. tomentosa* seja atribuída majoritariamente aos alcaloides oxindólicos (HEITZMAN *et al.*, 2005; ZHANG *et al.*, 2015), outros constituintes da espécie como os derivados triterpênicos (DIETRICH *et al.*, 2014) e compostos fenólicos (DREIFUSS *et al.*, 2013) também demonstraram potencial antitumoral.

A morte das células tumorais parece ocorrer via apoptose induzida pela ativação de caspases (SHENG *et al.*, 1998; BACHER *et al.*, 2006; DE MARINO *et al.*, 2006; CHENG *et al.*, 2007; RINNER *et al.*, 2009). Entretanto, a via apoptótica pode ser induzida alternativamente pela inibição da ativação do fator de transcrição NF-κB, que parece ser dependente do tipo celular e seu estado de ativação (ALLEN-HALL *et al.*, 2010; PILARSKI *et al.*, 2013). Além disso, o extrato das cascas de *U. tomentosa* e a fração enriquecida em alcaloides oxindólicos pentacíclicos deste foram capazes de inibir a ativação de genes que regulam a proliferação e diferenciação celular, mediante inibição da via de sinalização Wnt, sendo esta superativada em determinadas células tumorais, como no caso do carcinoma colorretal (SW480) (GURROLA-DÍAZA *et al.*, 2011).

Aspectos toxicológicos

A utilização de preparações de *U. tomentosa* é considerada segura (VALÉRIO JR.; GONZALEZ, 2005). Diversos estudos foram conduzidos visando avaliar o potencial toxicológico da espécie tanto *in vitro* quanto *in vivo*, contudo nenhuma alteração significativa nos padrões toxicológicos avaliados foi verificada. Além disso, preparações de *U. tomentosa* demonstraram baixo potencial genotóxico e mutagênico (VALÉRIO JR.; GONZÁLEZ, 2005; ROMERO-JIMÉNEZ *et al.*, 2005). Contrariamente, extratos de *U. tomentosa* tem aumentado a capacidade de reparação em danos ao DNA induzidos por radiação UV (RIZZI *et al.*, 1993; MAMMONE *et al.*, 2006; CAON *et al.*, 2014). Além disso, a utilização de três comprimidos contendo extrato seco de cascas de *U. tomentosa* durante 19 dias do ciclo de tratamento como terapia complementar foi capaz de reduzir significativamente a neutropenia induzida

pela quimioterapia empregando a associação 5-fluorouracil, doxorubicina e ciclofosfamida em pacientes acomentidos de cancer de mama (ARAÚJO *et al.*, 2012).

Aspectos analíticos

Inicialmente os métodos cromatográficos desenvolvidos destinaram-se ao monitoramente dos alcaloides oxindólicos em *U. tomentosa*, principalmente os pentacíclicos (Tabela 1b). STUPPNER *et al.* (1992) e posteriormente LAUS e KEPLINGER (1994) desenvolveram métodos via CLAE-UV destinados a quantificação dos alcaloides oxindólicos utilizando resfriamento do sistema (12 ºC e 15 ºC) o que dificulta a sua reprodutibilidade. Posteriormente, GANZERA *et al.* (2001) propuseram método isocrático via CLAE-UV visando avaliar os alcaloides oxindólicos com prévia extração em fase sólida de compostos fenólicos utilizando poliamida. Por outro lado, MONTORO *et al.* (2004), GRIEBELER (2006) e PAVEI *et al.* (2011) propuseram métodos via CLAE-EM e UV destinados a quantificação dos alcaloides oxindólicos que apresentavam como ponto de convergência a baixa seletividade entre isomitrafilina e pteropodina. BERTOL *et al.* (2012) propuseram método via CLAE-UV com adequada seletividade de separação entre isomitrafilina e pteropodina, mas a temperatura de análise (15 ºC) e a extração em fase sólida prévia da amostra com poliamida dificultam a implementação desta metodologia na rotina de análise. Por sua vez, KAISER *et al.*, (2013a) desenvolveram e validaram método via CLAE-UV/EM destinado a análise e quantificação dos alcaloides oxindólicos pentacíclicos e tetracíclicos a temperatura ambiente (23 ºC), sem a necessidade prévia de *clean-up* da amostra mantendo a adequada seletividade entre isomitrafilina e pteropodina.

Tabela 1b. Condições cromatográficas empregadas na análise de metabólitos secundárias relevantes em *Uncaria tomentosa* (Adaptado de KAISER, 2012).

Parte vegetal (Grupo químico)	Coluna *(Temperatura)*	Fase Móvel	Detecção	Referência
Raízes (alcaloides oxindólicos [a])	Lichrospher CH-18 *(15 °C)*	CH_3OH:CH_3CN: tampão fosfato pH 6,6 (20:20:60 v/v); gradiente	UV (245 nm)	STUPPNER *et al.* (1992)
Cascas de raízes e tronco (alcaloides oxindólicos [a])	LichroCART RP-18 *(12 °C)*	CH_3CN:éter: tampão fosfato pH 7,7 (34:1:65 v/v); isocrático	UV (254 nm)	LAUS e KEPLINGER (1994)
Cascas do caule (alcaloides oxindólicos [a b])	Luna RP-18 *(23 °C)*	Tampão fosfato pH 7,0:CH_3CN (65:35 v/v); gradiente	UV (245 nm)	GANZERA *et al.* (2001)
Cascas e folhas (alcaloides oxindólicos [a] e derivados triterpênicos)	Lichrsorb RP-18 e Symmetry RP-18 *(23 °C)*	CH_3OH:CH_3CN: tampão acetato pH5.0; gradiente	EM	MONTORO *et al.* (2004)
Cascas do caule e extrato seco (alcaloides oxindólicos [a])	Lichrospher RP-18 *(28 °C)*	Tampão fosfato pH 7,0:CH_3CN (60:40 v/v); isocrático	UV (245 nm)	GRIEBELER (2006)
Cascas do caule e raízes (polifenóis)	Gemini RP-18 *(23 ºC)*	TFA 0,1% (v/v): (metanol:TFA; 99,9:0,1; v/v); gradiente	UV (325 nm)	PAVEI *et al.* (2010)
Cascas do caule e extratos secos (alcaloides oxindólicos [a])	Gemini RP-18 *(35 ºC)*	Tampão fosfato pH 7,0:(CH_3CN:tampão fosfato pH 7; 95:5; v/v); gradiente	UV (245 nm)	PAVEI *et al.* (2011)
Cascas do caule (alcaloides oxindólicos [a b])	Zorbax XDB *(15 ºC)*	Tampão acetato de amônio 35 mM (pH 6,9): CH_3CN; gradiente	UV (245 nm)	BERTOL *et al.* (2012)
Cascas do caule e fração enriquecida (derivados triterpênicos)	Sinergy Fusion RP-18 *(35 ºC)*	Ácido fórmico 0,1%:(CH_3CN:ácido fórmico 0,1%; 90:10, v/v); gradiente	UV/EM (205 nm)	PAVEI *et al.* (2012)
Cascas do caule (alcaloides oxindólicos [a b])	Gemini-NX RP-18 *(23 ºC)*	Tampão acetato de amônio 10 mM (pH 7,0): CH_3CN; gradiente	UV/EM (245 nm)	KAISER *et al.* (2013a)
Cascas do caule (alcaloides oxindólicos [a b])	L1 *end-capped* (3µm) *(23 ºC)*	Tampão fosfato pH 7,0:CH_3CN:(CH_3OH:ácido acético; 99:1, v/v)	UV (245 nm)	USP (2015)

[a] pentacíclicos; [b]tetracíclicos; UV = Ultravioleta; EM = Espectrometria de massas.

Atualmente, a monografia da Farmacopéia Americana (USP, 2016) propõe metodologia via CLAE-UV destinada ao controle de qualidade da matéria-prima vegetal (cascas do caule de *U. tomentosa*) e de derivados desta, como extratos secos, comprimidos e cápsulas. A metodologia propõe o emprego de temperatura ambiente

(23 ºC) com adequada seletividade entre isomitrafilina e pteropodina, contudo mantém o processo de *clean-up* da amostra utilizando poliamida. De acordo com as especificações da monografia, a matéria-prima vegetal deve apresentar teor de alcaloides oxindólicos pentacíclicos superior a 0,3% (m/m) e teor de alcaloides oxindólicos tetracíclicos inferior a 0,05% (m/m). Para os derivados como extratos secos, comprimidos e cápsulas, o teor de alcaloides oxindólicos tetracíclicos é limitado a 25% (m/m) em relação ao teor de acalóides oxidólicos pentacíclicos determinado.

Em relação às demais frações majoritárias da espécie, a saber, polifenóis e derivados triterpênicos, o desenvolvimento de metodologias pode ser considerado incipiente quando comparado aos alcaloides oxindólicos. Inicialmente, MONTORO *et al.* (2004) propuseram metodologia destinada à análise de derivados triterpênicos em cascas do caule e folhas de *U. tomentosa* por CLAE-MS. Posteriormente, PAVEI *et al.* (2012) desenvolveram e validaram metodologia por CLAE-UV destinada à análise e quantificação dos sete derivados triterpênicos majoritários em cascas do caule de *U. tomentosa* utilizando α-hederina como padrão externo. Análises complementares por CLAE-MS possibilitaram a identificação de quatro derivados monoglicosilados, dois diglicosilados e um triglicosilado sendo todos derivados do Ácido quinóvico (PAVEI *et al.*, 2012). Além disso, PAVEI *et al.* (2010) desenvolveram e validaram metodologia via CLAE-UV destinada à análise da fração polifenólica das cascas do caule e raízes de *U. tomentosa*. Majoritariamente, cinco polifenóis foram detectados e quantificados, dentre os quais puderam ser identificados mediante comparação com substâncias de referência os ácidos cafeico e clorogênico bem como a rutina. Os demais picos apresentaram espetros de UV característicos de flavonóides, porém sua estrutura química não pode ser completamente elucidada (PAVEI *et al.*, 2010).

Ciclodextrinas

Ciclodextrinas são oligossacarídeos cíclicos de origem natural que apresentam uma superfície externa hidrofílica e um núcleo ou cavidade hidrofóbica (DEL VALLE, 2004; LOFTSSON *et al.*, 2005; KURKOV; LOFTSSON, 2013). As ciclodextrinas

naturais são formadas por seis (α-ciclodextrina; α-CD), sete (β-ciclodextrina; β-CD) ou oito (γ-ciclodextrina; γ-CD) unidades de glicopiranose. Ainda que as ciclodextrinas naturais apresentem características hidrofílicas, a β-CD apresenta limitada hidrossolubilidade devido à elevada energia de sua rede cristalina (LOFTSSON *et al.*, 2005). Assim foram desenvolvidos derivados hidrossolúveis da β-CD mediante modificações químicas nas hidroxilas secundárias sendo as mais comumente empregadas a hidroxipropil-β-ciclodextrina (HP-βCD) e a sulfobutil-éter-β-ciclodextrina (SBE-βCD) (LOFTSSON *et al.*, 2005). Em virtude de sua limitada hidrossolubilidade, a β-CD é utilizada apenas em formulações destinadas a via tópica e oral, enquanto que a HP-βCD e a SBE-βCD são também utilizadas em formulações destinadas à via parenteral (DEL VALLE, 2004; LOFTSSON *et al.*, 2005; KURKOV; LOFTSSON, 2013).

Em virtude de suas propriedades físico-químicas, as ciclodextrinas são muito utilizadas na indústria tanto para aumentar a hidrossolubilidade de moléculas pouco solúveis, quanto para preservar a estabilidade de moléculas susceptíveis a degradação mediante a formação de complexos entre as ciclodextrinas e a molécula de interesse (LOFTSSON *et al.*, 2005). Os complexos formados podem ser de inclusão, quando parte da molécula de interesse é imobilizada no interior da cavidade hidrofóbica a nível molecular, ou de adsorção, quando o complexo é formado mediante interação de grupamentos da molécula de interesse com os grupamentos da superfície externa da ciclodextrina (DEL VALLE, 2004; LOFTSSON *et al.*, 2005; KURKOV; LOFTSSON, 2013). Em virtude de sua capacidade de complexação com moléculas de interesse, a velocidade de degradação e isomerização da astilbina, um didroflavonol encontrado em *Hypericum perforatum*, pode ser minimizada significativamente mediante complexação com β-CD e γ-CD (ZHANG *et al.*, 2013). Além disso, a isomerização do *trans*-resveratrol a *cis*-resveratrol induzida pela exposição do resveratrol a luz solar foi minimizada após complexação com α-CD (BERTACCHE *et al.*, 2006). Assim, a complexação com as ciclodextrinas parece ser uma promissora alternativa para minizar a isomerização dos alcaloides oxindólicos de *U. tomentosa.*

Análise multivariada

A análise multivariada de dados tem como finalidade básica racionalizar a informação de uma matriz complexa de dados facilitando assim a visualização de correlações entre as variáveis que dificilmente seriam verificadas mediante análise univariada. Assim, pela própria definição, a utilização deste tipo de abordagem tem como pressuposto básico um sistema complexo. Matrizes vegetais, devido a sua natureza multicomponente, se enquadram perfeitamente nesta definição. Consequentemente, a utilização da análise multivariada em associação com métodos analíticos têm aumentado nos últimos anos, principalmente em abordagens destinadas à análise metabolômica (LIU *et al.*, 2016; GAD *et al.*, 2013a). Além disso, o seu emprego na diferenciação e no reconhecimento de adulteração em espécies de interesse comercial também tem sido muito efetivo (GAD *et al.*, 2013a; GAD *et al.*, 2013b).

De acordo com o padrão de reconhecimento do sistema e com a finalidade ao qual se destina a análise multivariada pode ser dividida em:

- *Análise não-supervisionada*: Tem como objetivo encontrar padrões em dados sem nenhum conhecimento prévio sobre a natureza dos mesmos. Destina-se basicamente à análise exploratória dos dados baseada na variância total do sistema. Enquadram-se nesta classe de métodos a análise de componentes principais (PCA), a análise de fatores (FA) e a análise de cluster (HCA), entre outros (BRERETON, 2003; HAIR *et al.*, 2009; GAD *et al.*, 2013a).

- *Análise supervisionada*: Tem como objetivo encontrar padrões em dados tendo como base o conhecimento prévio sobre as características qualitativas das amostras. Assim, é possível construir um modelo de classificação com base exclusivamente nas variáveis altamente correlacionadas com a característica qualitativa em questão. O modelo proposto depois de calibrado pode ser então avaliado usando um conjunto de amostras independentes de característica qualitativa conhecida para validar as propriedades de previsão do modelo proposto, antes de utilizá-lo em um conjunto de amostras desconhecidas. Enquadram-se nesta classe de

métodos a análise do vizinho mais próximo (*k*-NN), *soft independent modeling of class analogy* (SIMCA) e a análise discriminante por mínimos quadrados parciais (PLS-DA), entre outros (BRERETON, 2003; HAIR *et al.*, 2009; GAD *et al.*, 2013);

- *Calibração multivariada*: Análise supervisionada que tem como objetivo específico quantificar uma determinada característica (***y***) a partir de um conjunto de variáveis (matriz ***x***), também denominados preditores. O modelo em questão pode ser calibrado utilizando-se a característica quantitativa conhecida (***y***) e sua correlação e covariância com as variáveis da matriz ***x*** (preditores). Na calibração multivariada o modelo proposto depois de calibrado, pode ser então avaliado mediante uso de um conjunto de amostras independentes de característica quantitativa conhecida (***y***) para validar as propriedades de previsão do modelo proposto, antes de utilizá-lo em um conjunto de amostras desconhecidas. Enquadram-se nesta classe de métodos a regressão linear múltipla (MLR), a regressão de componentes principais (PCR) e a regressão por mínimos quadrados parciais (PLS); entre outros (BRERETON, 2003; HAIR *et al.*, 2009; GAD *et al.*, 2013).

Capítulo 1. Diferenciação química entre *Uncaria tomentosa* e *Uncaria guianensis* mediante análises de CLAE-PDA, IV e UV associadas à análise multivariada de dados: uma ferramenta para o reconhecimento de adulteração em *Uncaria tomentosa*.

Introdução

Dentre as 34 espécies que compõe o gênero *Uncaria*, apenas as espécies *U. tomentosa* e *U. guianensis* são encontradas no América do Sul (LAUS, 2004; HEITZMAN *et al.*, 2005; ZHANG *et al.*, 2015). Ambas são comumente conhecidas como unha-de-gato e ocupam o mesmo habitat, sendo que *U. guianensis* apresenta maior densidade populacional (GATTUSO *et al.*, 2004; POLLITO; TOMAZELLO, 2006). No entanto, o conhecimento relacionado ao emprego farmacológico de *U. tomentosa* e também em relação aos aspectos toxicológicos é maior se comparada o *U. guianensis*. Além disso, *U. tomentosa* apresenta maior valor comercial se comparada a *U. guianensis*, sendo que ambas são obtidas principalmente via extrativismo. Assim, práticas de substituição e/ou adulteração em *U. tomentosa* utilizando *U. guianensis* podem ser recorrentes.

A diferenciação entre *U. tomentosa* e *U. guianensis* baseada em aspectos morfoanatômicos e microscópicos parece ser efetiva para o reconhecimento de substituição quando aplicada a matéria-prima *in natura* ou até mesmo seca e cominuída (GATTUSO *et al.*, 2004; POLLITO; TOMAZELLO, 2006). Contudo, para derivados da espécie como extratos secos, comprimidos e cápsulas, a diferenciação e, consequentemente, o reconhecimento de substituição e adulteração em *U. tomentosa* se limita a sua composição química. Assim, o presente capítulo foi destinado à diferenciação química entre *U. tomentosa* e *U. guianensis* mediante emprego de distintas abordagens analíticas associadas à análise multivariada de dados visando, portanto, estabelecer parâmetros indicativos de adulteração em *U. tomentosa*.

Este capítulo é apresentado na forma de artigo a ser submetido para publicação em periódico relevante que se enquadre no escopo do presente estudo.

Artigo 1. Chemical differentiation between *Uncaria tomentosa* and *Uncaria guianensis* by LC-PDA, FT-IR and UV methods coupled to multivariate analysis: a reliable tool for adulteration recognition

Chemical differentiation between *Uncaria tomentosa* and *Uncaria guianensis* by LC-PDA, FT-IR and UV methods coupled to multivariate analysis: a reliable tool for adulteration recognition

Samuel Kaiser, Ânderson Ramos Carvalho, Vanessa Pittol, Evelyn Maribel Peñaloza, Pedro Ernesto de Resende, George González Ortega*

Faculdade de Farmácia, Programa de Pós Graduação em Ciências Farmacêuticas (PPGCF), Universidade Federal do Rio Grande do Sul (UFRGS), Av. Ipiranga, 2752, Santana, Porto Alegre – RS – Brazil – CEP: 90610-000.

* Correspondence to: S.Kaiser, Av. Ipiranga, 2752, Sala 606, Santana, Porto Alegre - RS – Brazil, CEP: 90610-000; Tel: +55 (51)3308 5415 Fax: +55 (51)3308 5437; E-mail: *samokaiser@yahoo.com.br*

ABSTRACT

Introduction − *Uncaria guianensis* (UG) and *Uncaria tomentosa* (UT) are widely found in the South America rainforest. Both species are popularly known as cat's claw but they can be easily differentiated in natural state through their morphological characteristics. However, the differentiation of derivatives obtained from both species, such as dried extracts, is limited to differences in their chemical composition, and consequently it requires analytical chemical methods to. Thus, several official compendia established identification criteria based on the oxindole alkaloids profile of UT stem bark, nonetheless, this analytical task can be troublesome owing to the natural variability of both species, including the occurrence of at least three chemotypes in UT.

Objective − To determine criteria directed toward the establishment of a consistent differentiation of both cat's claw species by multivariate analysis from FT-IR, UV, and LC-PDA data, as well to establish reliable parameters for adulteration recognition in *U. tomentosa* stem bark.

Material and Methods − Six authentic UT stem bark samples, two UG stem bark samples and eighteen UT samples spiked with UG at three levels (10%, 30% and 50%, w/w) were properly extracted. All samples were analyzed by FT-IR analysis; direct UV analysis; UV analysis after basification and complexation with KOH and $AlCl_3$, respectively; LC-PDA analysis of oxindole alkaloids, quinovic acid glycosides, and polyphenols. Classification (SIMCA and *k*-NN models) and calibration (PCR and PLS models) multivariate models were applied for adulteration recognition and quantification of their level, respectively. LC-PDA-QTOF analyses were performed to characterize the main compounds responsible by adulteration recognition. Additionally, ten stem bark samples of cat's claw obtained from folk market and three from commercial suppliers were evaluated to corroborate the applicability of the models developed.

Results − The LC-PDA analysis of oxindole alkaloids was insufficient for differentiate genuine UT stem bark samples of those purposely spiked with UG stem bark. In opposition, the LC-PDA analysis of polyphenols and the UV analysis after

basification with KOH and complexation with $AlCl_3$ coupled to SIMCA and PLS multivariate models, allowed a conclusive differentiation between UT and UG, as well the recognition of UT stem bark samples mixed with UG. In that context, flavonoids appear to be key-compounds for the differentiation between UT and UG, as well as for adulteration recognition. Two tri-O-glycosylated flavonols derived from quercitin and kaempferol responsible by differentiation between UT and UG and, consequently, with adulteration recognition, were characterized from LC-PDA-QTOF analysis. In addition, two UT stem bark samples from Peruvian folk market were recognized as adulterated by the analytical approach here proposed.

Conclusion – The UV-based analysis of the cat's claw polyphenols seems to be the method of choice aiming an initial screening for the identification of genuine *U. tomentosa* samples. Furthermore, a more conclusive approach can be achieved by the LC-PDA analysis of polyphenols. In addition, alkaloid-based methods were not suffice neither for identification nor for recognition of adulteration in *U. tomentosa* stem bark with *U. guianensis* owing its natural variability and chemotypes.

Keywords: *Uncaria tomentosa*; *Uncaria guianensis*; cat's claw; stem bark; multivariate analysis; adulteration recognition.

INTRODUCTION

The genus *Uncaria* (Rubiaceae) includes about thirty four species spread worldwide, but only *Uncaria tomentosa* (Will.) DC. and *Uncaria guianensis* (Aubl.) Gmel. can be found in the Amazon rainforest (Heitzman et al., 2005; Keplinger et al., 1999; Pollito & Tomazello, 2006; Reinhard, 1999; Zhang et al., 2015). Both species are lianas known as cat's claw or "Uña de Gato" owing the presence curved hooked thorns (Keplinger et al., 1999; Pollito & Tomazello, 2006; Reinhard, 1999). Aqueous preparations from stem bark of both species have been used as anti-inflammatory, immunostimulant, antiviral and antitumor in folk medicine (Heitzman et al., 2005; Keplinger et al., 1999; Reinhard, 1999). Thus, the two South American *Uncaria* species are frequently confused (Keplinger et al., 1999). However, the safety and the pharmacological activities of *U. tomentosa* preparations were extensively explored when compared to *U. guianensis* preparations (Heitzman et al., 2005; Keplinger et al., 1999). Moreover, incipient differences in the chemical composition of both species have been reported. Higher levels of pentacyclic (POA) and tetracyclic oxindole alkaloids (TOA) can be found in stem bark of *U. tomentosa* when compared to *U. guianensis* (Sandoval et al., 2002), while the distribution of polyphenols (PPH), such as caffeoylquinic derivatives and flavonoids, as well as of mono- di- and tri-glycosylated quinovic acid glycosides (QAG) have been slightly evaluated.

The differentiation about both species can be easily performed by morphological characteristics of their thorns and leaves, as well from its wood and stem bark (Pollito & Tomazello, 2006; Silva et al., 1998; Lindorf, 2001). In contrast, the identification of derivatives obtained from both species, such as dried extracts, capsules and tablets containing powdered extract, is harder and limited to differences in their chemical composition, since show identical organoleptic properties. Currently, only the oxindole alkaloids (POA and TOA) have been used as chemical markers in quality control of raw material and derivatives from *U. tomentosa* (USP, 2016). Moreover, three-chemotypes were found in *U. tomentosa* wild population based on their oxindole alkaloid profile, namely, chemotype I (POA with *cis* D/E ring junction); chemotype II (POA with *trans* D/E ring junction); and chemotype III (TOA) (Peñaloza, et. al.,

2015). Thus, the *U. tomentosa* U.S. pharmacopeia monographs specifications based only in oxindole alkaloids might not be enough to adulteration detection with *U. guianensis*.

The adulteration of *U. tomentosa* with *U guianensis* can be related with misconceptions at collection, since both species have the same habitat and are obtained mostly from wild populations due to early status of cat's claw forest management (Peñaloza, et. al., 2015; Torrejón et al., 2010). In addition, the lower market value of the *U. guianensis* stem bark compared to *U. tomentosa* and its larger wild population (Pollito & Tomazello, 2006) also can contribute to adulteration occurrence.

Supervised multivariate analysis, such as *k*-nearest neighbors (*k*-NN) and soft independent modeling of class analogy (SIMCA) allow selecting variables responsible by differentiation even in complex systems, as plant derivatives. On the other hand, multivariate calibration methods, such as principal component regression (PCR) and partial least squares (PLS), allow the quantification of a specific response (compound level or spike level) from a multivariate system (Brereton; 2003; Gad et. al., 2013a). For building supervised and multivariate calibration models are necessary previous knowledge about sample classification or response level, respectively.

The present study aims to determine chemical composition criteria that enable the differentiation between stem bark from both cat's claw species (*U. tomentosa* and *U. guianensis*) by multivariate analysis, as well as, to establish quality control parameters applied to adulteration recognition of *U. tomentosa* with *U. guianensis* in the raw material and its pharmaceutical derivatives.

EXPERIMENTAL

Reagents and standards

Acetonitrile (Tedia, USA), methanol (Tedia, USA), ammonium acetate (Tedia, USA), formic acid (FA)(Tedia, USA), Trifluoroacetic acid (TFA) (Sigma, USA) NH_4OH (Merck, Germany), KOH (Merck, Germany), $AlCl_3$ (Merck, Germany) and ultra-pure

water from Milli-Q® system (Millipore, USA) were used for LC and spectrophotometric analyses. Mitraphylline (Phytolab, batch 2946, Germany), chlorogenic acid (Fluka, batch 455159/1, Switzerland), caffeic acid (Extrasynthèse, batch 0381024, France), rutin (Sigma, batch 128K1177, USA) were used as external standards. The leucine-enkephalin (Waters, batch W24021502, USA) used as lock mass in the LC-PDA-QTOF analysis. All other reagents used were of analytical grade.

Plant material

Six genuine *U. tomentosa* stem bark samples (UT_1-UT_6) and two *U. guianensis* stem bark samples (UG_1-UG_2) collected in Peruvian Amazon (November 2012) were certified by J.R. Campos De la Cruz (Museo de Historia Natural de la Universidad Nacional Mayor de San Marcos, Lima, Peru). The *U. tomentosa* samples were purposely selected to cover the three chemotypes recognized in this specie (Peñaloza, et al., 2015), namely, POA with *trans* D/E ring junction (UT_1 and UT_2), TOA (UT_3 and UT_4) and POA with *cis* D/E ring junction (UT_5 and UT_6) (**Table 1**). The vouchers of specimens (ICN157757- ICN157762) were deposited at Herbarium of Universidade Federal do Rio Grande do Sul (Porto Alegre, Brazil). All samples were comminuted in a cutter mill (SK1 Retsch, Germany) after dried in air-circulating convection oven (Memmert, Germany) at 40 ºC. For analysis of simulated adulteration, three genuine *U. tomentosa samples* (UT_1, UT_3 and UT_6) were spiked with UG_1 and UG_2 in three levels (10%, 30% and 50%, w/w) totalizing eighteen samples (**Table 1**).

Table 1

Extraction procedure

Powdered samples (106–250 µm particle size range selected) were extracted by 2-h dynamic maceration under magnetic stirring at 300 rpm (IKA RH basic 1, Germany), using ethanol:water 61:39 (v/v) as solvent, and a plant:solvent ratio of 0.5:10 (w/v) (Kaiser, et al. 2013a). The resulting extractive solutions were filtered (Paper filter Whatman nº 2, UK) and reconstituted to their original value with the same solvent.

FT-IR analysis

Separately, 10-mL aliquots were concentrated under vacuum at 40 °C up to half of their original weights (Büchi R-114, Switzerland) and freeze-dried at once (Modulyo 4L, Edwards, USA). The freeze dried samples were analyzed at FT-IR Spectrometer (Spectrum BX, Perkin Elmer, Germany) using the diamond ATR sensor and the absorbance were measured in the range 400 − 4400 cm^{-1} with a resolution of 4 cm^{-1}. Twenty scan were performed for each sample.

UV analysis

Separately, aliquots of 40μL from extractive solutions were properly diluted with 2 mL of ethanol:water 61:39 (v/v) solution and evaluated in UV-VIS spectrophotometer (Hewlett-Packard, USA) in the 200-500 nm range at once (I), after addition of 40 μL KOH 1M solution (II) and 20-min after addition of 40 μL $AlCl_3$ solution (5% in methanol; w/v) (III). Blanks solution were prepared with 40 μL ethanol:water solution 61:39 (v/v), instead of samples aliquots.

LC-PDA analysis

All analyses were performed in a Prominence high performance liquid chromatography (HPLC) system (Shimadzu, Japan) composed by an FCV-10 AL system controller, an LC-20 AT pump system, an SIL-20 A automatic injector and an SPD-M20A detector. The extractive solutions were properly diluted and filtered through a 0.45 μm membrane (Millipore, USA) prior the analysis of oxindole alkaloids (TOA and POA) (Kaiser et al., 2013b), quinovic acid glycosides (QAG) (Pavei et al., 2012) and polyphenols (PPH) (Pavei et al., 2010) in accordance with previously validated methods (Supporting information, **Table S1**). All results were processed by LC-Solution Multi-PDA software (Shimadzu, Japan).

LC-PDA-QTOF analysis

All analyses were performed in an Acquity ultra performance liquid chromatography (UPLC™) system (Waters, USA) coupled to an Acquity PDA detector and a QTOF analyzer (SYNAPT G2 Si, Waters, USA). The UPLC analysis parameters were adjusted from HPLC analysis of polyphenols by using of Acquity UPLC Columns calculator software (Waters, USA). An Acquity BEH C18 column (10 x 2.1 mm i.d., 1.7 μm) (Waters, USA) was used as stationary phase. Formic acid solution 0.1% (v/v) (A) and acetonitrile:formic acid (99.9:0.1, v/v) (B) were used as mobile phase in a linear gradient program: 30-40% B (0-2.5 min); 40-60% B (2.5-4.5 min); 60% B (4.5-5.5 min); 60-30% B (5.5-7.0 min); and stop (8.0 min). The flow rate was kept constant at 0.35 mL/min and analyses were performed at constant temperature (50 ± 1°C) using an injection volume of 30 nL. The analysis was performed in both ESI^- and ESI^+ modes with TOF operating in resolution mode (R = 20,000). All MS experiments were performed in MS^E continuum mode. The source conditions used were: 2 kV of capillarity; 120°C and 500°C of source and desolvation temperatures, respectively; 30 V and 80 V for sampling cone and source offset, respectively; 50 L/h and 1,000 L/h of cone and desolvation gases flow, respectively; and 6.5 bar of nebulizer gas flow. The nitrogen was employed as desolvation gas, cone gas and nebulizer gas while the argon was employed as collision gas at transfer collision cell (20 – 40 eV). A wide mass range (50-1000 *m/z*) was monitored with a scan time of 0.3 s and interscan delay of 0.015 s. The leucine-enkephalin solution (1μg/mL) (554.2615 *m/z* in ESI^-; 556.2771 in ESI^+) was employed as lock mass solution. All results were processed by Mass Lynx 4.1 and MS^E data viewer softwares (Waters, USA).

Separately, 2 mg-aliquots of freeze dried extracts from UT_3 and UT_3 + UG_1_50 were properly dissolved to obtain solution of 5μg/mL in water:acetonitrile (70:30, v/v) and filtered through a 0.22 μm membrane (PVDF, Millipore, USA) prior to analysis.

Multivariate analysis

The chromatograms obtained from LC analyses were aligned by the correlation optimized warping (COW) algorithm (Pravdova et al., 2002) before the proposed model fitting. The Kennard–Stone algorithm (Kennard; Stone, 1969) was employed for selection of calibration set (n=18) and prediction set (n=8) (**Table 1**). Different transforms and preprocessing methods were employed to obtain a better fitting to proposed model. All analyses were performed at Pirouette 3.11 (Woodinville, WA, USA).

For the discrimination analysis, soft independent modeling class analogy (SIMCA) and *k*-nearest neighbors (*k*-NN) models were employed (Brereton; 2003; Gad et. al., 2013a). The sensitivity or true positive rate (**1**) (percentage of spiked samples that were indicated by model as spiked) and specificity or true negative rate (**2**) (percentage of authentic samples that were indicated by model as authentic) were evaluated for proposed models.

$$sensitivity(\%) = \frac{a}{b} \times 100 \qquad (\mathbf{1})$$

$$specificity(\%) = \frac{c}{d} \times 100 \qquad (\mathbf{2})$$

where *a* represents the number of spiked *U. tomentosa* stem bark samples classified as spiked by the model, and *b* the total number of spiked samples; *c* represents the number of authentic *U. tomentosa* stem bark samples classified as authentic by the model, and *d* the total number of genuine samples.

For multivariate calibration, principal component regression (PCR) and Partial least squares (PLS) models were employed (Brereton; 2003; Gad et. al., 2013a). The leave-one-out method was used for cross validation. The root mean square error of calibration (RMSEC) and cross validation (RMSECV) and prediction (RMSEP) were the parameters considered in the fitting of the proposed models. The number of principal components or latent variables was determined from lowest RMSECV value for each proposed model.

Evaluation of market samples

Ten cat's claw samples obtained from Peruvian folk market and three cat's claw samples available from commercial suppliers were evaluated (I-XIII) (Supporting information, **Table S2**). Additionally, nine UT samples spiked with *U. guianensis* (A-I) (which were not present in the calibration and prediction sets used in building of models) were analyzed for validation of the multivariate models. The root mean square error of validation (RMSEV) was used for evaluation of the predictive capacity of the models. All samples were prepared as described above in the *Extraction procedu*re.

RESULTS AND DISCUSSION

U.S. pharmacopeia specifications for *U. tomentosa* stem bark quality control

The current U.S. pharmacopeia monographs specifications for quality control of UT stem bark raw material, as well as for their derivatives, such as powdered dried extract, capsules and tables has been based mainly on their oxindole alkaloids content (USP, 2016). In accordance with U.S. pharmacopeia requirements, the POA content obtained by sum of individual concentration of speciophylline, uncarine F, mitraphylline, isomitraphylline, pteropodine, isopteropodine must be higher than 0.3% (w/w) of dried raw material, while the TOA content, obtained by sum of rhyncophylline and isorhyncophylline, must be lower than 0.05% (w/w). Moreover, for the powdered dried extracts, capsules and tablets, the TOA content must be lower than 25% of the labeled amount of POA ones (USP, 2016).

Clearly, the differentiation between authentic UG and UT stem bark samples could be verified, mainly due to higher content of oxindole alkaloid found in UT stem bark (about 20 times higher in some cases) in comparison with that found in UG (**Figure 1**). Despite the clear decrease of the POA and TOA contents verified after intentional spiking of UT samples with UG, both maximal POA and minimal TOA content were achieved in accordance with U.S. pharmacopeia requirements, especially those having high POA contents, as UT_1 and UT_2 samples. The sample UT_3 showed TOA content

higher than threshold (0.05%, w/w) even before intentional adulteration, while the UT_6 was reproved only after addition of 50% (w/w) of spiking amount with UG (**Figure 1**). Thus, the U.S. pharmacopoeia requirements were inadequate for adulteration recognition in UT stem bark samples.

Figure 1

Evaluation multivariate models

The multivariate analysis is an important tool for adulteration recognition in herbal medicines (Brereton; 2003; Gad et. al., 2013a). Thus, in this occasion were evaluated seven classification models (**Table 2**) and seven calibration models (**Table 3**) from data of FT-IR, UV and LC-PDA analyses aiming at challenging the capability for adulteration recognition and quantification of spiking level in the UT stem bark purposely adulterated with UG stem bark.

The classification and calibration models proposed showed suitable predictive capacity, without indicative of overfitting, as verified from the sensitivity and sensibility levels for the calibration and prediction samples sets in the classification models (**Table 2**), root mean square errors of calibration (RMSEC), cross-validation (RMSECV), and prediction (RMSEP) in the calibration models (**Table 3**), except for the model based on LC-PDA analysis of oxindole alkaloids. The SIMCA models showed higher capacity for adulteration recognition, compared to *k*-NN models (**Table 2**), while the PLS models showed higher capacity for quantification of spiking levels compared to PCR models (**Table 3**). Both classification and calibration models obtained from UV data (UV spectrum, UV+KOH spectrum and UV+AlCl3 spectrum) and LC-PDA analysis of polyphenols showed superior performance for the recognition and quantification of the simulated adulteration in the UT stem bark samples.

Table 2

Table 3

FT-IR analysis

The FT-IR analysis provides a semi-quantitative profile about the chemical constitution of samples. Although it shows a limited application for quantitative analysis of complex samples, FT-IR technique supports the direct analysis of samples in solid state such as powdered extracts or tablets containing them without prior sample preparation. Consequently, the association of FT-IR and multivariate analysis has been used for the analysis of complex samples, including plant raw material and powdered dried extracts (Bunaciu et al., 2011; Gad et al., 2013a).

From FT-IR spectra of both UT and UG samples (Supporting information, **Figure S1A**), no clear differentiation region could be observed and, therefore, any consistent criteria for the recognition of the simulated adulteration of UT with UG could be determined. Consequently, aiming the improvement in the discrimination and quantification capacity of the models, the fingerprint region of FT-IR spectra (1600–730 cm^{-1}) was used. Nevertheless, no practical advantage was verified, as revealed by the poor specificity of the SIMCA model (**Table 2,** Supporting information, **Figure S1B**) and high RMSCV and RMSEP values (higher than 10%) from the PLS model (**Table 3**). In general, the high discrimination power from SIMCA model was associated to absorptions bands (1100–1020 cm^{-1}; 840–790 cm^{-1}) (Supporting information, **Figure S1C**) corresponding to C−O stretching vibration from alcohols and aromatic C−H out of plane bending, respectively (Silverstein et. al., 2005). However, the high chemical complexity of stem bark extracts hindered a definitive identification of the class of compounds responsible by differentiation between both species as well the unambiguous recognition of adulteration in UT stem bark samples spiked with UG.

UV analysis

The analysis by UV spectroscopy has been extensively employed for quantification mainly due to its low cost, practicality and robustness. Although UV analysis shows low specificity, its association with multivariate analysis had increased aiming the

analysis of complex matrix such as plant extracts (Gad et. al., 2013a; Gad et. al., 2013b).

From UV spectra, a clear differentiation could be verified among authentic UT samples alone and those spiked samples with UG. The absorption peak at 344 nm noticed in UG samples was almost absent in UT authentic samples (**Figure 2A**). Moreover, the high sensitivity and specificity obtained from SIMCA model indicated that the UV analysis and the proposed model were able to discriminate both species straightforward (**Table 2**, **Figure 2B**). The highest discriminative power observed in the classification model was ascribed to the absorption peak at 344 nm (**Figure 2C**), which seems to be a clear indicative of adulteration of UT stem bark samples using UG.

Figure 2

Furthermore, the spiking level using UG could be determined with suitable accuracy by all proposed calibration models (**Table 3**). The regression errors (RMSEC, RMSECV and RMSEP) obtained from both PLS and PCR models were lower than 2.5 % (w/w), demonstrating therefore a suitable correlation among predicted spiked amounts and experimental spiked amounts (r_C, r_{CV} and $r_P > 0.99$) (**Table 3**). More specifically, the intensity of absorption peak at 344 nm could be related to spiked amount in UT samples, as indicated by higher regression vector in PLS model (**Figure 2D**). Thus, the presence of a significant absorption peak at 344 nm is a strong indicative of adulteration in UT stem bark samples such as earlier verified by SIMCA model, and its intensity could be related to UG spiking level.

The UV analysis performed with addition of chemical reagents also allowed further analytical possibilities. Thus, a significant bathochromic shift could be verified in the UV spectrum of the UG samples after medium basification (Supporting information**,** **Figure S2A**). The characteristic absorption peak noticed in the spiked samples was shifted to 398 nm. This behavior is characteristic of acid compounds with π conjugated systems such as cinnamoyl system present in polyphenols, more specifically

flavonoids (De Rijke et. al., 2006; Mabry et. al., 1970). After medium basification, both classification (SIMCA model, Supporting information**, Figure S2B**) and calibration models (PLS and PCR models) were able to recognize the simulated adulteration in UT stem bark samples and also to quantify the spiked amount (**Tables 2** and **3**). According to SIMCA and PLS models, the absorption peak at 398 nm showed highest discriminative power (Supporting information, **Figure S2C**) and regression vector (Supporting information, **Figure S2D**), respectively. It appears, therefore, as a reliable indicative to recognize the adulteration in UT stem bark samples with UG.

The addition of $AlCl_3$ produced a characteristic bathochromic shift in the UV spectra of UG samples and UT samples spiked with UG, revealing two absorption peaks at 360 nm and 402 nm (Supporting information, **Figure S3**). These spectra remained stable after medium acidification (Data not shown), a behavior often noticed in 3-hydroxyflavones, 5-hydroxyflavones and 3,5-hydroxyflavones (De Rijke et. al., 2006; Mabry et. al., 1970). In contrast to that verified with UV data without addition of reagents, the SIMCA model showed low specificity (50%) in the prediction set after the complexation with $AlCl_3$ (**Table 2**), indicative of the false positive occurrence. Nevertheless, both PLS and PCR models were able to determine the spiked amount of UG in UT stem bark samples after addition of $AlCl_3$ (**Table 3**).

LC-PDA analysis

The LC-PDA analysis has been extensively employed for the quality control of medicinal plants due to its specificity, a very critical point for analysis of complex matrix, such as plant derivatives (Gad et. al., 2013a). At present, the quality control of UT stem bark samples is based in the LC-PDA analysis of oxindole alkaloids (USP, 2016). However, as earlier demonstrated (**Figure 1**), the simulated adulteration was not recognized by the oxindole alkaloids analysis. Essentially, oxindole alkaloids content did not present any relation with the spiking level in UT stem bark samples, as verified from values of RMSEC, RMSECV and RMSEP (higher than 20%) and

regression coefficients (r_C, r_{CV} and r_P) (**Table 3**). The negative regression vectors in the PLS model indicate that decrease in the oxindole alkaloids content with the increase in the spiked level occurred due to lower oxindole alkaloid content present in the UG (Supporting information, **Figure S4D**). Moreover, the low sensitivity (33%) and specificity (50%) in the prediction set obtained from SIMCA model evidence the occurrence of false negatives and false positives, respectively (**Table 2**). On the other hand, the classification and calibration models obtained from the quinovic acid glycosides analysis by LC-PDA showed superior performance compared to models obtained from oxindole alkaloids. The higher discriminating power and regression vectors (Supporting information, **Figure S5C** and **Figure S5D**) could be related to peak Q7, a monoglycosylated derivative (Pavei et al., 2012). However, the low specificity (50%) verified from SIMCA model (**Table 2**) is a consistent indicative of false positive occurrence.

As earlier verified from UV analysis, the polyphenols composition seems to be closely related with the adulteration recognition in UT stem bark samples. The SIMCA model obtained from LC-PDA analysis of polyphenols (**Table 2**), showed high sensitivity (100%) and specificity (100%), while from calibration model (PLS) the low values of RMSEC, RMSECV and RMSEP (lower than 2.1%) and high regression coefficients (r_C, r_{CV} and $r_P > 0.99$) (**Table 3**) suggest that the polyphenols composition is related with the spiking level in UT stem bark. The peak P4, previously characterized as flavonoid from its UV spectrum (Pavei at al., 2010), showed the highest discriminative power (**Figure 3C**) and regression vector (**Figure 3D**) observed in SIMCA and PLS models, respectively. Therefore, the presence of peak P4 in significant amounts seems to be an important indicative of adulteration in UT stem bark samples.

Figure 3

The UV spectra of the extractive solutions obtained from UG stem bark are very similar than spectrum associated to peak P4 obtained from LC-PDA analysis of polyphenols (Supporting information, **Figure S6**). More specific, the absorption peak

at 344 nm in UG stem bark samples and the absorption peak at 347 nm in the UV spectrum of peak P4 seem related with electrons transition in π conjugated of the cinnamoyl system (Mabry et. al., 1970). This finding reinforces the potential use of the UV spectrum for initial screening aiming the differentiation between UT and UG stem bark, as well as for adulteration recognition in UT stem bark.

LC-PDA-QTOF analysis

In order to characterize the main compounds responsible by adulteration recognition in UT stem bark, LC-QTOF analyses were performed (Supporting information, **Figure S7**). The major peaks verified between 2.0 min and 4.0 min in the ESI^+ chromatograms (Supporting information, **Figure S7A** and **Figure S7C**) showed *m*/*z* at 369.1814 $[M+H]^+$ or 385.2127 $[M+H]^+$, characteristic of POA and TOA, respectively. In the ESI^- chromatograms the same peaks could not be verified, since the oxindole alkaloids due to their alkalinity don't ionize in the negative mode (Supporting information, **Figure S7B** and **Figure S7D**). Moreover, all peaks showed λ_{max} at 245 nm very similar to λ_{max} of oxindole alkaloids (Kaiser et al., 2013b). However, no clear relation between oxindole alkaloid profile and the adulteration recognition was established, such as previously showed from multivariate analysis.

On the other hand, from ESI^- chromatograms two minor peaks at 1.56 min and 1.96 min showed higher content in the UT sample spiked with 50% of UG (Supporting information, **Figure S7B**), compared to authentic UT sample (Supporting information, **Figure S7D**). Thus, seem to be related to adulteration recognition in the UT samples. Moreover, both peaks showed UV spectra similar to Peak 4 (Supporting information, **Figure S6B**), with two λ_{max} about 265 nm and 350 nm, characteristic of flavonoids. From their fragmentation pattern, both peak at 1.56 min and 1.96 min were characterized as tri-O-glycosylated flavonols derived from quercitin and kaempferol, respectively (**Table 4**). The aglycones were suitably characterized as flavonols by presence of fragments $^{1,3}A^+$, $^{1,3}A^-$ for peak at 1.56 min and fragments $^{0,2}A^+$, $^{1,3}A^+$ and $^{0,2}B^+$ for peak at 1.96 min, common for this flavonoid class (De Rijke et al., 2006;

Ma et al., 1997) . These fragments, mainly the $^{1,3}A^{+}$, $^{1,3}A^{-}$, were generated by retro-Diels-Alder reactions (De Rijke et al., 2006; Ma et al., 1997). In addition, the fragments with *m*/*z* at 303.0487 $[M+H-162-146-146]^{+}$ and *m*/*z* at 300.0277 $[M-2H-162-146-146]^{-}$ indicated that peak at 1.56 min is a tri-O-glycosylated quercitin derivative with the glycosidic chain formed by hexose−6-deoxy-hexose−6-deoxy-hexose. On the other hand, the fragments with *m*/*z* at 287.0541 $[M+H-162-146-146]^{+}$ and *m*/*z* at 284.0316 $[M-2H-162-146-146]^{-}$ indicated that peak at 1.96 min is a tri-O-glycosylated kaempferol derivative with the glycosidic chain formed by hexose−6-deoxy-hexose−6-deoxy-hexose. Therefore, these results reinforce that the higher content of flavonoids in *U. guianensis* compared to *U. tomentosa* stem bark seems to be related with differentiation between both cat's claw species and, consequently, with adulteration detection in authentic *U. tomentosa* stem bark samples.

The kaempferitrin, a di-O-glycosylated flavonol found only in UG leaves and absent in UT leaves was proposed as chemical marker for differentiation of both species, despite its content in UG stem bark was thirty six times lower than that found in leaves (Valente et al., 2009). Consequently, the differentiation between the stem bark of UT and UG by kaempferitrin seems to be doubtful at least. The rutin also was proposed as a chemical marker for differentiation between stem bark of UT and UG from TLC analysis (Van Ginkel, 1997). Moreover, the presence of rutin by TLC analysis in UT stem bark samples was considered an adulteration indicative (Van Ginkel, 1997). However, our results demonstrated that rutin level in the UT stem bark samples was weakly correlated with the spiking level. Thus, the rutin could not be considered a reliable chemical marker for adulteration recognition in UT stem bark samples.

Table 4

Evaluation of market samples

The UT stem bark has been used in Asháninka medicine for over two thousand years (Keplinger et al., 1999). Hence, the use of UT preparations in Peru mainly in the folk medicine is very common. Aiming to evaluate the adulteration in the UT stem bark

samples commercialized, ten samples obtained from Peruvian folk market and three obtained from commercial suppliers were evaluated (I-XIII). In addition, nine UT stem bark samples spiked with UG (*A-I*) were evaluated for validation of SIMCA and PLS models established from UV data, used in the initial screening of unknown samples.

From UV initial screening, only six intentional spiked samples (*D-I*) and one sample obtained from folk market (IX) were classified as adulterated from SIMCA model (**Table 5** and **Figure 4**). The samples A, B, C and XI that could not classified by SIMCA model probably due to its conservative feature, but other unknown samples were classified as authentic UT stem bark samples. Complementarily, the predicted spiking amounts obtained from PLS model established from UV data showed suitable agreement to experimental spiking amounts (RMSEV = 6.12%; r_V = 0.99) for all intentional spiked samples (*A-I*) (**Table 5**). Except for samples IX and XI that showed predicted spiking amount of 47% and 91% (w/w) indicative of adulteration practice, all other samples obtained from Peruvian local market showed predicted spiking amounts lower than RMSEV, characteristic of authentic UT samples. In addition, the high intensity of absorption peak at 344 nm in the UV spectrum (**Figure 4**) associated to higher content of peak P4 obtained from LC-PDA analysis of polyphenols allowed the adulteration recognition in both IX and XI samples (**Table 5**). Coincidentally, both samples did not meet the U.S. pharmacopeia requirements due to their low POA content. Nevertheless, three UT authentic samples (*B*, *D* and *E*) intentionally spiked with UG also fulfilled these U.S. pharmacopeia requirements demonstrating clearly its deficiency in relation to adulteration recognition.

Figure 4

Table 5

CONCLUSIONS

From U.S. pharmacopeia requirements employed in quality control of *U. tomentosa* stem bark raw material based on its oxindole alkaloids profile was not possible to

recognize the simulated adulteration with *U. guianensis*. Among the alternative multivariate methods employed to recognize the simulated adulteration in *U. tomentosa* stem bark with *U. guianensis*, the UV analysis seems to be the method of choice for an initial screening of sample, followed by analysis of polyphenols by LC-PDA. The levels of absorption peak at 344 nm in the UV spectrum and peak P4 in the LC-PDA analysis could be correlated with the spiking level in the *U. tomentosa* stem bark samples. The differential distribution of flavonoids, present in higher levels in *U. guianensis* in comparison with *U. tomentosa* stem bark, were the compounds responsible by differentiation between both cat's claw species. In addition, the analysis of cat's claw market samples revealed that adulteration occurred in two samples of eleven samples of *U. tomentosa* stem bark evaluated. It reinforces the need of alternative methods able to recognize the adulteration in *U. tomentosa* stem bark by using of *U. guianensis* stem bark in raw material and its pharmaceutical derivatives.

ACKNOWLEDGMENTS

The authors are grateful to Brazilian Conselho Nacional de Desenvolvimento Científico e Tecnológico (CNPq) and Coordenação de Aperfeiçoamento de Pessoal de Nível Superior (CAPES) for financial support to conduct this study.

SUPPORTING INFORMATION

Supporting information can be found in the online version.

REFERENCES

Brereton RG. 2003. *Chemometrics: Data analysis for the laboratory systems and chemical plants* (1st Edn.). John Wiley & Sons Ltda: Chichester.

Bunaciu AA, Aboul-Enein HY, Fleschin S. 2011. Recent Applications of Fourier Transform Infrared Spectrophotometry in Herbal Medicine Analysis. *Applied Spectroscopy Reviews* **46:** 251-260.

De Rijke E, Out P, Niessen WMA, Ariese F, Gooijer C, Brinkman UAT. 2006. Analytical separation and detection methods for flavonoids. *J Chromatogr A* **1112:**31–63.

Gad HA, El-Ahmady SH, Abou-Shoer MI, Al-Azizi MM. 2013a. Application of chemometrics in authentication of herbal medicines: a review. *Phytochemical Anal* **24:** 1–24.

Gad HA, El-Ahmady SH, Abou-Shoer MI, Al-Azizia MM. 2013b. A Modern Approach to the Authentication and Quality Assessment of Thyme Using UV Spectroscopy and Chemometric Analysis. *Phytochem Anal* **24:** 520–526.

Heitzman ME, Neto CC, Winiarz E, Vaisberg AJ, Hammond GB. 2005. Ethnobotany, phytochemistry and pharmacology of *Uncaria* (Rubiaceae). *Phytochemistry* **66:** 5–29.

Kaiser S, Verza SG, Moraes RC, De Resende PE, Barreto F, Pavei C, Ortega GG. 2013b. Cat's claw oxindole alkaloid isomerization induced by common extraction methods. *Quim Nova* **36:** 808–814.

Kaiser S, Verza SG, Moraes RC, Pittol V, Peñaloza EMC, Pavei C, Ortega GG. 2013a. Extraction optimization of polyphenols, oxindole alkaloids and quinovic acid glycosides from cat's claw bark by Box–Behnken design. *Ind Crop Prod* **48:** 153–161.

Kennard RW, Stone LA. 1969. Computer Aided Design of Experiments. *Technometrics* **11:** 137–148.

Keplinger K, Laus G, Wurm M, Dierich MP, Teppner H. 1999. *Uncaria tomentosa* (Wild). Ethnomedicinal uses and new pharmacological, toxicological and botanical results. *J Ethnopharmacol* **64:** 23–34.

Lindorf H. 2001. *Reconocimiento al microscopia de la corteza y el polvo farmaceutico de la "uña de gato": 1ª Reunión Internacional del Género Uncaria "uña de gato"* . Pontificia Universidad Católica del Perú: Iquitos, Perú.

MaY-L, Li QM, van den Heuvel H, Claeys M. 1997. Characterization of flavone and flavonol aglycones by collision-induced dissociation tandem mass spectrometry. *Rapid Commun Mass Spectrom* **11**: 1357–1364

Mabry TJ, Markham KR, Thomas MB. 1970. *The Systematic Identification of Flavonoids* (1st Edn.). Springer-Verlag: New York.

Pavei C, Kaiser S, Borré GL, Ortega GG. 2010. Validation of a LC method for polyphenols assay in cat's claw (*Uncaria tomentosa*). *J Liq Chromatogr Relat Technol* **33:** 1–11.

Pavei C, Kaiser S, Verza SG, Borré GL, Ortega GG. 2012. HPLC-PDA method for quinovic acid glycosides assay in Cat's claw (*Uncaria tomentosa*) associated with UPLC/Q-TOF–MS analysis. *J Pharm Biomed Anal* **62:** 250–257.

Peñaloza EMC, Kaiser S, Resende PE, Pittol V, Carvalho AR, Ortega GG. 2015 Chemical composition variability in the *Uncaria tomentosa* (cat's claw) wild population. *Quim Nova* **38:** 378-386.

Pollito PAZ, Tomazello M. 2006. Anatomia do lenho de *Uncaria guianensis* e *U. tomentosa* (Rubiaceae) do estado do Acre, Brasil. *Acta Amazônica* **36:** 1–21.

Pravdova V, Walczak B, Massart DLA. 2002. Comparison of two algorithms for warping of analytical signals. *Anal Chim Acta* **456:** 77–92.

Reinhard KH. 1999. *Uncaria tomentosa* (Willd.) D.C.: Cat's claw, Uña de Gato, or Saventaro. *The Journal of Alternative Complementary Medicine* **5:** 143–151.

Sandoval M, Okuhama NN, Zhang X-J, Condezo LA, Lao J, Angeles FM, Musah RA, Bobrowski P, Miller MJS. 2002. Anti-inflammatory and antioxidant activities of cat's claw (*Uncaria tomentosa* and *Uncaria guianensis*) are independent of their alkaloid content. *Phytomedicine* **9:** 325–337.

Silva DH, Alvarado DR, Hidalgo HJ, Cerrutti ST, Garcia RJ, Dávila MW, Mestanza DM, Rios IF, Nina CE, Nonato LR. 1998. *Monografia de Uncaria tomentosa (Willd.) DC*. Instituto Peruano de Seguridad Social-Instituto de Medicina Tradicional: Iquitos.

Silverstein RM, Webster FX, Kielme DJ. 2005. *Spectrometric identification of organic compounds* (7th Edn.). John Wiley & Sons Ltda: Chichester.

Torrejón GD, Martín JJG, Loayza DG, Alanoca R. 2010. Contenido de alcaloides en corteza de *U. tomentosa* (Wild.) DC procedentes de diferentes hábitats de la región Ucayali-Perú. *Rev Soc Quim Peru* **76:** 271–278.

USP. 2016. *United States Pharmacopeia* (39th Edn.). U.S. Pharmacopeia: Rockville.

Valente LMM, Bizarri CHB, Liechocki S, Barboza RS, Paixão D, Almeida MBS, Benevides PJC, Magalhães A, Siani AC. 2009. Kaempferitrin from *Uncaria guianensis* (Rubiaceae) and its Potential as a Chemical Marker for the Species. *J Braz Chem Soc* **20:** 1041-1045.

Van Ginkel A. 1997. Identificação of the alkaloids and flavonoids from *Uncaria tomentosa* bark by TLC in quality control. *Phytother Res* **10:** 9–18.

Zhang Q, Zhao JJ, Xu J, Feng F, Qu W. 2015. Medicinal uses, phytochemistry and pharmacology of the genus *Uncaria*. *J Ethnopharmacol* **173:** 48–80.

FIGURES

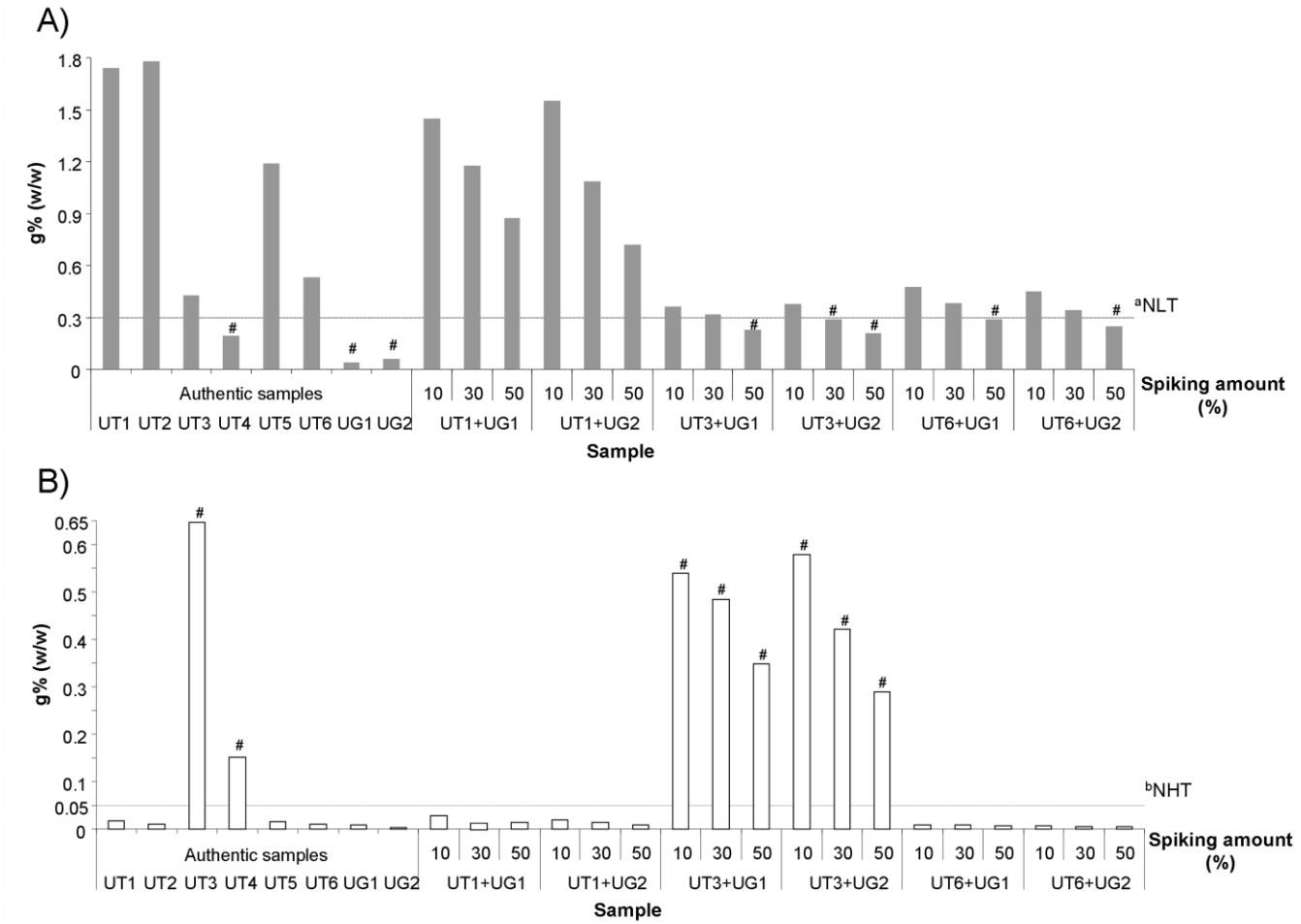

Figure 1. Total content of pentacyclic (POA) (**A**) and tetracyclic oxindole alkaloids (TOA) (**B**) in *U. tomentosa* stem bark samples (UT1-UT6), *U. guianensis* stem bark samples (UG1 and UG2) and intentionally spiked *U. tomentosa* samples with *U. guianensis* stem bark in three levels (10; 30; 50%, w/w). [a]minimum POA content (NLT: not lower than 0.3 %, w/w) in accordance with U.S. pharmacopeia requirements; [b]maximum TOA content (NHT: not higher than 0.05%, w/w) in accordance with U.S. pharmacopeia requirements. *POA content*: obtained from sum of speciophylline, uncarine F, mitraphylline, isomitraphylline, pteropodine, and isopteropodine contents expressed as mitraphylline; *TOA content*: obtained from sum of rhyncophylline and isorhyncophylline contents expressed as mitraphylline; [#]samples reproved in accordance with U.S. pharmacopeia monograph specifications.

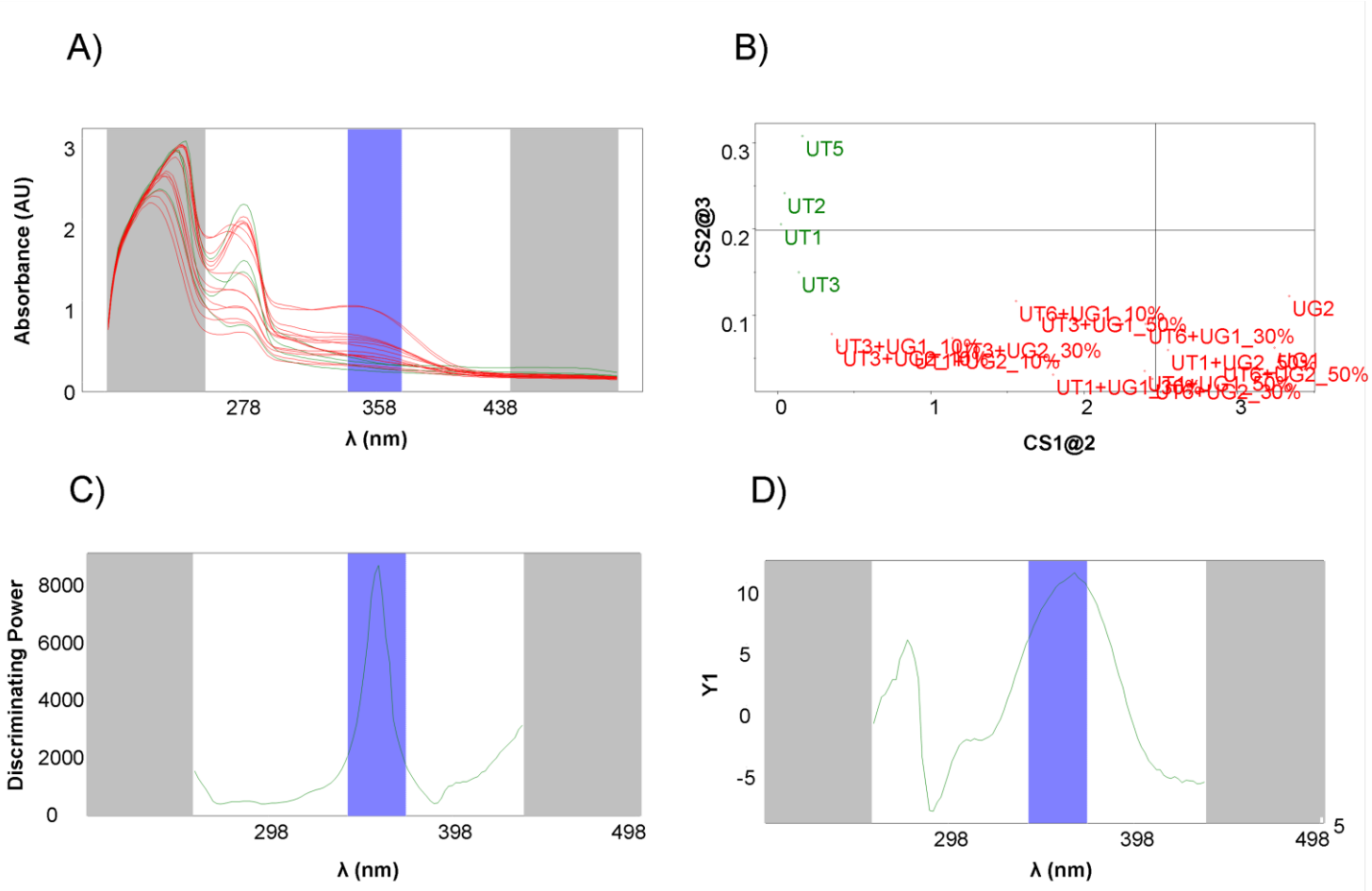

Figure 2. Overlaid of UV spectra (200–500 nm) obtained from analyses of extractive solutions (**A**); *In green*, authentic *U. tomentosa* stem bark samples; *In red*, *U. tomentosa* stem bark samples intentionally spiked with *U. guianensis* stem bark; *White region*: selected region from UV spectra (260–440 nm); *Blue region*: main differentiation peak (320–380 nm) from UV spectra between spiked samples and authentic samples. Class distance plot obtained from classification SIMCA model (**B**); Discriminating power obtained from classification SIMCA model (**C**); Regression vector obtained from calibration PLS model (**D**).

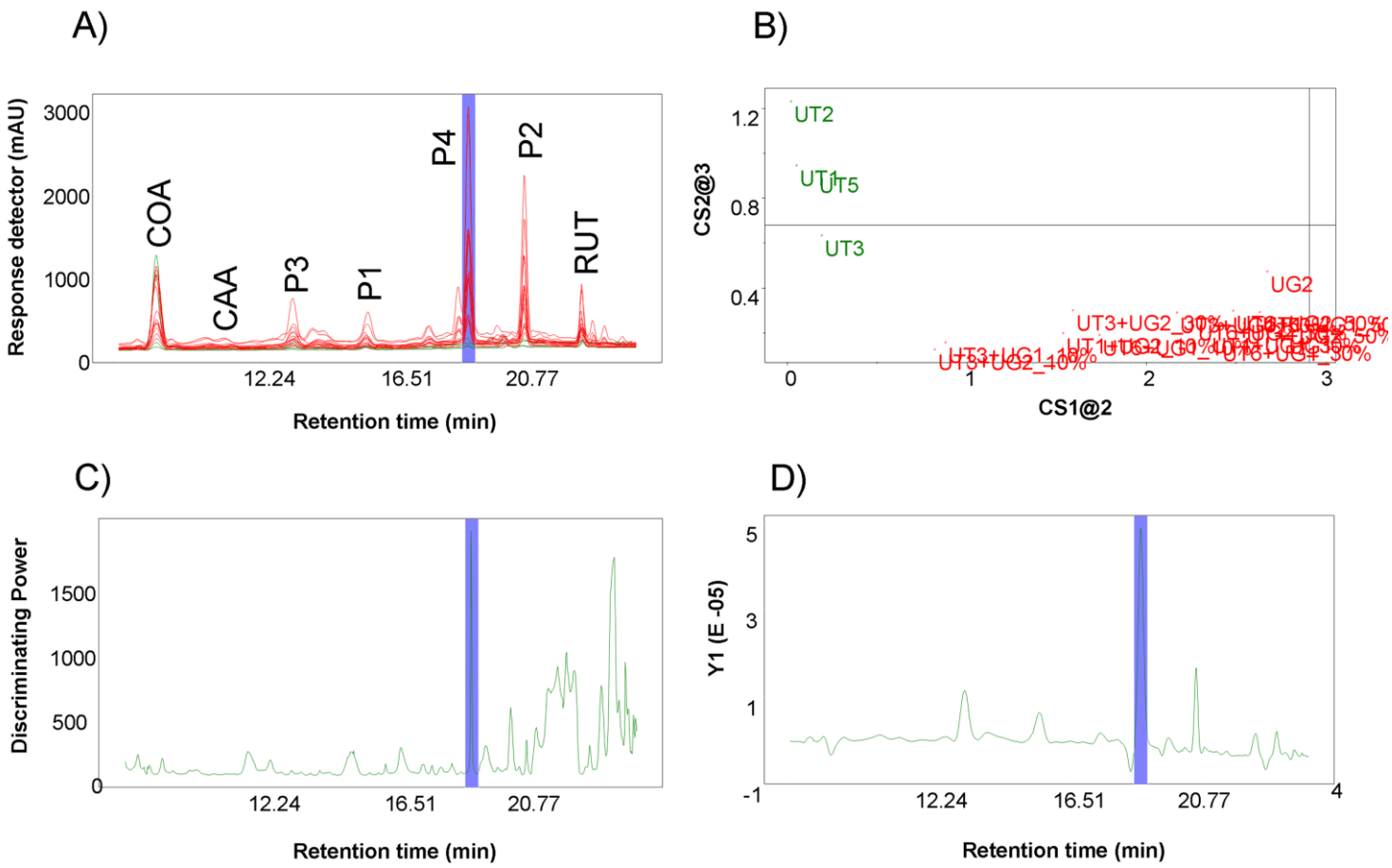

Figure 3. Overlaid of LC-PDA profiles (325 nm) from polyphenols analyses of extractive solutions (**A**); *In green*, authentic *U. tomentosa* stem bark samples; *In red*, *U. tomentosa* stem bark samples intentionally spiked with *U. guianensis* stem bark; *Blue region*: main differentiation peak (peak 4) from LC-UV profiles between spiked samples and authentic samples. Class distance plot obtained from classification SIMCA model (**B**); Discriminating power from classification SIMCA model (**C**); Regression vector obtained from calibration PLS model (**D**). Chlorogenic acid (COA), caffeic acid (CAA), peak P3 (Flavonoid), peak P4 (Flavonoid), peak P2 (Flavonoid), rutin (RUT).

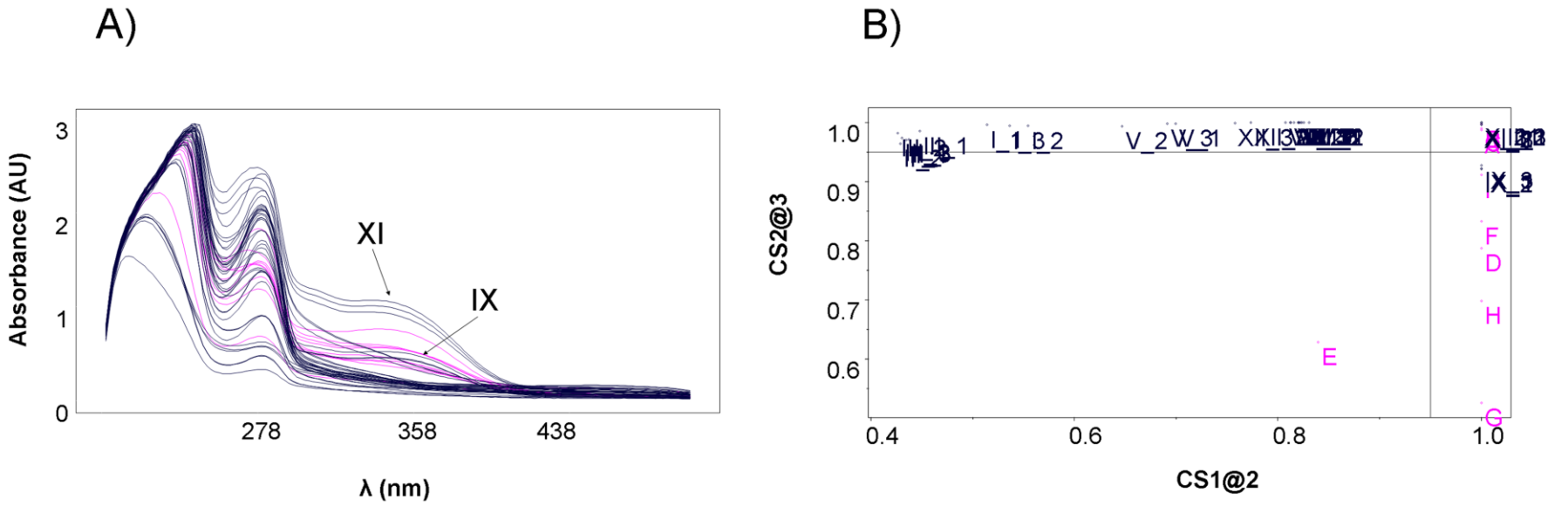

Figure 4. Overlaid of UV spectra (200–500 nm) obtained from analyses of extractive solutions (**A**); *In blue*, unknown samples obtained from folk market and commercial suppliers (I-XIII); *In pink*, *U. tomentosa* stem bark samples intentionally spiked with *U. guianensis* stem bark (*A-I*); Class distance probability plot obtained from classification SIMCA model (**B**).

TABLES

Table 1. Detailed descriptions of cat's claw stem bark samples used in the building of multivariate models.

Sample	Sample description	Spiked amount (%, w/w)	Chemotype[a]
1	UT_1	0	POA with *trans* D/E
2	UT_2	0	POA with *trans* D/E
3	UT_3	0	TOA
4	UT_4	0	TOA
5	UT_5	0	POA with *cis* D/E
6	UT_6	0	POA with *cis* D/E
7	UG_1	0	ND
8	UG_2	0	ND
9	UT_1 + UG_1_10	10	POA with *trans* D/E
10	UT_1 + UG_1_30	30	POA with *trans* D/E
11	UT_1 + UG_1_50	50	POA with *trans* D/E
12	UT_1 + UG_2_10	10	POA with *trans* D/E
13	UT_1 + UG_2_30	30	POA with *trans* D/E
14	UT_1 + UG_2_50	50	POA with *trans* D/E
15	UT_3 + UG_1_10	10	TOA
16	UT_3 + UG_1_30	30	TOA
17	UT_3 + UG_1_50	50	TOA
18	UT_3 + UG_2_10	10	TOA
19	UT_3 + UG_2_30	30	TOA
20	UT_3 + UG_2_50	50	TOA
21	UT_6 + UG_1_10	10	POA with *cis* D/E
22	UT_6 + UG_1_30	30	POA with *cis* D/E
23	UT_6 + UG_1_50	50	POA with *cis* D/E
24	UT_6 + UG_2_10	10	POA with *cis* D/E
25	UT_6 + UG_2_30	30	POA with *cis* D/E
26	UT_6 + UG_2_50	50	POA with *cis* D/E

[a]based on the oxindole alkaloid profile; POA: Pentacyclic oxindole alkaloids; TOA: Tetracyclic oxindole alkaloids; ND: not defined.

Table 2. Classification models for the recognition of adulteration in authentic *U. tomentosa* stem bark samples.

Method	Classification Model	Preprocessing *Transformation*	Number of components for each class or Neighbors	Sensitivity (%) *Specificity (%)*	
				Calibration set	Prediction set
FT-IR	SIMCA	Mean Centred *SNV, 1st Derivative*	2 and 3	100 *100*	100 *0*
	k-NN	Mean Centred *SNV, 1st Derivative*	3	100 *25*	100 *0*
UV	SIMCA	Mean Centred *Nor*	2 and 3	100 *100*	100 *100*
	k-NN	Mean Centred *Nor*	3	100 *50*	100 *50*
UV+KOH	SIMCA	Mean Centred *Nor*	2 and 3	100 *100*	100 *100*
	k-NN	Mean Centred *Nor*	3	100 *100*	100 *100*
UV+$AlCl_3$	SIMCA	Mean Centred *Nor*	2 and 3	100 *100*	100 *50*
	k-NN	Mean Centred *Nor*	3	100 *50*	100 *50*
LC analysis POA+TOA	SIMCA	Auto scale *Nor*	2 and 3	93 *100*	33 *50*
	k-NN	Mean centred *Nor*	3	93 *75*	83 *0*
LC analysis QAG	SIMCA	Mean Centred *MSC, Nor*	2 and 3	100 *100*	100 *50*
	k-NN	Mean Centred *MSC, Nor*	5	93 0	100 *0*
LC analysis PPH	SIMCA	Mean Centred *Nor*	2 and 3	100 *100*	100 *100*
	k-NN	Mean Centred *Nor*	3	100 *100*	100 *50*

SIMCA: soft independent modeling class analogy; *k*-NN: *k*-nearest neighbors; SNV: Standard normal deviation; MSC: Multiplicative scattering correlation; Sensitivity: percentage of spiked samples that were indicated by model as spiked; Specificity: percentage of authentic samples that were indicated by model as authentic; Nor: Normalization (100); POA: Pentacyclic oxindole alkaloids; TOA: Tetracyclic oxindole alkaloids; QAG: Quinovic acid glycosides; PPH: Polyphenols; UV+KOH: UV analysis after basification with KOH; UV+$AlCl_3$: UV analysis after complexation with $ALCl_3$.

Table 3. Calibration models for determination of the spiking level in *U. tomentosa* stem bark samples.

Method	Model	Preprocessing *Transformation*	LV or PC selected	RMSEC (%) *RMSECV (%)*	r_C r_{CV}	RMSEP (%)	r_P
FT-IR	PCR	Mean Centred *SNV, 1st Derivative**	4	9.37 *12.92*	0.965 *0.908*	9.09	0.888
	PLS	Mean Centred *SNV, 1stDerivative**	6	3.25 *10.68*	0.996 *0.937*	15.21	0.675
UV	PCR	Auto scale *None*	6	2.03 *2.42*	0.998 *0.996*	1.52	0.999
	PLS	Mean Centred *None*	5	2.12 *2.40*	0.998 *0.997*	1.63	0.999
UV+KOH	PCR	Auto scale *None*	4	1.38 *2.39*	0.999 *0.998*	3.37	0.987
	PLS	Auto scale *None*	4	1.32 *2.38*	0.999 *0.998*	3.31	0.987
UV+$AlCl_3$	PCR	Auto scale *None*	6	1.43 *1.88*	0.999 *0.998*	2.02	0.997
	PLS	Auto scale *None*	6	1.34 *1.84*	0.999 *0.998*	2.02	0.998
LC analysis POA+TOA	PCR	Mean Centred *None*	2	22.27 *23.08*	0.742 *0.650*	29.71	-0.084
	PLS	Mean Centred *None*	2	20.71 *22.68*	0.782 *0.674*	30.85	-0.076
LC analysis QAG	PCR	Mean Centred *MSC*	3	12.77 *14.23*	0.929 *0.884*	11.02	0.857
	PLS	Mean Centred *MSC*	3	9.70 *13.79*	0.960 *0.893*	10.14	0.925
LC analysis PPH	PCR	None *None*	6	1.32 *1.72*	0.999 *0.998*	1.73	0.997
	PLS	None *None*	4	1.38 *1.82*	0.999 *0.998*	2.07	0.997

*(first-degree derivative and 5 points were used); PCR: Principal components regression; PLS: Partial least-squares analysis; SNV: Standard normal deviation; MSC: Multiplicative scattering correlation; LV: Number of latent variables; PC: Number of principal components; RMSEC: Root mean square error of calibration; RMSECV: Root mean square error of cross validation; RMSEP: Root mean square error of prediction; r_C: calibration regression coefficient; r_{CV}: cross validation regression coefficient; r_P: prediction regression coefficient; POA: Pentacyclic oxindole alkaloids; TOA: Tetracyclic oxindole alkaloids; QAG: Quinovic acid glycosides; PPH: Polyphenols; UV+KOH: UV analysis after basification with KOH; UV+$AlCl_3$: UV analysis after complexation with $ALCl_3$.

Table 4. Characterization of peaks related to adulteration recognition in *U. tomentosa* stem bark samples from LC-PDA-QTOF analysis in MS^E mode.

RT (min)	λ_{max} (nm)	Low energy mass spectrum					
		ESI^+ (*m*/*z*)	ESI^- (*m*/*z*)	Measured monoisotopic mass (Da)	Theoretical monoisotopic mass (Da)	Δ ppm [a]	Molecular formula [b]
1.56	270; 353	$[M+Na]^+$= 779.2003 $[M+H]^+$ = 757.2181	$[M-H]^-$ = 755.2057	756.2119	756.2113	0.80	$C_{33}H_{40}O_{20}$
1.96	265; 350	$[M+Na]^+$= 763.2057 $[M+H]^+$ = 741.2237	$[M-H]^-$ = 739.2109	740.2173	740.2164	1.21	$C_{33}H_{40}O_{19}$

RT (min)	High energy mass spectrum (20 – 40 eV) [c]	
	ESI^+ fragmentation pattern (*m*/*z*)	ESI^- fragmentation pattern (*m*/*z*)
1.56	611.1622 $[M+H-146]^+$ 465.1042 $[M+H-146-146]^+$ 303.0487 $[M+H-162-146-146]^+$ 153.0178 $^{1,3}A^+$	300.0277 $[M-2H-162-146-146]^-$ 151.0029 $^{1,3}A^-$
1.96	595.1659 $[M+H-146]^+$ 449.1075 $[M+H-146-146]^+$ 287.0541 $[M+H-162-146-146]^+$ 165.0177 $^{0,2}A^+$ 153.0177 $^{1,3}A^+$ 121.0278 $^{0,2}B^+$	284.0316 $[M-2H-162-146-146]^-$

RT: Retention time; λ_{max}: wavelength of maximum absorption from UV spectrum; ESI: Electrospray ionization; [a]mass difference between measured monoisotopic mass and theoretical monoisotopic in parts per million (ppm); [b]Determined from isotopic pattern; [c]collision energy ramp; $^{0,2}A^+$; $^{1,3}A^+$; $^{1,3}A^-$; $^{0,2}B^+$ mass fragments from aglycone name in accordance with Ma et al. (1997).

Table 5. Determination of peak P4, POA and TOA contents in *U. tomentosa* stem bark samples spiked with *U. guianensis*, and unknown samples from Peruvian folk market and commercial suppliers.

Sample	Spiking amount (%, w/w)	Predicted spiking amount[a] (%, w/w)	Peak P4 content[b] (%, w/w)	POA content[c] (%, w/w)	TOA content[d] (%, w/w)
$UT_1 – UT_6$[*]	0	-2.20 – 1.04	0.001 – 0.015	0.193 – 1.779	0.010 – 0.646
$UG_1 – UG_2$[*]	0	99.99 – 103.21	0.429 – 0.504	0.038 – 0.058	0.003 – 0.008
UT + UG_10[*]	10	9.73 – 11.04	0.039 – 0.058	0.362 – 1.553	0.008 – 0.579
UT + UG_30[*]	30	26.04 – 33.79	0.118 – 0.152	0.285 – 1.176	0.006 – 0.421
UT + UG_50[*]	50	45.70 – 53.97	0.191 – 0.227	0.209 – 0.871	0.004 – 0.288
A	14	10.05[##]	0.086	0.065[###]	0.178[###]
B	45	34.32[##]	0.192	0.386	0.029
C	32	29.14[##]	0.188	0.277[###]	0.008
D	54	50.86[#]	0.347	0.811	0.002
E	16	17.42[#]	0.133	1.159	0.003
F	60	49.73[#]	0.272	0.329	0.252[###]
G	87	78.54[#]	0.233	0.098[###]	0.070[###]
H	64	52.59[#]	0.377	0.157[###]	0.005
I	41	35.23[#]	0.430	0.074[###]	0.001
I	unknown	1.01	0.004	0.885	ND
II	unknown	-3.22	0.001	0.388	0.053[###]
III	unknown	1.56	0.013	0.670	0.579[###]
IV	unknown	3.03	0.005	0.939	0.017
V	unknown	-3.73	0.010	1.500	0.011
VI	unknown	-4.99	0.008	1.446	0.001
VII	unknown	-1.68	0.010	1.474	0.754[###]
VIII	unknown	-0.61	0.008	0.293[###]	0.427[###]
IX	unknown	47.01[#]	0.391	0.042[###]	0.057[###]
X	unknown	4.29	0.011	0.201[###]	0.011
XI	unknown	91.05[##]	0.734	0.046[###]	0.002
XII	unknown	-1.57	0.029	0.258[###]	0.034
XIII	unknown	6.09	0.087	0.247[###]	0.041

[a]PLS model established from UV data; [b]expressed as rutin; [c]calculated from sum of speciophylline, uncarine F, mitraphylline, isomitraphylline, pteropodine, and isopteropodine contents expressed as mitraphylline; [d]calculated from the sum of rhyncophylline and isorhyncophylline contents expressed as mitraphylline; [*]range obtained from samples employed in the establishment of the multivariate models (calibration and classification models); [#]classified as spiked sample by SIMCA model established from UV data; [##]not classified sample by SIMCA model established from UV data; ND: not detected; [###]samples in disagree with U.S. pharmacopeia requirements (USP, 2016); all experimental result were obtained from mean of three determinations.

SUPPORTING INFORMATION

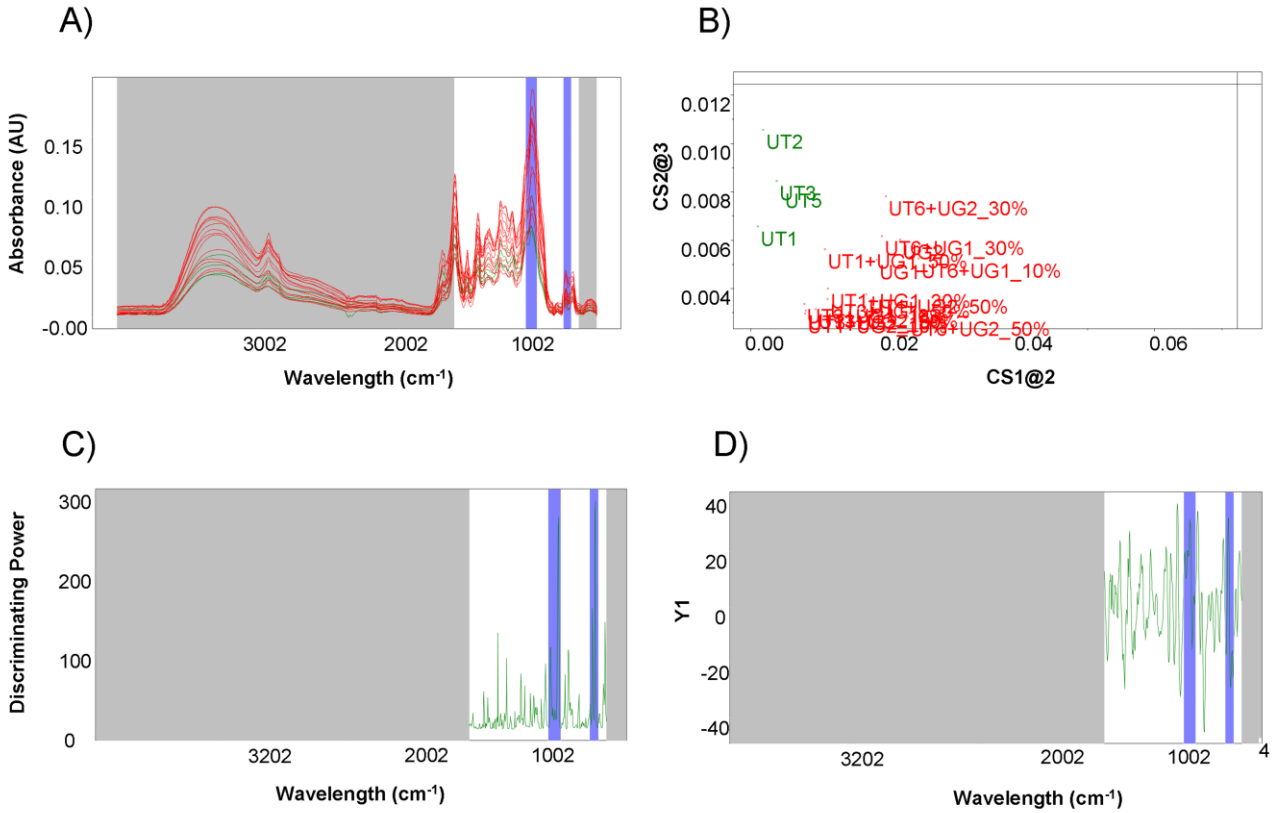

Figure S1. Overlaid of FT-IR spectra (4000–600 cm^{-1}) obtained from analyses of freeze dried stem bark sample (**A**); *In green*, authentic *U. tomentosa* stem bark samples; *In red*, *U. tomentosa* stem bark samples intentionally spiked with *U. guianensis* stem bark; *White region*: selected region from FTIR spectra (1600–730 cm^{-1}); *Blue region*: main differentiation bands (1100–1020 cm^{-1}; 840–790 cm^{-1}) from FRTIR spectra between spiked samples and authentic samples. Class distance plot obtained from classification SIMCA model (**B**); Discriminating power obtained from classification SIMCA model (**C**); Regression vector obtained from calibration PLS model (**D**).

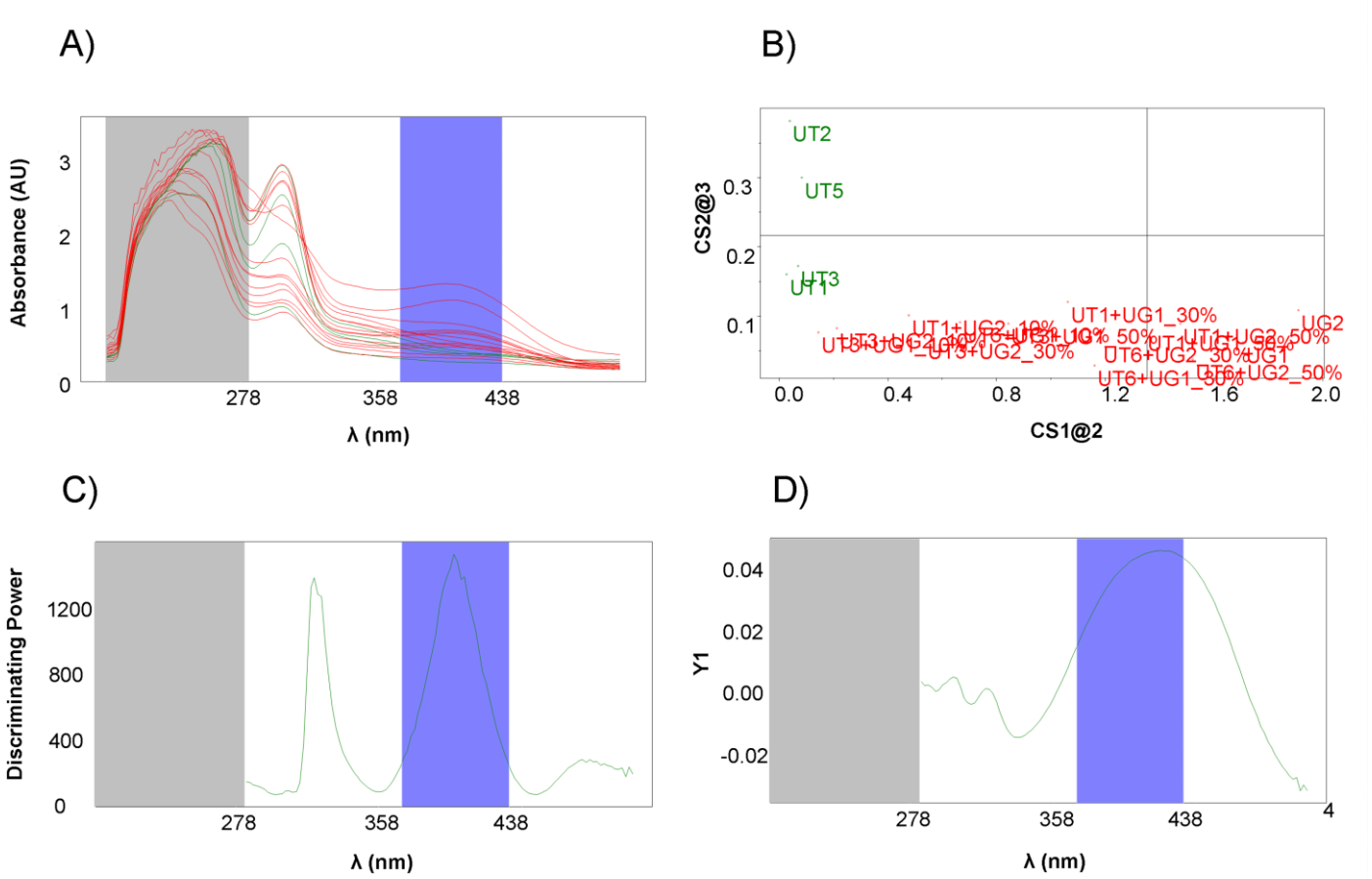

Figure S2. Overlaid of UV spectra (200–500 nm) obtained from analyses of extractive solutions after basification with KOH 1M (**A**); *In green*, authentic *U. tomentosa* stem bark samples; *In red*, *U. tomentosa* stem bark samples intentionally spiked with *U. guianensis* stem bark; *White region*: selected region from UV spectra (280–500 nm); *Blue region*: main differentiation peak (360–440 nm) from UV spectra between spiked samples and authentic samples. Class distance plot obtained from classification SIMCA model (**B**); Discriminating power obtained from classification SIMCA model (**C**); Regression vector obtained from calibration PLS model (**D**).

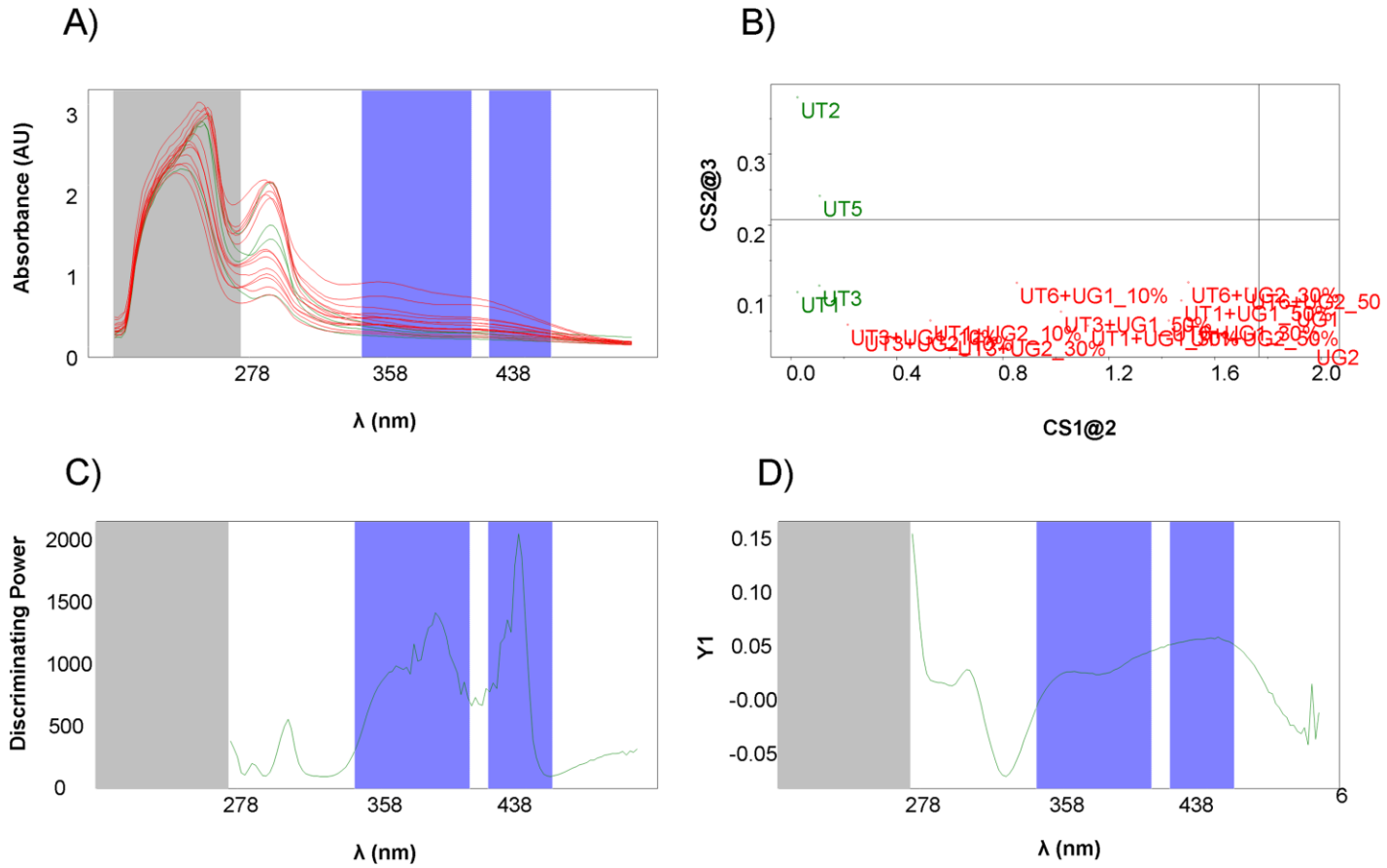

Figure S3. Overlaid of UV spectra (200–500 nm) obtained from analyses of extractive solutions after complexation with $AlCl_3$ 5% (**A**); *In green*, authentic *U. tomentosa* stem bark samples; *In red*, *U. tomentosa* stem bark samples intentionally spiked with *U. guianensis* stem bark; *White region*: selected region from UV spectra (280–500 nm); *Blue region*: main differentiation peak (400–460 nm) from UV spectra between spiked samples and authentic samples. Class distance plot obtained from classification SIMCA model (**B**); Discriminating power obtained from classification SIMCA model (**C**); Regression vector obtained from calibration PLS model (**D**).

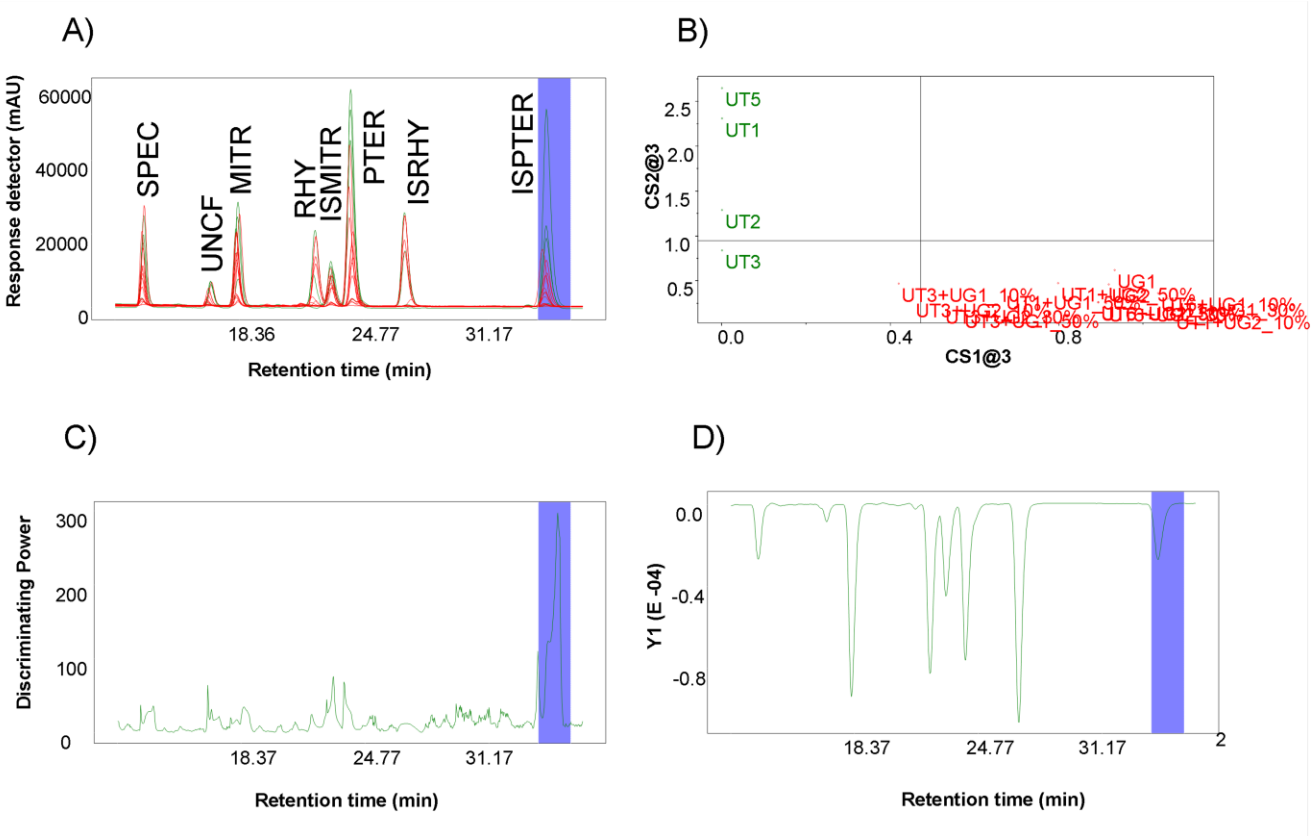

Figure S4. Overlaid of LC-PDA profiles (245 nm) obtained from oxindole alkaloid analyses of extractive solutions (**A**); *In green*, authentic *U. tomentosa* stem bark samples; *In red*, *U. tomentosa* stem bark samples intentionally spiked with *U. guianensis* stem bark; *Blue region*: main differentiation peak (ISPTER) from LC-UV profiles between spiked samples and authentic samples. Class distance plot obtained from classification SIMCA model (**B**); Discriminating power obtained from classification SIMCA model (**C**); Regression vector obtained from calibration PLS model (**D**). Speciophylline (SPEC), uncarine F (UNCF) mitraphylline (MIT), rhynchophylline (RHY), isomitraphylline (ISMITR), pteropodine (PTER), isorhynchophylline (ISRHY), isopteropodine (ISPTER).

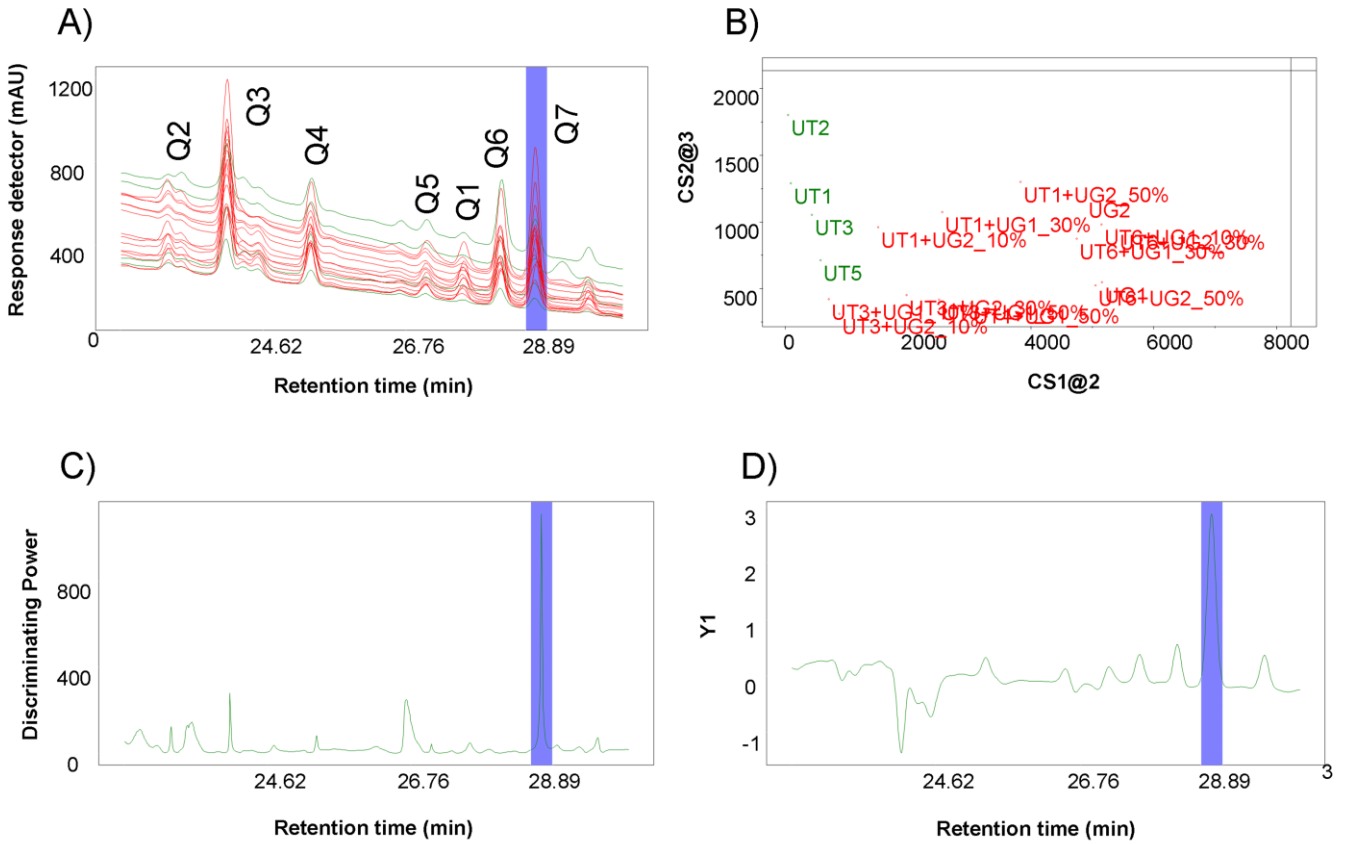

Figure S5. Overlaid of LC-PDA profiles (205 nm) obtained from quinovic acid glycosides analyses of extractive solutions (**A**); *In green*, authentic *U. tomentosa* stem bark samples; *In red*, *U. tomentosa* stem bark samples intentionally spiked with *U. guianensis* stem bark; *Blue region*: main differentiation peak (peak 7) from HPLC-UV profiles between spiked samples and authentic samples. Class distance plot obtained from classification SIMCA model (**B**); Discriminating power obtained from classification SIMCA model (**C**); Regression vector obtained from calibration PLS model (**D**). Peak Q2 (triglycosilated derivative), peak Q3 (diglycosilated derivative), peak Q4 (monoglycosilated derivative), peak Q5 (diglycosilated derivative), peak Q1 (monoglycosilated derivative) peak Q6 (monoglycosilated derivative); peak Q7 (monoglycosilated derivative).

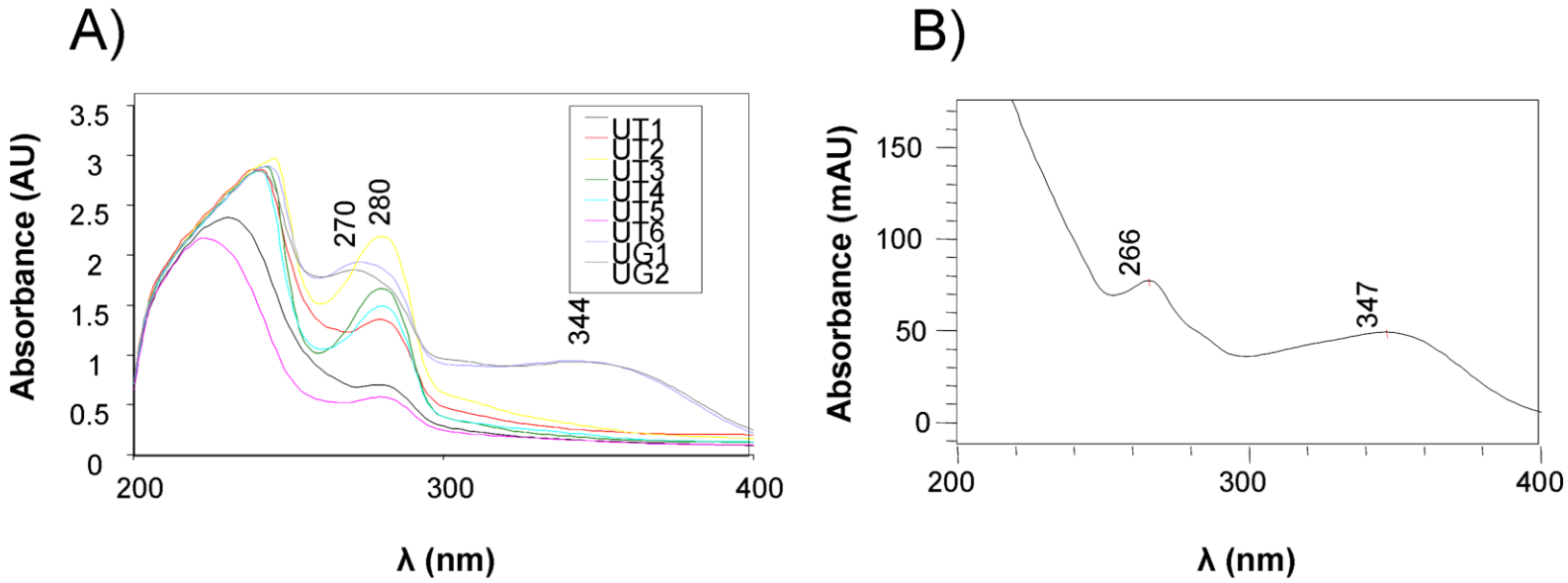

Figure S6. UV spectra (200–400 nm) obtained from analyses of authentic *U. tomentosa* (UT) and *U. guianensis* (UG) stem bark extractive solutions (**A**) and UV spectrum (200–400 nm) of Peak P4 obtained from HPLC-PDA analysis of polyphenols (**B**).

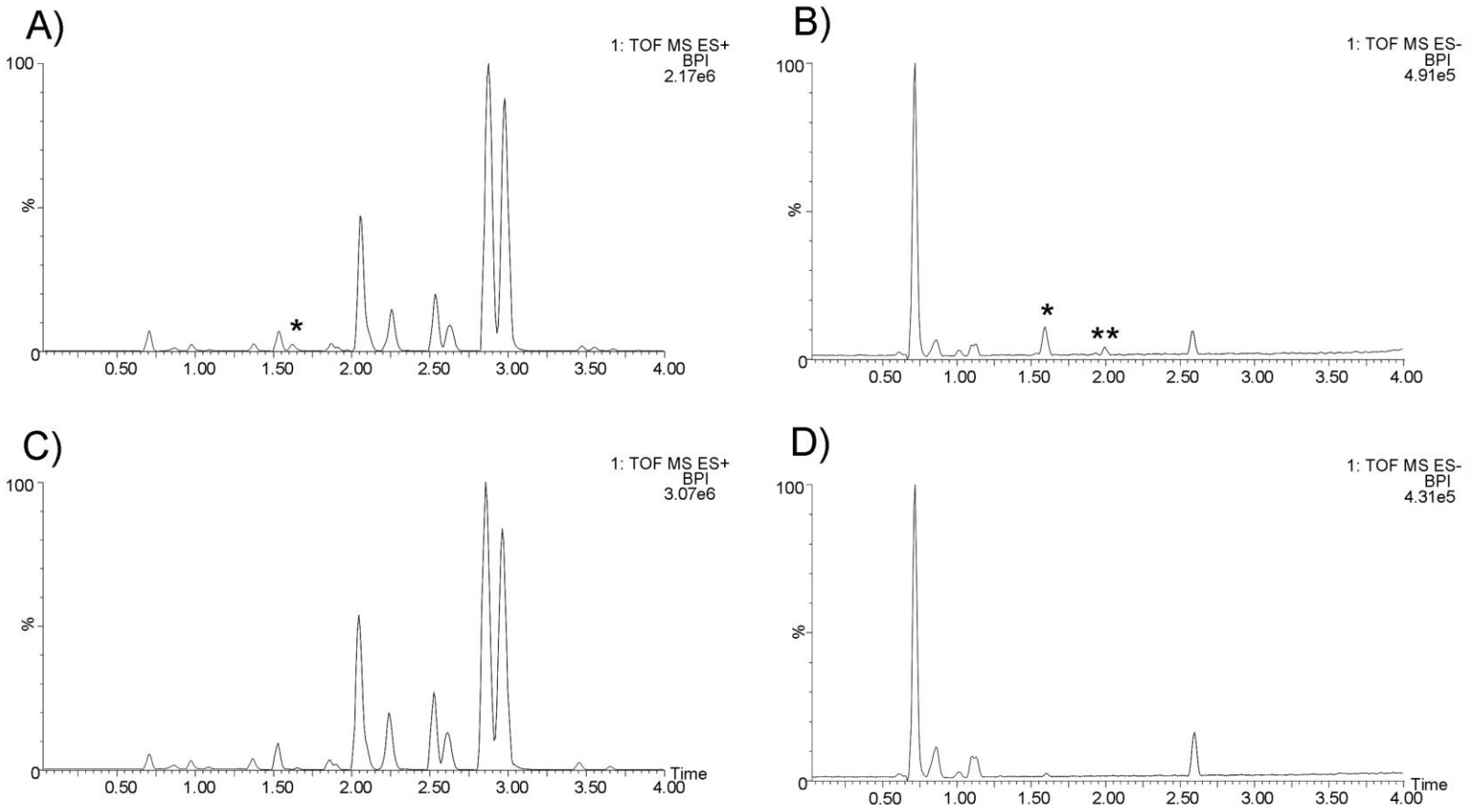

Figure S7. Base peak intensity (BPI) chromatograms from LC-PDA-QTOF (50-1000 *m/z*) analyses of *U. tomentosa* (UT) spiked with 50% (w/w) of *U. guianensis* (UG) in both ionization modes (ESI^+ (**A**); ESI^- (**B**)) and authentic *U. tomentosa* (UT) sample in both ionization modes (ESI^+ (**C**); ESI^- (**D**)). *peak at 1.56 min and **peak at 1.96 min related with adulteration recognition in *U. tomentosa* stem bark samples.

Table S1. LC-PDA conditions for analysis of oxindole alkaloids, polyphenols and quinovic acid glycosides.

Method	Column	Mobile phase *Diluent* (*Sample dilution factor)*	Flow rate (mL/min) Temperature (ºC) λ (nm)	Compound (*RRT* [a] *– min*)	Reference
Oxindole alkaloids (POA and TOA)	Gemini-NX RP-18 column (250 x 4.6 mm i.d., 5 µm) (Phenomenex, USA)	Ammonium acetate buffer 10 mM (pH 7.0) (A) and acetonitrile (B) in a linear gradient program. *acetonitrile:H_2O (50:50, v/v)* (*10 times*)	1.00 mL/min 23 ±1 ºC 245 nm	speciophylline (SPEC) (*1.00*[b]) uncarine F (UNCF) (*1.26* [b]) mitraphylline (MIT) (*1.36* [b]) rhynchophylline (RHY) (*1.65*[b]) isomitraphylline (ISMITR) (*1.71*[b]) pteropodine (PTER) (*1.78*[b]) isorhynchophylline (ISRHY) (*1.99*[b]) isopteropodine (ISPTER) (*2.53*[b])	Kaiser, et al., 2013b
Polyphenols (PPH)	Gemini RP-18 column (250 x 4.6 mm i.d., 5 µm) (Phenomenex, USA)	TFA 0.1% (v/v) (A) and methanol: TFA (99.9:0.1, v/v) (B) in a linear gradient program. *methanol:TFA 0.1% (v/v)* (*two times)*	0.90 mL/min 23±1 ºC 325 nm	chlorogenic acid (COA) (*1.00*[c]) caffeic acid (CAA) (*1.23*[c]) peak P3 (Flavonoid*) (*1.46*[c]) peak P1 (Flavonoid*) (*1.71*[c]) peak P4 (Flavonoid*) (*2.05*[c]) peak P2 (Flavonoid*) (*2.24*[c]) rutin (RUT) (*2.44*[c])	Pavei, et al., 2010
Quinovic acid glycosides (QAG)	Sinergy Fusion RP-18 column (150 x 4.6 mm i.d., 4 µm) (Phenomenex, USA)	FA 0.01% (v/v) (A) and acetonitrile: FA 0.01% (90:10, v/v) (B) in a linear gradient program. *acetonitrile: FA 0.01% (30:70, v/v)* (*two times*)	1.00 mL/min 35±1 ºC 205 nm	peak Q2 (triglycosilated derivative**) (*1.00*[d]) peak Q3 (diglycosilated derivative**) (*1.04*[d]) peak Q4 (monoglycosilated derivative**) (*1.09*[d]) peak Q5 (diglycosilated derivative**) (*1.17* [d]) peak Q1 (monoglycosilated derivative**) (*1.19*[d]) peak Q6 (monoglycosilated derivative**) (*1.21*[d]) peak Q7 (monoglycosilated derivative**) (*1.24*[d])	Pavei, et al., 2012

[a]RRT: Relative retention time; [b]reference speciophylline peak; [c]reference cholorogenic acid peak; [d]reference peak Q1; * chemical class inferred from UV spectrum ** putatively identified from MS analysis.

Table S2. Detailed descriptions of *U. tomentosa* stem bark samples spiked with *U. guianensis* and unknown samples obtained from Peruvian folk market and commercial suppliers.

Sample	Package identification	Source	Spiking amount (%, w/w)
I	*"san roque"*	Folk market	NA
II	*"sanatel vida"*	Folk market	NA
III	*"la bella durmiente"*	Folk market	NA
IV	*"herbosh el shipibo"*	Folk market	NA
V	*"herbosteria los ficus"*	Folk market	NA
VI	ND	Folk market	NA
VII	ND	Folk market	NA
VIII	ND	Folk market	NA
IX	ND	Folk market	NA
X	Supplier 1	Commercial supplier	NA
XI	*"janeiro 2004"*	Folk market	NA
XII	Supplier 2	Commercial supplier	NA
XIII	Supplier 3	Commercial supplier	NA
A	NA	Collected from Peruvian amazon	14
B	NA	Collected from Peruvian amazon	45
C	NA	Collected from Peruvian amazon	32
D	NA	Collected from Peruvian amazon	54
E	NA	Collected from Peruvian amazon	16
F	NA	Collected from Peruvian amazon	60
G	NA	Collected from Peruvian amazon	87
H	NA	Collected from Peruvian amazon	64
I	NA	Collected from Peruvian amazon	41

ND: not determined; NA: not applied;

Capítulo 2. Relevância dos quimiotipos em relação à genoxicidade e citotoxicidade dos alcaloides oxindólicos em *Uncaria tomentosa*

Introdução

Reconhecidamente, as atividades imunoestimulante e antitumoral em *U. tomentosa* têm sido atribuídas aos alcaloides oxindólicos (HEITZMAN *et al.*, 2005; ZHANG *et al.*, 2015). O monitoramente inicial do perfil dos alcaloides oxindólicos em diferentes anos e estágios de maturidade da espécie revelou uma grande variabilidade em seu perfil de alcaloides (STUPPNER *et al.* 1992a). Assim foi proposta a existência de dois quimiotipos em *U. tomentosa* botanicamente indistinguíveis entre si, a saber, quimiotipo *pentacíclico* e *tetracíclico* (LAUS *et al.*, 1997). Recentemente, a partir da avaliação da constituição química de 22 amostras de cascas de caule, galhos e folhas de *U. tomentosa* de origem Peruana, evidenciou-se que os quimiotipos eram ainda mais específicos na espécie (PEÑALOZA *et al.* 2015). Consequentemente, três quimiotipos foram verificados em função do perfil de alcaloides oxindólicos da espécie: *quimiotipo I*, composto majoritariamente por alcaloides oxindólicos pentacíclicos com conformação dos anéis D/E em *cis* (especiofilina, uncarina F, pteropodina e isopteropodina); *quimiotipo II*, composto majoritariamente por alcaloides oxindólicos pentacíclicos com conformação dos anéis D/E em *trans* (mitrafilina e isomitrafilina); *quimiotipo III*, composto majoritariamente por alcaloides oxindólicos tetracíclicos (rincofilina e isorrincofilina).

Em relação à atividade imunoestimulante, os alcaloides tetracíclicos e pentacíclicos possuem efeitos antagônicos (KEPLINGER *et al.*, 1999). Enquanto os alcaloides oxindólicos pentacíclicos estimularam a proliferação de linfócitos T e B em células endoteliais, os tetracíclicos foram capazes de inibir o efeito estimulante. Neste tocante, o presente capítulo visou avaliar a influência dos diferentes quimiotipos sobre a citoxicidade e seletividade em células tumorais em comparação a células não-malignas (leucócitos humanos) bem como seu potencial genotóxico em células não-malignas.

O presente capítulo é constituído por artigo científico publicado, conforme referência abaixo:

Kaiser S, Carvalho AR, Pittol V, Dietrich F, Manica F, Machado MM, De Oliveira LFS, Battastini AMO, Ortega GG. 2016. Genotoxicity and cytotoxicity of oxindole alkaloids from *Uncaria tomentosa* (cat's claw): Chemotype relevance. *J Ethnopharmacol* **189**: 90-98.

Artigo 2. Genotoxicity and cytotoxicity of oxindole alkaloids from *Uncaria tomentosa* (cat's claw): Chemotype relevance

Journal of Ethnopharmacology 189 (2016) 90–98

Contents lists available at ScienceDirect

Journal of Ethnopharmacology

journal homepage: www.elsevier.com/locate/jep

Genotoxicity and cytotoxicity of oxindole alkaloids from *Uncaria tomentosa* (cat's claw): Chemotype relevance

Samuel Kaiser [a,*], Ânderson Ramos Carvalho [a], Vanessa Pittol [a], Fabrícia Dietrich [b], Fabiana Manica [b], Michel Mansur Machado [c], Luis Flávio Souza de Oliveira [c], Ana Maria Oliveira Battastini [b], George González Ortega [a]

[a] Laboratório de Desenvolvimento Galênico (LDG), Faculdade de Farmácia, Universidade Federal do Rio Grande do Sul (UFRGS), Porto Alegre, RS, Brazil
[b] Laboratório de Enzimologia, Departamento de Bioquímica Universidade Federal do Rio Grande do Sul (UFRGS), Porto Alegre, RS, Brazil
[c] Laboratório de Imunologia Clínica e Toxicologia, Universidade Federal do Pampa (UNIPAMPA), Campus Uruguaiana, RS, Brazil

ARTICLE INFO

Article history:
Received 17 February 2016
Received in revised form
1 May 2016
Accepted 3 May 2016
Available online 13 May 2016

Keywords:
Uncaria tomentosa
Cat's claw
Genotoxicity
Cytotoxicity
Oxindole alkaloids
Chemotypes

Chemical compounds studied in this article:
Mitraphylline (PubChem CID: 94160)
Isomitraphylline (PubChem CID: 11726520)
Speciphylline (PubChem CID: 168985)
Uncarine F (PubChem CID: 12304288)
Pteropodine (PubChem CID: 10429112)
Isopteropodine (PubChem CID: 9885603)
Rhynchophylline (PubChem CID: 5281408)
Isorhynchophylline (PubChem CID: 3037048)

ABSTRACT

Ethnopharmacological relevance: *Uncaria tomentosa* (Willdenow ex Roemer & Schultes) DC. (Rubiaceae) or cat's claw is a climber vine from the South American rainforest used in folk medicine for cancer treatment. Its antitumor activity has been mostly ascribed to pentacyclic oxindole alkaloids (POA) from stem bark and leaves while the activity of tetracyclic oxindole alkaloids (TOA) remains unknown. In recent times, the occurrence of three chemotypes based on its oxindole alkaloid profile was noticed in *U. tomentosa*, namely, chemotype **I** (POA *cis* D/E ring junction); chemotype **II** (POA *trans* D/E ring junction) or chemotype **III** (TOA). Consequently, the relationship between the chemotype and cytotoxic and genotoxic activities deserves attention.

Aim of the study: To evaluate the influence of cat's claw chemotypes on genotoxicity and cytotoxicity against non malignant and malignant human cell line models.

Material and methods: Four authentic stem bark cat's claw samples (S_I-S_{IV}) and two leaf samples (L_{II} and L_{III}) were analyzed by HPLC-PDA, properly extracted and fractioned by ion-exchange to obtain oxindole alkaloid purified fractions (OAPFs). The freeze-dried fractions were assayed for genotoxicity and cytotoxicity against human leukocytes (non malignant cell line) by the micronuclei frequency method and the alkaline comet DNA assay, and the trypan blue method, respectively. Moreover, the cytotoxicity of each OAPF was evaluated against a human bladder cancer cell line (T24) and human glioblastoma cell line (U-251-MG) by MTT method (malignant cell lines). Additionally, the isomerization of oxindole alkaloids throughout the course of cell incubation was monitored by HPLC-PDA.

Results: Based on HPLC-PDA analyses, sample S_I was characterized as chemotype **I**, while samples S_{II} and L_{II} were characterized as chemotype **II**, and samples S_{III}, S_{IV} and L_{III} as chemotype **III**. The chemotypes showed comparable cytotoxic activity toward malignant cell lines (T24 and U-251-MG) unlike human leukocytes (non malignant cell line), where this activity was clearly distinct. Chemotype **II** (POA *trans* D/E ring junction) showed a higher selectivity index (SI) against malignant cells (SI = 1.11–3.04) than chemotype **I** (SI = 0.10 – 0.19) and **III** (SI = 0.21–0.57). No important genotoxic potential was found by micronuclei frequency and alkaline comet DNA assays. Despite the isomerization of oxindole alkaloids during the cell incubation, the chemotype of the cat's claw samples remained unchanged.

Conclusion: Cat's claw chemotypes showed different selectivity against human malignant cells, so that the correct identification of each chemotype seems to be important to better understand its antitumor potential.

1. Introduction

Uncaria tomentosa (Willdenow ex Roemer & Schultes) DC. (Rubiaceae), popularly known as cat's claw or "Uña de Gato", is a climber vine from the South American rainforest traditionally employed as immunostimulant, anti-inflammatory and also for cancer treatment (Heitzman et al., 2005; Keplinger et al., 1999;

Abbreviations: POA, pentacyclic oxindole alkaloids; TOA, tetracyclic oxindole alkaloids; OAPFs, oxindole alkaloid purified fractions; T24, human bladder cancer cell line; U-251-MG, human glioblastoma cell line; SI, selectivity index; SPEC, speciophylline; UNCF, uncarine F; PTER, pteropodine; ISPTER, isopteropodine; MIT, mitraphylline; ISMITR, isomitraphylline; RHY, rhynchophylline; ISRHY, isorhynchophylline; S, stem bark samples; L, leaf samples; CE, crude extract

* Corresponding author.
E-mail address: samokaiser@yahoo.com.br (S. Kaiser).

http://dx.doi.org/10.1016/j.jep.2016.05.026
0378-8741/

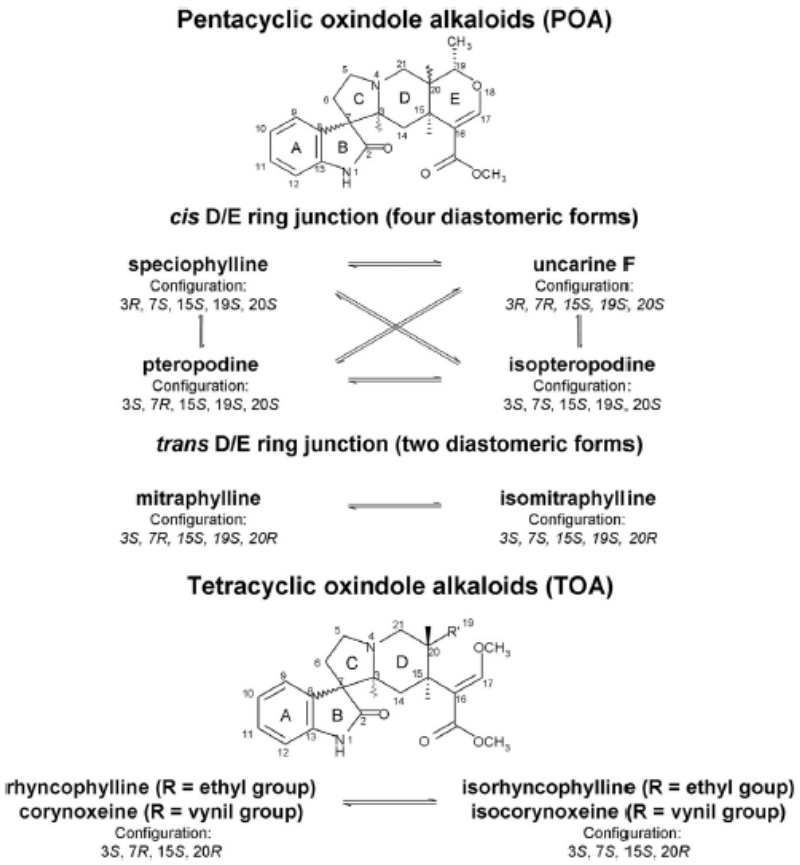

Fig. 1. Main oxindole alkaloids reported in cat's claw and their isomerization process.

Zhang et al., 2015). Antitumor activity has been mostly ascribed to its stem bark oxindole alkaloids (Heitzman et al., 2005; Kaiser et al., 2013a; Pilarski et al., 2010), which can occur as pentacyclic (POA) or tetracyclic (TOA) derivatives (Fig. 1). Both POA and TOA are susceptible to isomerization. The isomerization rate depending on pH, temperature and medium polarity (Laus et al., 1996). For POA with *trans* D/E ring junction, isomerization leads to one pair of interconvertible diastereomeric forms (mitraphylline and isomitraphylline), while for POA with *cis* D/E ring junction undergoes isomerization to four interconvertible diastereomeric forms (speciophylline, uncarine F, pteropodine and isopteropodine) (Laus et al., 1996). Concerning TOA, two pairs of interconvertible diastereomeric forms are found, which differ in the group attached at C-20 (ethyl group – rhyncophylline and isorhyncophylline; vinyl group – corynoxeine and isocorynoxeine) (Laus et al., 1998).

The occurrence of two chemotypes in cat's claw based on its oxindole alkaloid profile (chemotype POA or TOA) was first reported by Laus et al. (1997). Recently, three specific chemotypes were found from the study of the chemical variability of a wild population of cat's claw from the Peruvian Amazon (Peñaloza et al., 2015). These chemotypes were named as chemotype **I**, composed mainly by POA with *cis* D/E ring junction; chemotype **II**, composed mainly by POA with *trans* D/E ring junction; and chemotype **III** composed mainly by TOA.

The occurrence of an antagonistic effect between TOA and POA has been reported. POA was able to stimulate the endothelial cells *in vitro* to produce a lymphocyte-proliferation-regulating factor, while the increased TOA concentration in the medium inhibited the factor production (Keplinger et al., 1999; Wurm et al., 1998). Probably based on these findings, the U. S. Pharmacopeia limited the TOA content to 0.05% (w/w) of the dried raw material, and up to 25% (w/w) in relation to the POA content in the cat's claw derivatives such as powdered dried extract, capsules and tables (USP, 2016). On the other hand, against human peripheral blood mononuclear cells (PBMC) stimulated with phytohaemagglutinin and concanavalin A, both POA and TOA showed similar suppression activity in immunobiochemical pathways induced by interferon-γ (Winkler et al., 2004). Thus, the antagonistic effect of TOA in relation to POA needs to be clarified.

Cat's claw preparations are considered effective and safe as a phytomedicine for human use, without major restrictions regarding their acute toxicity, genotoxicity or cytotoxicity (Keplinger et al., 1999; Romero-Jiménez et al., 2005; Valerio Jr and Gonzales, 2005). Despite the antitumor activity found for cat's claw quinovic acid glycosides (Dietrich et al., 2014), it has been mostly reported for the cat's claw oxindole alkaloids (Heitzman et al., 2005; Kaiser et al., 2013a; Pilarski et al., 2010; Zhang et al., 2015). However the effect of the different oxindole alkaloid profiles found in cat's claw on antitumor activity remains unknown. Thus, the present study aims to evaluate the influence of the cat's claw chemotypes on the genotoxicity and cytotoxicity against human non malignant cell line (human leukocytes) and cytotoxicity against human malignant cell lines (T24 human bladder cancer cell line and U-251-MG human glioblastoma cell line).

2. Material and methods

2.1. Plant material and extraction procedure

Four authentic cat's claw stem bark samples (S_I–S_{IV}) and two leaf samples (L_{II}–L_{III}) were collected from the Peruvian Amazon (November 2012) and certified by J. R. Campos De la Cruz (Museo de Historia Natural de la Universidad Nacional Mayor de San Marcos, Lima, Peru) (Table 1). The botanical vouchers were deposited at the Herbarium of Universidade Federal do Rio Grande do Sul (Porto Alegre, Brazil). All samples were comminuted in a cutter mill (SK1 Retsch, Germany) after drying at 40 °C in an air-circulating convection oven (Memmert, Germany), and extracted to obtain the maximum yield of oxindole alkaloids (Kaiser et al., 2013b). Separately, 10 g of powdered samples were extracted by 2-h dynamic maceration in a magnetic stirrer at 300 rpm (IKA RH basic 1, Germany) with hydroethanolic solution 63% (v/v) at a plant: solvent ratio of 0.5:10 (w/v). The resulting solutions were filtered through paper filter (Paper filter Whatman no. 2, UK), concentrated under vacuum at 40 °C up to half of their original weights (Büchi R-114, Germany), and immediately freeze-dried (Modulyo 4 L, Edwards, USA). For comparative purposes, the crude extract from S_{II} (CES_{II}) was used in the genotoxicity and cytotoxicity evaluation.

2.2. Obtaining the oxindole alkaloid purified fractions (OAPFs)

Oxindole alkaloid purified fractions were obtained separately from the crude extracts of each stem bark (S_I-S_{IV}) and leaf (L_{II} and L_{III}) samples by ion-exchange fractionation as previously described (Kaiser et al., 2013a). Aliquots of crude extract (200 mL) were mixed with 0.8 g of crossliked Polyvinylpyrrolidone (PVPP) (Divergan RS, BASF, Germany) and stirred magnetically at 300 rpm for 1 h at room temperature (23 ± 1 °C). This mixture was filtrated through paper filter and acidified with formic acid solution (10%, v/v) to pH 3.0. After, acidified filtrated was submitted to ion-exchange process using a glass column (2.7 × 50 cm) previously filled with 30 g of strong anionic resin (Dowex Marathon, Sigma Aldrich, USA) and drained off at constant flow (5 mL/min). Non-adsorbed compounds were washed out with 150 mL of hydroethanolic solution 40% (v/v) and discarded. The column was washed with 300 mL of ammonium acetate buffer 0.3 M (pH 7.0) for resin neutralization. Finally, the oxindole alkaloids were extracted from resin with 300 mL of hydroethanolic solution 80% (v/v). The first 40-mL subfraction was drained off, and the next 260 mL containing the oxindole alkaloids were acidified with formic acid solution 10% (v/v) to pH 5.5, concentrated under vacuum up to 50 mL at 40 °C and immediately freeze-dried. All alkaloid fractions (S_I-S_{IV}; L_{II} and L_{III}) were obtained by pool of three consecutive batches from purification process.

2.3. Oxindole alkaloids analysis

The oxindole alkaloids were assayed employing a previously validated HPLC-PDA method (Kaiser et al., 2013c) using mitraphylline as external standard (Phytolab, Germany). A Gemini-NX RP-18 column (250 × 4.6 mm i.d., 5 μm) (Phenomenex, USA) protected by an RP-18 guard column was used as stationary phase. Ammonium acetate buffer 10 mM (pH 7.0) and acetonitrile were used as mobile phase in a linear gradient program. The temperature (23 °C) and the flow rate (1.0 mL/min) were kept constant throughout the analysis. All samples were properly diluted in acetonitrile: water solution (50:50, v/v), and filtered through a 0.45 μm membrane (Millipore, USA) prior to analyses. The total oxindole alkaloid content was determined in triplicate and expressed by the sum of individual alkaloid contents (speciophylline, uncarine F, pteropodine and isopteropodine – POA with *cis* D/E ring junction; mitraphylline, isomitraphylline – POA with *trans* D/E ring junction) for POA, and (rhyncophylline and isorhyncophylline) for TOA.

2.4. Genotoxicity and cytotoxicity evaluation against human leukocytes

2.4.1. Cellular proliferation and viability assay

Human leukocyte cultures were prepared using 500 μL of venous blood collected by venipuncture from a male volunteer (survey approved by the Ethics Committee of the Federal University of Santa Maria, letter of approval number: 23,081) and immediately transferred to RPMI 1640 medium supplemented with 10% fetal bovine serum, 1% streptomycin/penicillin and 1% of phytohemaglutinin (Dos Santos Montagner et al., 2010). First the dose-effect cytotoxicity of the OAPFs (S_I-S_{IV}; L_{II} and L_{III}) in leukocytes was evaluated. Concentrations ranging from 18.7 to 935.4 μM for all purified fractions and 1.2–59.5 μM for crude extract from S_{II}(CES_{II}) expressed by total oxindole alkaloid content (sum of POA and TOA contents) in relation to weighted molecular weight (Eq. (1)) were prepared in phosphate buffered saline (PBS, pH 7.2).

$$WMW = (MW_{POA} \times (\%POA/100)) + (MW_{TOA} \times (\%TOA/100)) \quad (1)$$

where WMW, MW_{POA} and MW_{TOA} represent the weighted molecular weight, POA average molecular weight (368.426 g/mol), TOA average molecular weight (384.469 g/mol), respectively, while %POA and %TOA represent the percentage of POA and TOA in relation to total oxindole alkaloid content.

The leukocyte cultures were maintained at 37 °C in a humid atmosphere saturated with 5% CO_2. After 72 h, cell viability was determined by the trypan blue method (Burow et al., 1998) employing PBS (pH 7.2) as negative control. The viable cells were determined by counting in a Neubauer chamber and the results were expressed as the percentage of cell viability in relation to

Table 1
Detailed geographic coordinates of the cat's claw samples used in the study.

Sample	Region	GPS coordinates		Voucher	Chemotype
		Latitude (deg)	Longitude (deg)		
Stem bark (S_I)	Padre Abad–Ucayali–Peru	−9.018	−75.489	ICN 157760	**I** (POA with *cis* D/E ring junction)
Stem bark (S_{II})[1]	Puerto Inca–Huánuco–Peru	−9.135	−75.009	ICN 157757	**II** (POA with *trans* D/E ring junction)
Stem bark (S_{III})[2]	José Crespo y Castillo–Huánuco–Peru	−9.125	−76.041	ICN157761	**III** (TOA)
Stem bark (S_{IV})	Padre Abad–Ucayali–Peru	−9.145	−75.778	ICN 157759	**III** (TOA)
Leaf (L_{II})[1]	Puerto Inca–Huánuco–Peru	−9.135	−75.009	ICN 157,757	**II** (POA with *trans* D/E ring junction)
Leaf (L_{III})[2]	José Crespo y Castillo–Huánuco–Peru	−9.125	−76.041	ICN157761	**III** (TOA)

[1] Stem bark and leaf samples collected from same plant (II).
[2] Stem bark and leaf samples collected from same plant (III).

negative control group by means of three independent experiments. A four-parameter Weibull non-linear model (Curve Expert 1.3 software) was applied to estimate the inhibitory concentration of 50% (IC_{50}).

For the genotoxicity evaluation (alkaline comet DNA assay and micronuclei frequency) of the OAPFs, three concentrations were employed for each purified fraction (18.7 μM, 187.1 μM and 935.4 μM) and CES_{II} (1.2 μM, 11.9 μM and 59.5 μM). Phosphate buffered saline (PBS, pH 7.2) was employed as negative control.

2.4.2. Micronuclei frequency assay

The leukocyte samples were placed in a conical tube with saline and centrifuged twice in 1000 rpm for 5 min About one milliliter containing the cell pellet was drained off and spread over a glass slide in replicate, and allowed to dry at room temperature. Slides were stained by the panoptic method (Schmid, 1975), and analyzed by optical microscopy in immersion lens. Each result expressed a 1000 cell-count.

2.4.3. Alkaline comet DNA assay

The alkaline comet DNA assay was performed as previously described (Singh et al., 1988; Tice et al., 2000). After incubation, leukocyte samples were mixed with low-melting point agarose and placed on a microscope slide pre-coated with normal melting point agarose. The slides were immersed in a lysis solution, and the electrophoretic analysis was performed at 300 mA and 25 V during 20 min The slides were neutralized, allowed to dry at room temperature overnight, re-hydrated for 10 min, and dried again as before. The last stage was the coloring and the use of stop solution. The slides were analyzed under blind conditions. The DNA damage index (DI) was calculated based on two criteria: completely undamaged (100 cells $\times 0$), and maximum damaged (100 cells $\times 4$).

2.5. Cytotoxicity against human malignant cells

The T24 human bladder cancer cell line (American Type Culture Collection – ATCC, USA) and U-251-MG human glioblastoma cell line (Sigma, USA) were maintained, respectively, in RPMI, and DMEM culture media, both supplemented with 0.5 U/mL penicillin/streptomycin and with 10% (v/v) fetal bovine serum. Separately, the cell lines were plated (96-well plate) at 3×10^3 (T24) and 8×10^3 (U-251-MG) per well, and treated with the working samples after reaching semi-confluence. About 7 mg of each OAPF sample (S_I-S_{IV}; L_{II}, L_{III} and CES_{II}) were dissolved in 100 μL of DMSO (Sigma-Aldrich), and properly transferred to a 96-well plate to yield concentrations ranging from 46.8 to 374.2 μM for OAPFs, and 2.97–23.74 μM for the CES_{II}. The culture medium (cell viability control) and DMSO (solvent control) were used as negative controls. Cisplatin (Sigma-Aldrich, USA) was used as positive control (5.0 μg/mL). The cell cultures were maintained at 37 °C, in a humid atmosphere saturated with 5% CO_2. After 48 h incubation, cell viability was determined by the MTT method (Mosmann, 1983). Absorbance was measured at 570 and 630 nm using an ELISA plate reader (Spectramax M5, Molecular Devices, USA), and the results were expressed as cell viability percent in relation to the solvent control group by means of three independent experiments. A four-parameter Weibull non-linear model (Curve Expert 1.3 software) was applied to estimate the inhibitory concentration of 50% (IC_{50}).

2.6. Monitoring of oxindole alkaloid profile throughout the cell incubation

Each OAPF sample (S_I-S_{IV}; L_{II} and L_{III}) was properly dissolved in PBS (pH 7.4) to obtain a final concentration of 187.1 μM. Separately, 100 μL aliquots were collected at the initial time and after 24 h of incubation in a humid atmosphere saturated with 5% CO_2, at 37 °C. Each sample was appropriately diluted tenfold with acetonitrile: water (50:50, v/v), and the individual alkaloid contents were determined by HPLC-PDA (Kaiser et al., 2013c).

2.7. Statistical analysis

The results were statistically evaluated by the Snedecor *f*-test for variance, followed by the Student *t*-test (Microsoft Excel software), and $p < 0.05$ values were considered significant.

3. Results and discussion

3.1. Plant material characterization

Together with two cat's claw chemotypes previously recognized by their oxindole alkaloid profiles (Laus et al., 1997), a third chemotype was recently detected in wild populations of the specie (Peñaloza et al., 2015). In the present work, the stem bark samples S_I and S_{II} were characterized as POA chemotype with *cis* (chemotype **I**) and *trans* (chemotype **II**) D/E ring junction, respectively, while S_{III} was characterized as TOA chemotype (chemotype **III**) (Fig. 2). Likewise, the leaf samples L_{II} and L_{III} were characterized as POA chemotype with *trans* D/E ring junction (chemotype **II**) and TOA chemotype (chemotype **III**), in that order. The cat's claw chemotype seems to be more clearly defined in L_{II} and L_{III} than in S_{II} and S_{III} (Fig. 2). This may be due to the fact the biosynthesis of these oxindole alkaloids occurs in leaves first, before they are distributed to other organs of the plant, where they undergo isomerization and bioconversion (Laus et al., 1997; Peñaloza et al., 2015). Although POA and TOA contents were quite similar in sample S_{IV}, it was classified as TOA chemotype (chemotype **III**) owing to the high content of the latter. Among all selected samples, only S_I, S_{II} and L_{II} (POA *cis* and *trans* chemotypes) showed a TOA content lower than 0.05% (w/w), thus fulfilling this U. S. pharmacopeia quality requirement (USP, 2016).

3.2. Obtaining and characterization of oxindole alkaloid purified fractions (OAPFs)

The fractionation method applied consisted in a multiple step ion-exchange process which avoids oxindole alkaloids isomerization allowing suitable yields, recovery and reproducibility, such as previously reported (Kaiser et al., 2013a). Although all samples were fully identified as *U. tomentosa*, the total alkaloid contents found in OAPFs were dissimilar among them (Table 2). Actually, these alkaloid contents ranged from 19.66% to 87.89% (w/w) and seemed unrelated to any of the chemotypes analyzed.

3.3. Cytotoxicity and genotoxicity evaluation against human leukocytes

Human leukocytes represent a recognized model aiming at the evaluation of cytotoxicity and genotoxicity in non malignant cells. Since other active substances occurring in the ethanolic crude extract from cat's claw stem bark can hinder univocal conclusion, the crude extract from S_{II} (CES_{II}) was also included this experiment. Concentrations ranging from 18.7 – 935.4 μM and 1.2 – 59.5 μM, respectively were employed for the cytotoxicity evaluation of the purified fractions (OAPFs) and crude extract (CES_{II}) (Fig. 3A). It is noteworthy that, against human leukocytes the oxindole alkaloids from cat's claw showed significant cytotoxic activity. Thus, cell viability decreased significantly even after treatment with the lowest concentration of 18.7 μM of S_I, S_{IV} and L_{III}. Comparable activity was noticed for S_{II}, S_{III} and L_{II}, but at a concentration higher than 187.04 μM. The IC_{50} values calculated

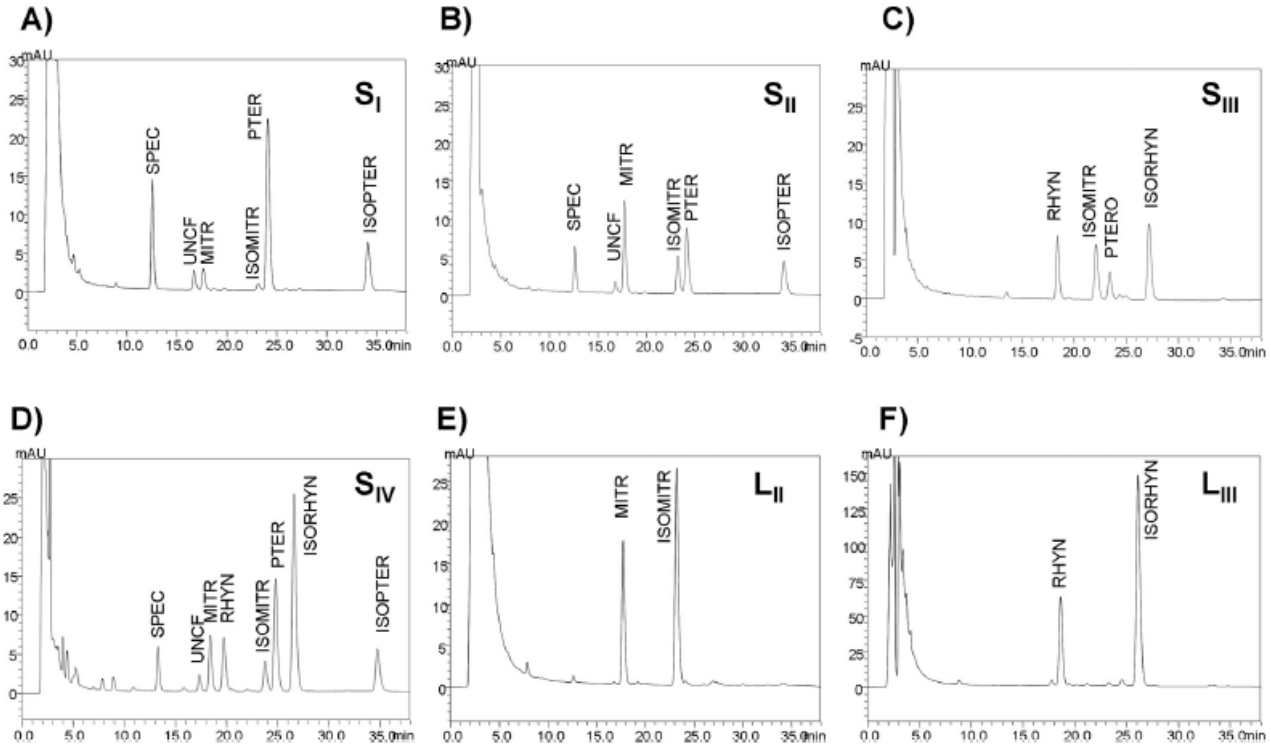

Fig. 2. Chromatographic profiles (245 nm) of tetracyclic (TOA) and pentacyclic oxindole alkaloids (POA) found in the different cat's claw chemotypes: chemotype **I** (POA with *cis* D/E ring junction) (A); chemotype **II** (POA with *trans* D/E ring junction) (B;E); chemotype **III** (TOA) (C;D;F). Speciophylline (SPEC) RT: 12.7 min; uncarine F (UNCF) RT: 16.7 min; pteropodine (PTER) RT: 24.1 min; isopteropodine (ISPTER) RT: 34.1 min – POA with *cis* D/E ring junction; mitraphylline (MIT) RT: 17.8 min; isomitraphylline (ISMITR) RT: 23.1 min – POA with *trans* D/E ring junction; rhynchophylline (RHY) RT: 19.1 min; isorhynchophylline (ISRHY) RT: 26.3 min – TOA.

from a four-parameter Weibull equation ranged from 33.80 to 736.23 µM for OAPFs, and 44.32 µM for CE (Table 3). Since the total alkaloid content of OAPF from S_{II} (75.16%, w/w) was clearly higher than that found in CES_{II} (4.45%, w/w), the lower IC_{50} value of CES_{II} compared to S_{II} suggests that other compounds present in the CES_{II}, such as quinovic acid glycosides and polyphenols can also contribute to the cytotoxic activity (Dietrich et al., 2014). In addition, the dissimilar cat's claw chemotypes showed different cytotoxicities against human leukocytes. Chemotype **I** (S_I) showed higher cytotoxic activity when compared to chemotype **II** (S_{II} and L_{II}) and chemotype **III** (S_{III}, S_{IV} and L_{III}). Therefore, the cytotoxicity of the cat's claw samples against human leukocytes, a non malignant cell model, seems to be closely related to pentacyclic oxindole alkaloids with *cis* D/E ring junction (speciophylline, uncarine F, pteropodine and isopteropodine). It should be mentioned that no significant cytotoxic effect was previously reported for cat's claw oxindole alkaloids by other non malignant cell line models. Rinner et al. (2009) did not found significant reduction in the viability of human skin fibroblast cells (HF-SAR) after 48 h of incubation with 200 µM of pteropodine and isopteropodine. On the

Table 2
Chemical constitution of crude extract obtained from cat's claw stem bark (CES_{II}) and oxindole alkaloids purified fractions (OAPFs) obtained from cat's claw stem bark (S_I–S_{IV}) and leaf samples (L_{II} and L_{III}).

Sample	Total oxindole alkaloid content (g%)[a]	Total POA with *cis* D/E ring junction content (g%)[b]	Total POA with *trans* D/E ring junction content (g%)[c]	TOA content (g%)[d]	TOA/POA ratio	Chemotype
S_I	19.66 ± 1.90	18.61 ± 1.70	1.05 ± 0.20	ND	NA	**I** (POA with *cis* D/E ring junction)
S_{II}	75.16 ± 3.26	46.56 ± 1.93	28.68 ± 1.34	ND	NA	**II** (POA with *trans* D/E ring junction)
S_{III}	54.49 ± 5.50	5.11 ± 0.35	18.23 ± 1.67	31.15 ± 3.85	1.33 ± 0.10	**III** (TOA)
S_{IV}	87.89 ± 10.42	36.52 ± 4.61	11.31 ± 1.26	40.06 ± 4.56	0.84 ± 0.01	**III** (TOA)
L_{II}	56.30 ± 1.52	4.25 ± 0.18	52.06 ± 1.34	ND	NA	**II** (POA with *trans* D/E ring junction)
L_{III}	83.60 ± 5.50	3.77 ± 0.20	6.34 ± 0.63	73.48 ± 4.74	7.25 ± 0.23	**III** (TOA)
CES_{II}	4.45 ± 0.10	2.49 ± 0.05	1.97 ± 0.05	ND	NA	**II** (POA with *trans* D/E ring junction)

Mean ± standard deviation of three consecutive batches (X ± SD, n = 3); POA: pentacyclic oxindole alkaloids; TOA: tetracyclic oxindole alkaloids; ND: Not detected; NA: Not applicable.

[a] Obtained by the sum of total POA and TOA contents.
[b] Obtained by the sum of individual alkaloid contents (speciophylline, uncarine F, pteropodine and isopteropodine).
[c] Obtained by the sum of individual alkaloid contents (mitraphylline, isomitraphylline).
[d] Obtained by the sum of individual alkaloid contents (rhyncophylline and isorhyncophylline).

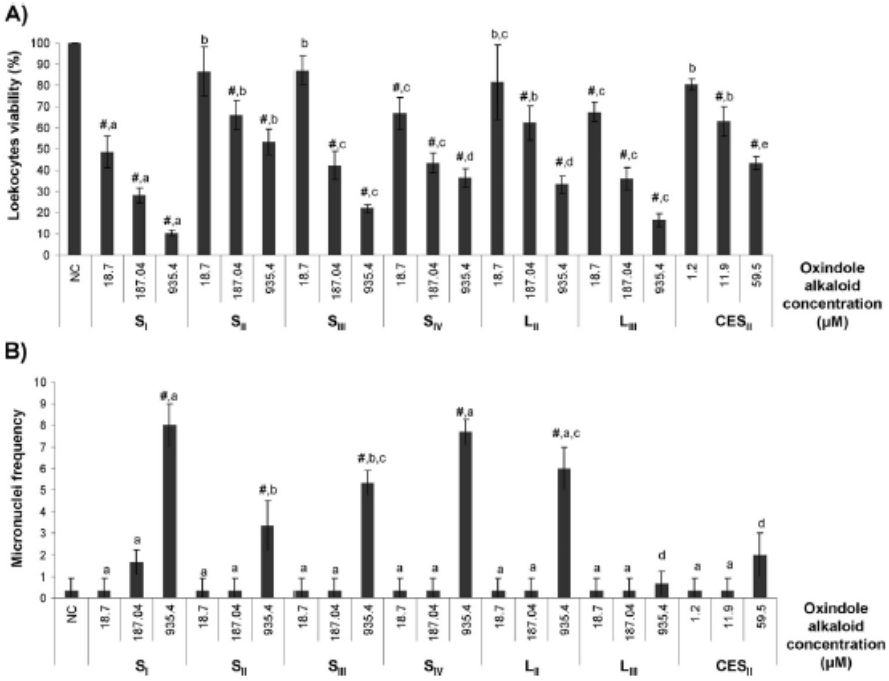

Fig. 3. Leukocyte viability assay (A) and micronuclei frequency assay (B) after treatment (72 h) with stem bark crude extract (CES_{II}) and oxindole alkaloid purified fractions obtained from stem bark (S_I-S_{IV}) and leaves (L_{II} and L_{III}) of the different cat's claw chemotypes (n=3). #statistical difference from negative control (NC, phosphate buffered saline PBS, pH 7.2) obtained from Snedecor *f*-test for variances followed by Student *t*-test ($p<0.05$). [a,b,c,d,e] Same letters indicate statistically equivalent results by Student *t*-test ($p>0.05$) for the same concentration level; S_I: chemotype **I** (pentacydic oxindole alkaloids (POA) with *cis* D/E ring junction); S_{II}, L_{II} and CES_{II}: chemotype **II** (POA with *trans* D/E ring junction); S_{III}, S_{IV} and L_{III}: chemotype **III** (tetracyclic oxindole alkaloids (TOA)).

Table 3
Inhibitory concentration 50% values (IC_{50}) of stem bark crude extract (CES_{II}) and oxindole alkaloids purified fractions (S_I-S_{IV}; L_{II} and L_{III}) evaluated in human bladder cancer cell line (T24), human glioblastoma cell line (U-251-MG) and human leukocytes, respectively.

Sample	IC_{50} (μM)			Chemotype
	T24	U-251-MG	Human leukocytes	
S_I	181.68 ± 8.36^{a} (SI=0.19)	351.64 ± 7.67^{a} (SI=0.10)	33.80 ± 6.10^{a}	**I** (POA with *cis* D/E ring junction)
S_{II}	$241.88 \pm 60.42^{a,b}$ (SI=3.04)	353.63 ± 38.27^{a} (SI=2.08)	736.23 ± 76.93^{b}	**II** (POA with *trans* D/E ring junction)
S_{III}	$263.97 \pm 53.54^{a,b}$ (SI=0.57)	327.58 ± 82.75^{a} (SI=0.46)	149.63 ± 14.48^{c}	**III** (TOA)
S_{IV}	$265.05 \pm 47.16^{a,b}$ (SI=0.43)	374.30 ± 34.78^{a} (SI=0.30)	$112.80 \pm 31.00^{c,e}$	**III** (TOA)
L_{II}	229.19 ± 26.10^{b} (SI=1.95)	403.50 ± 33.54^{a} (SI=1.11)	446.18 ± 30.63^{d}	**II** (POA with *trans* D/E ring junction)
L_{III}	$197.79 \pm 0.68^{a,b}$ (SI=0.43)	398.69 ± 2.13^{a} (SI=0.21)	85.09 ± 7.13^{e}	**III** (TOA)
CES_{II}	9.54 ± 0.89^{c} (SI=4.64)	NI	44.32 ± 2.09^{f}	**II** (POA with *trans* D/E ring junction)

Mean ± standard deviation of three independent experiments (X ± SD, n=3); selectivity index value SI=IC_{50} human leukocytes/IC_{50} T24 or U-251-MG cell lines; NI: No inhibitory activity at concentration range evaluated (2.97 – 23.74 μM) expressed as total oxindole alkaloids content present in the extract. [a,b,c,d,e,f]Same letters indicate results statistically equivalents by Student *t*-test ($p>0.05$) for each cell line evaluated.

other hand, Muhammad et al. (2001) found different IC_{50} values after the incubation of VERO cells with oxindole alkaloids with *cis* D/E ring junction. Speciophylline showed lower IC_{50} value (39 μg/mL equivalent to 106 μM) compared to pteropodine (higher than 50 μg/mL equivalent to 136 μM) and isopteropodine, which was inactive in the concentration range evaluated.

Micronuclei frequency, an important indicative of DNA mutagenesis, was increased significantly after treatment with 935.4 μM of all samples, excepting L_{III} and CES_{II}, where no significant increase could be observed (Fig. 3B). The higher micronuclei frequency was noted with S_I (chemotype **I**), followed by S_{IV} (chemotype **III**) and L_{II} (chemotype **II**). Moreover, from the comet assay data, no significant DNA damage was found either after treatment with OAPFs or with CES_{II} (Fig. 4). Previous studies performed with cat's claw preparations from stem bark also revealed weak genotoxic potential (Romero-Jiménez et al., 2005; Valerio Jr and Gonzales, 2005). Therefore, both OAPFs and CES_{II} showed weak DNA

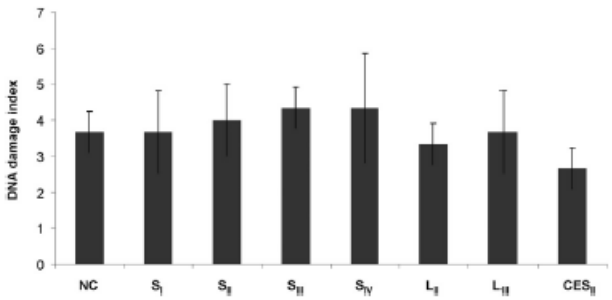

Fig. 4. Comet assay after treatment with stem bark crude extract (CES_{II}) (11.9 μM) and oxindole alkaloid purified fractions (18.7 μM) obtained from stem bark (S_I-S_{IV}) and leaves (L_{II} and L_{III}) of the different cat's claw chemotypes (n=3). S_I: chemotype **I** (pentacyclic oxindole alkaloids (POA) with *cis* D/E ring junction); S_{II}, L_{II} and CES_{II}: chemotype **II** (POA with *trans* D/E ring junction); S_{III}, S_{IV} and L_{III}: chemotype **III** (tetracyclic oxindole alkaloids (TOA)).

damage in the concentration range evaluated, and no clear relationship could be found between the different chemotypes and genotoxicity against human leukocytes.

3.4. Cytotoxicity evaluation against human malignant cells

The antitumor activity of cat's claw has been mostly ascribed to oxindole alkaloids (Heitzman et al., 2005; Kaiser et al., 2013a; Pilarski et al., 2010; Zhang et al., 2015), but without any distinction among chemotypes. On this occasion, the cytotoxicity of the cat's claw chemotypes was evaluated against human bladder cancer (T24) and human glioblastoma (U-251-MG) cell lines. From a four-parameter Weibull equation, the IC_{50} value estimated for T24 cell line ranged from 181.68 to 267.05 μM for OAPFs, and 9.54 μM for CES_{II} (Table 3). For the U-251-MG cell line, it ranged from 351.64 to 403.50 μM for OAPFs, CES_{II} being ineffective (Table 3). As previously reported (Dietrich et al., 2014), the quinovic acid glycoside purified fraction from cat's claws showed a higher cytotoxic potential against human bladder cancer cell line (T24) compared to oxindole alkaloid purified fraction. On the other hand, the cytotoxicity of CES_{II} against the human glioblastoma (U-251-MG) cell line was much weaker (non significant) than all the OAPFs evaluated. Therefore, these results suggest some relationship between this activity and the high content of oxindole alkaloids found in those fractions.

The grouped IC_{50} values against malignant cell lines (T24 and U-251-MG) and non malignant cell line (human leukocytes) revealed that all cat's claw chemotypes were effective against both malignant cell lines (Figs. 5A and B), but they showed different cytotoxicity against a non malignant cell line (Fig. 5C). Consequently, chemotype **II** (S_I) was more selective (selectivity index (SI) > 1) against malignant cell lines, when compared to chemotype **I** (S_{II} and L_{II}) and chemotype **III** (TOA) (selectivity index (SI) < 1) (Table 3). In addition, any antagonistic effect between POA and TOA could be verified for antitumor activity against the cell lines evaluated differently from the behavior observed in relation to immunomodulatory activity (Keplinger et al., 1999; Wurm et al., 1998). However, the presence of TOA in the alkaloid profile seems to decrease its selectivity against the malignant cell lines, as could be verified from S_{IV} (SI = 0.30 – 0.43; Chemotype **III**), that presents an equivalent content of POA and TOA, compared to S_{II} (SI = 2.08 – 3.04; Chemotype **II**) composed only by POA (Figs. 2B, D and Table 3).

3.5. Monitoring of oxindole alkaloid profile throughout the cell incubation

Isomerization of oxindole alkaloids has been often reported and its rate is dependent of pH, solvent polarity and temperature of the medium (Laus et al., 1996). About cat's claw oxindole alkaloids, their isomerization was recently reported in cell viability assays performed in buffered medium at pH 7.4, at 37 °C (Kaiser et al., 2013a). In the present work, a similar outcome was found, namely, the individual concentrations of POA and TOA also varied through the 24 h-incubation, until a new equilibrium among isomers was reached (Figs. 6A and C). As can be seen, the individual content ratios of the oxindole alkaloids were originally different, but they became equivalent after 24 h of incubation. Nonetheless,

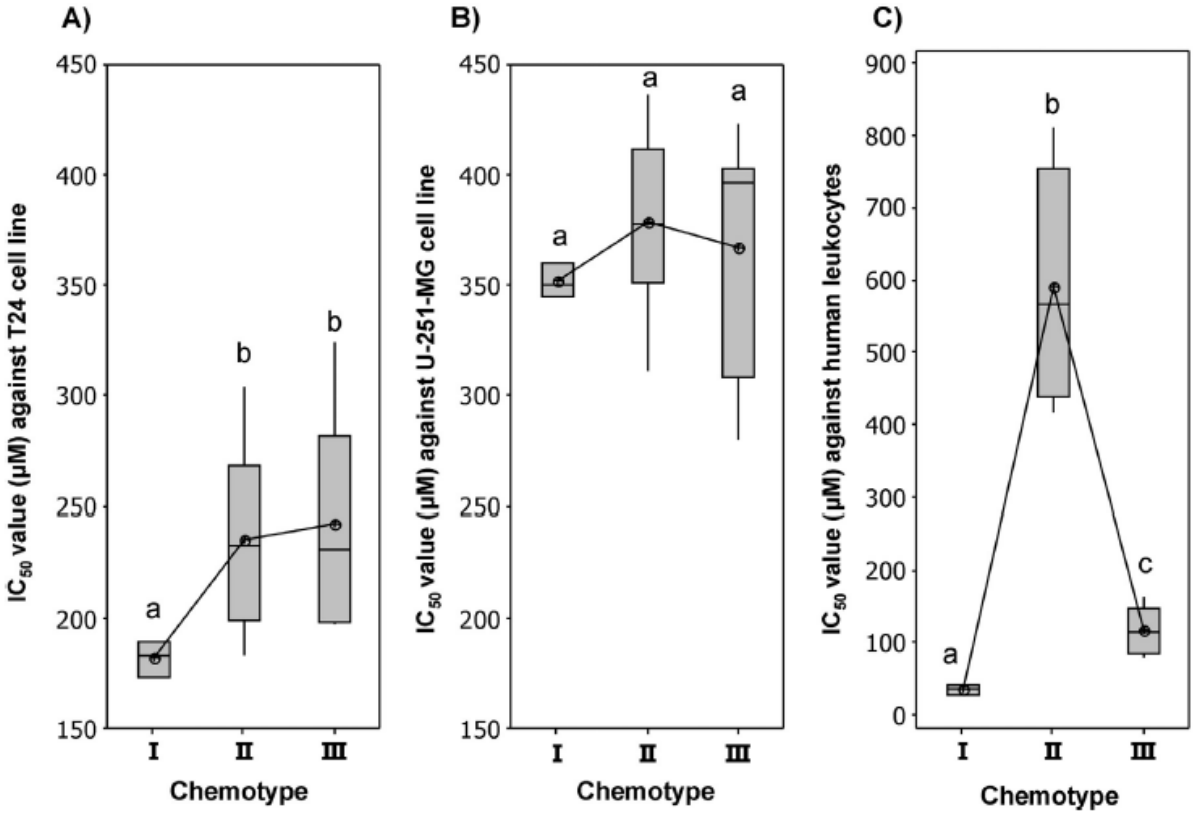

Fig. 5. Box-plot of IC_{50} values obtained from the evaluation of oxindole alkaloid purified fractions (OAPFs) against human bladder cancer cell line (T24) (A), human glioblastoma cell line (U-251-MG) (B) and human leukocytes (C). ^{a,b,c} Same letters indicate statistically equivalent results by Student *t*-test ($p > 0.05$) for each cell line evaluated. Chemotype **I** (pentacyclic oxindole alkaloids (POA) with *cis* D/E ring junction; S_I); chemotype **II** (POA with *trans* D/E ring junction; S_{II}, L_{II}); chemotype **III** (tetracyclic oxindole alkaloids (TOA); S_{III}, S_{IV} and L_{III}).

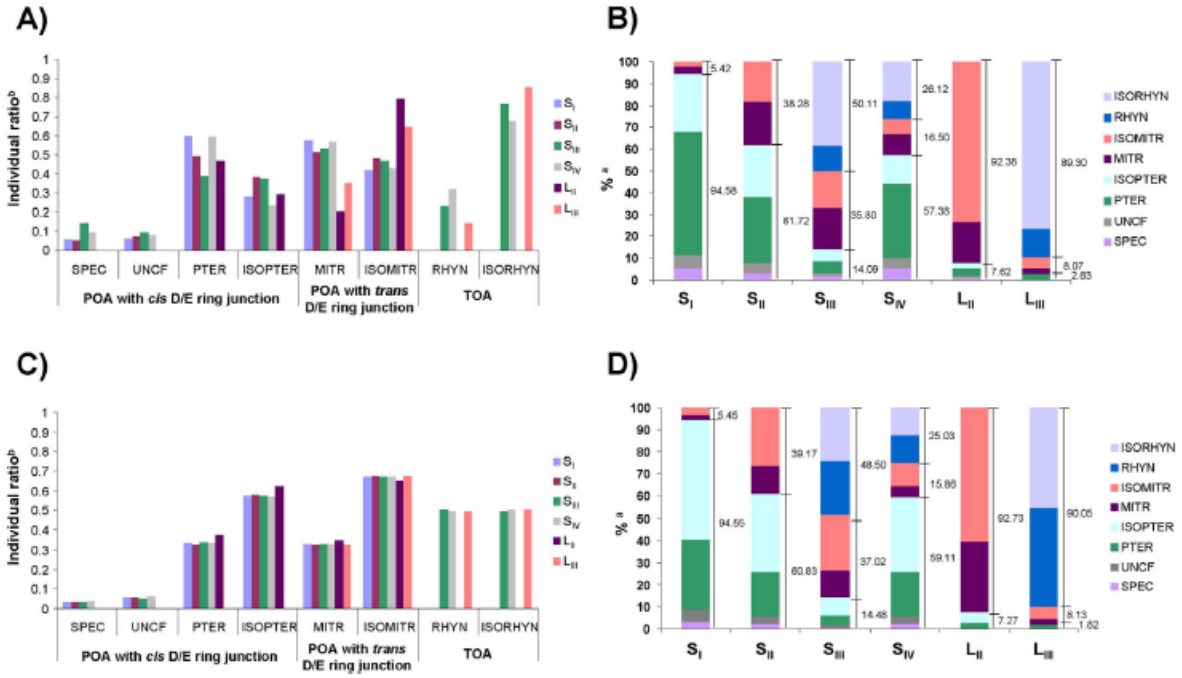

Fig. 6. Oxindole alkaloid profiles and individual oxindole alkaloid ratios in the oxindole alkaloid purified fractions (OAPFs) obtained from cat's claw stem bark (S_I-S_{IV}) and leaves (L_{II} and L_{III}) at initial time (A and B) and after 24 h of incubation (C and D) under similar conditions to those employed in cell treatment (PBS, pH 7.4 at 37 °C in a humid atmosphere saturated with 5% CO_2). [a]percentage in relation to total alkaloid content (sum of individual contents of pentacyclic (POA) and tetracyclic oxindole alkaloids (TOA)). [b]individual ratio in relation to total POA with *cis* D/E ring junction (sum of speciophylline (SPEC), uncarine F (UNCF), pteropodine (PTER), isopteropodine (ISPTER) individual contents); total POA with *trans* D/E ring junction (sum of mitraphylline (MIT), isomitraphylline (ISMITR) individual contents) and total TOA (sum of rhynchophylline (RHY) isorhynchophylline (ISRHY) individual contents).

the original D/E junction ring conformation of each type of isomer remained unaffected as well as the original chemotype attributed to each sample (Figs. 6B and D). For instance, speciophylline, uncarine F, and pteropodine were isomerized to isopteropodine. Hence, even after isomerization the *cis* D/E ring junction was preserved, consequently sample S_I continue to belong to chemotype **I**. Likewise, the *trans* D/E ring junction remained unaffected in samples S_{II} and L_{II}, despite the isomerization of mitraphylline to isomitraphylline, consequently chemotype **II** remains unchanged. Regarding samples S_{III}, S_{IV} and L_{III} from chemotype **III** (TOA), the conversion of isorhyncophylline to rhyncophylline also did not alter the initial chemotype of the samples.

4. Conclusions

The cat's claw chemotypes (**I**, **II** and **III**) showed similar cytotoxicity against malignant cell lines evaluated (T24 and U-251-MG). On the other hand, chemotype **I** (POA with *cis* D/E ring junction) followed by chemotype **III** (TOA) showed higher cytotoxic potential against the non malignant cell line evaluated (human leukocytes) when compared to chemotype **II** (POA with *trans* D/E ring junction). Consequently, chemotype **II** was more selective against malignant cell lines. Concerning genotoxicity, no major alteration was found in the micronuclei frequency or DNA damage index after treatment with the different cat's claw chemotypes in their effective cytotoxic concentration range against malignant or non malignant cell lines. Only after treatment with 935.4 µM were verified significant increases in the micronuclei frequency. Although alkaloid isomerization was found throughout the cell incubation, the original cat's claw chemotype of each sample remains unchanged. Therefore, selection and definition of the adequate cat's claw chemotype seems to be very important for antitumor activity, since it influences cytotoxic selectivity against malignant cells.

Conflicts of interest

We declare that we do not have any financial or other relationships that might lead to a conflict of interest.

Funding sources

None.

Authorship

The experiments were conceived and designed by: SK FD MMM LFSO AMOB GGO. The experiments were performed by: SK ARC VP FD FM. The data were analyzed by: SK FD MMM GGO. The following contributed reagents/materials/analysis tools: SK FD LFSO AMOB. The paper was written by: SK GGO.

Acknowledgments

The authors are grateful to the Brazilian Conselho Nacional de Desenvolvimento Científico e Tecnológico (CNPq) (Grant no. 159461/2012-0) and Coordenação de Aperfeiçoamento de Pessoal de Nível Superior (CAPES) for financial support to conduct this study.

References

Burow, M.E., Weldon, C.B., Tang, Y., Navar, G.L., Krajewski, S., Reed, J.C., Hammond, T. G., Clejan, S., Beckman, B.S., 1998. Differences in susceptibility to tumor necrosis factor α-induced apoptosis among MCF-7 breast cancer cell variants. Cancer Res. 58, 4940–4946.

Dietrich, F., Kaiser, S., Rockenbach, L., Figueiró, F., Bergamin, L.S., da Cunha, F.M., Morrone, F.B., Ortega, G.G., Battastini, A.M.O., 2014. Quinovic acid glycosides purified fraction from *Uncaria tomentosa* induces cell death by apoptosis in the T24 human bladder cancer cell line. Food Chem. Toxicol. 67, 222–229.

Dos Santos Montagner, G.F.F., Sagrillo, M., Machado, M.M., Almeida, R.C., Mostardeiro, C.P., Duarte, M.M.M.F., Da Cruz, I.B., 2010. Toxicological effects of ultraviolet radiation on lymphocyte cells with different manganese superoxide dismutase Ala16Val polymorphism genotypes. Toxicol. In Vitro 24, 1410–1416.

Heitzman, M.E., Neto, C.C., Winiarz, E., Vaisberg, A.J., Hammond, G.B., 2005. Ethnobotany, phytochemistry and pharmacology of *Uncaria* (Rubiaceae). Phytochemistry 66, 5–29.

Kaiser, S., Dietrich, F., de Resende, P.E., Verza, S.G., Moraes, R.C., Morrone, F.B., Batasttini, A.M.O., Ortega, G.G., 2013a. Cat's claw oxindole alkaloid isomerization induced by cell incubation and cytotoxic activity against T24 and RT4 human bladder cancer cell lines. Planta Med. 79, 1413–1420.

Kaiser, S., Verza, S.G., Moraes, R.C., Pittol, V., Peñaloza, E.M.C., Pavei, C., Ortega, G.G., 2013a. Extraction optimization of polyphenols, oxindole alkaloids and quinovic acid glycosides from cat's claw bark by Box–Behnken design. Ind. Crops Prod. 48, 153–161.

Kaiser, S., Verza, S.G., Moraes, R.C., De Resende, P.E., Barreto, F., Pavei, C., Ortega, G. G., 2013b. Cat's claw oxindole alkaloid isomerization induced by common extraction methods. Quim. Nova 36, 808–814.

Keplinger, K., Laus, G., Wurm, M., Dierich, M.P., Teppner, H., 1999. *Uncaria tomentosa* (Wild). Ethnomedicinal uses and new pharmacological, toxicological and botanical results. J. Ethnopharmacol. 64, 23–34.

Laus, G., Brössner, D., Keplinger, K., 1997. Alkaloids of Peruvian *Uncaria tomentosa*. Phytochemistry 45, 855–860.

Laus, G., Brössner, D., Senn, G., Wurst, K., 1996. Analysis of the kinetics of isomerization of spirooxindole alkaloids. J. Chem. Soc. Perkin Trans. 2, 1931–1936.

Laus, G., 1998. Kinetics of isomerization of tetracyclic spirooxindole alkaloids. J. Chem. Soc. Perkin Trans. 2, 315–331.

Mosmann, T., 1983. Rapid colorimetric assay for cellular growth and survival: application to proliferation and cytotoxicity assays. J. Immunol. Methods 65, 55–63.

Muhammad, I., Dunbar, D.C., Khan, R.A., Ganzera, M., Khan, I.A., 2001. Investigation of Uña De Gato I. 7-deoxyloganic acid and 15 N NMR spectroscopic studies on pentacyclic oxindole alkaloids from *Uncaria tomentosa*. Phytochemistry 57, 781–785.

Peñaloza, E.M.C., Kaiser, S., Resende, P.E., Pittol, V., Carvalho, A.R., Ortega, G.G., 2015. Chemical composition variability in the *Uncaria tomentosa* (cat's claw) wild population. Quim. Nova 38, 378–386.

Pilarski, R., Filip, B., Wietrzyk, J., Kurás, M., Gulewicz, K., 2010. Anticancer activity of the *Uncaria tomentosa* (Willd.) DC. preparations with different oxindole alkaloid composition. Phytomedicine 17, 1133–1139.

Rinner, B., Li, Z.X., Haas, H., Siegl, V., Sturm, S., Stuppner, H., Pfragner, R., 2009. Antiproliferative and pro-apoptotic effects of *Uncaria tomentosa* in human medullary thyroid carcinoma cells. Anticancer Res. 29, 4519–4528.

Romero-Jiménez, M., Campos-Sánchez, J., Analla, M., Muñõz-Serrano, A., Alonso-Moraga, A., 2005. Genotoxicity and *anti*-genotoxicity of some traditional medicinal herbs. Mutat. Res./Genet. Toxicol. Environ. Mutagen. 585, 147–155.

Schmid, W., 1975. The micronucleus test. Mutat. Res./Environ. Mutagen. Relat. Subj. 31, 9–15.

Singh, N.P., McCoy, M.T., Tice, R.R., Schneider, E.L., 1988. A simple technique for quantitation of low levels of DNA damage in individual cells. Exp. Cell Res. 175, 184–191.

Tice, R.R., Agurell, E., Anderson, D., Burlinson, B., Hartmann, A., Kobayashi, H., Miyamae, Y., Rojas, E., Ryu, J.C., Sasaki, Y.F., 2000. Single cell gel/comet assay: guidelines for *in vitro* and *in vivo* genetic toxicology testing. Environ. Mol. Mutagen. 35, 206–221.

USP, 2016. United States Pharmacopeia, 39th ed. U.S. Pharmacopeia., Rockville.

Valerio Jr, L.G., Gonzales, G.F., 2005. Toxicological aspects of the South American herbs cat's claw (*Uncaria tomentosa*) and maca (*Lepidium meyenii*). Toxicol. Rev. 24, 11–35.

Winkler, C., Wirleitner, B., Schroecksnadel, K., Schennach, H., Mur, E., Fuchs, D., 2004. *In vitro* effects of two extracts and two pure alkaloid preparations of *Uncaria tomentosa* on peripheral blood mononuclear cells. Planta Med. 70, 205–210.

Wurm, M., Kacani, L., Laus, G., Keplinger, K., Dierich, M.P., 1998. Pentacyclic oxindole alkaloids from *Uncaria tomentosa* induce human endothelial cells to release a lymphocyte-proliferation regulating factor. Planta Med. 64, 701–704.

Zhang, Q., Zhao, J.J., Xu, J., Feng, F., Qu, W., 2015. Medicinal uses, phytochemistry and pharmacology of the genus *Uncaria*. J. Ethnopharmacol. 173, 48–80.

Capítulo 3. Influência da complexação com ciclodextrinas sobre a isomerização dos alcaloides oxindólicos de *Uncaria tomentosa*

Introdução

Os alcaloides oxindólicos de *U. tomentosa* apresentam elevada susceptibilidade à isomerização em solução sendo a velocidade dependente do pH do meio, polaridade do solvente e temperatura (LAUS *et al.*, 1996). Em decorrência disso, a isomerização pode ocorrer durante o processo extrativo e até mesmo durante incubação dos alcaloides oxindólicos sob condições normalmente utilizadas em experimentos com cultura de células (KAISER *et al.*, 2013a; KAISER *et al.*, 2013c). Consequentemente, com a alteração do perfil de alcaloides em função do período de incubação não é possível estabelecer uma relação entre o mesmo e a atividade observada. Em estudo *in silico* via *docking* molecular foi possível demonstrar que a mitrafilina apresenta maior afinidade ao sítio de ligação da enzima diidrofolato redutase, um importante alvo para moléculas com potencial antitumoral e antimicrobiano, em relação aos demais alcaloides oxindólicos (KOZIELEWICZ *et al.*, 2014). Contudo, preservar a mitrafilina em solução sem que ocorra sua isomerização a isomitrafilina é muito difícil.

A complexação com ciclodextrinas pode minimizar efetivamente a degradação e a isomerização de moléculas lábeis, como é o caso da astilbina e do *trans*-resveratrol (BERTACCHE *et al.*, 2006; ZHANG *et al.*, 2013). Assim o presente capítulo visou avaliar a influência da complexação com ciclodextrinas sobre a isomerização dos alcaloides oxindólicos de *U. tomentosa*.

Este capítulo é apresentado na forma de artigo a ser submetido para publicação em periódico relevante que se enquadre no escopo do presente estudo.

Artigo 3. Effect of cyclodextrins on the cat's claw oxindole alkaloids isomerization

Effect of cyclodextrins on the cat's claw oxindole alkaloids isomerization

Samuel Kaiser*, Vanessa Pittol, Sara Elis Bianchi, Ânderson Ramos Carvalho, Valquiria Linck Bassani, George González Ortega

Laboratório de Desenvolvimento Galênico (LDG), Faculdade de Farmácia, Universidade Federal do Rio Grande do Sul (UFRGS), Porto Alegre, RS, Brazil

* Correspondence to: S.Kaiser, Av. Ipiranga, 2752, Sala 606, Santana, Porto Alegre - RS – Brazil, CEP: 90610-000; Tel: +55 (51)3308 5415 Fax: +55 (51)3308 5437; E-mail: *samokaiser@yahoo.com.br*

ABSTRACT

Introduction – The *Uncaria tomentosa* or cat's claw is composed mainly by polyphenols, quinovic acid glycosides, tetracyclic (TOA) and pentacyclic oxindole alkaloids (POA), to which have been assigned important biological activities, such as immunostimulant and the antitumor. However, the oxindole alkaloids are susceptible to isomerization even in the cell incubation conditions. In contrast, the cyclodextrins (CD) are able to reduce not only the degradation, but also the isomerization of compounds mainly due to their ability for inclusion of the labile moiety of compound into hydrophobic cavity.

Objective – To evaluate the effect of cyclodextrins on the isomerization of the oxindole alkaloids from cat's claw under incubation conditions commonly used in the culture cells experiments.

Material and Methods – An authentic cat's claw stem bark sample was properly extracted and submitted to ion exchange process to obtain an oxindole alkaloids purified fraction (OAPF). Excessive amounts of OAPF (5 mg) were used in the phase-solubility studies with β-CD (1 – 10 mM), HP-βCD (2 – 20 mM) and SBE-βCD (2 – 20 mM). After, the oxindole alkaloids/SBE-βCD solid complex and a coresponding physical mixture obtained from freeze drying and spatulation, respectively, were properly characterized by DSC, FT-IR, SEM and their oxindole alkaloids content was determined by HPLC-PDA. The isomerization kinetics of oxindole alkaloids in the OAPF, solid complex and physical mixture was evaluated under cell incubation (PBS 10 mM pH 7.4) at 37 ºC.

Results – The oxindole alkaloids/βCD and oxindole alkaloids/HP-βCD phase-solubility diagrams indicate that complexes obtained showed limited aqueous solubility or negative deviation from linearity. On the other hand, the oxindole alkaloids/SBE-βCD phase-solubility diagram showed linear relationships between increases in the aqueous solubility of oxindole alkaloids (POA and TOA) and SBE-βCD concentration, characteristic of A_L-type curve. A stoichiometric ratio of 1:1 were obtained for both POA (*Ks* 122.47 M^{-1}) and TOA (*Ks* 25.57 M^{-1}) with enhancement of

2.92 and 1.33 fold in the aqueous solubility of POA and TOA, respectively, in the presence of 20 mM of SBE-βCD, in comparison with their intrinsic solubility. The contents of oxindole alkaloids found in oxindole alkaloids/SBE-βCD solid complex and physical mixture were 7.3 % (w/w) and 11.1 % (w/w), respectively and their characterization by DSC and FT-IR suggest that complexation occurs even in solid state. Moreover, the complexation of oxindole alkaloids with SBE-βCD reduced the isomerization rate of oxindole alkaloids under cell incubation conditions.

Conclusions – The complexation of oxindole alkaloids with SBE-βCD in solid state reduce the isomerization rate of oxindole alkaloids from cat's claw under incubation conditions commonly used in cell experiments.

Keywords: *Uncaria tomentosa*; cat's claw; oxindole alkaloids; isomerization; cyclodextrins; Sulfobutyl ether β-cyclodextrin.

INTRODUCTION

Uncaria tomentosa (Willd.) DC. (Rubiaceae) have been used in the Asháninka medicine for treatment of several immunological and inflammatory diseases, as well as of the cancer (Keplinger et al., 1999; Heitzman et al., 2005). This specie, popularly known as cat's claw or "Uña de Gato" due to curved hooked thorns, is composed mainly by polyphenols, quinovic acid glycosides, tetracyclic (TOA) and pentacyclic oxindole alkaloids (POA), to which have been assigned important biological activities, such as immunostimulant and antitumor (Keplinger et al., 1999; Heitzman et al., 2005; Kaiser et al., 2013a).

Nevertheless, the oxindole alkaloids can be easily isomerized even under extraction or cell incubation conditions (Kaiser et al., 2013a; Kaiser et al., 2013b). For POA with *cis* D/E ring junction, four interconvertible diastomeric forms are found (speciophylline, uncarine F, pteropodine and isopteropodine) while for POA with *trans* D/E ring junction only one pair of interconvertible diastomeric forms are found (mitraphylline and isomitraphylline) (Laus et al., 1996) (**Figure 1**). For TOA two pairs of interconvertible diastomeric forms are found (rhyncophylline and isorhyncophylline; corynoxeine and isocorynoxeine) (Laus et al., 1998) (**Figure 1**). The isomerization process involves a retro-Mannich reaction concerning the stereogenic centers C-3 and C-7 with the formation of the zwitterionic intermediate, being the isomerization rate dependent mainly of the temperature, pH and solvent polarity (Laus et al., 1996). Basically, the increase in the medium temperature enhances the isomerization rate (Laus et al., 1996). Under acid conditions the formation of the hydrogen bond between protonated N-4 and lactam carbonyl, when the groups in a *syn* position to each other (mitraphylline, pteropodine and isopteropodine), inhibits the formation of the zwitterionic intermediate slowing down the isomerization rate (Laus et al., 1996). In addition, the high solvent polarity stabilizes the zwitterionic intermediate increasing the isomerization rate in comparison with less polar solvents, being the isomerization rate inversely proportional to Dimroth-Reichardt polarity parameter of the solvent (Laus et al., 1996).

Figure 1

Cyclodextrins are cyclic oligosaccharides from natural source with a hydrophilic external surface and a lipophilic cavity, which have been extensively used to increase aqueous solubility of poorly soluble compounds, to improve their bioavailability and the stability due to the formation of the inclusion complex (Loftsson et al., 2005; Kurkov & Loftsson, 2013). β-cyclodextrin (β-CD) and their hydrophilic derivatives hydroxypropyl β-cyclodextrin (HP-βCD) and sulfobutyl ether β-cyclodextrin (SBE-βCD) have been used as complexing agents because of their commercial availability and cavity size which is suitable for interaction with aromatic and heterocyclic rings (Del Valle, 2004; Kurkov & Loftsson, 2013). For these reasons they are employed in about 77% of the formulation with use of cyclodextrins available in the commercial market (Kurkov & Loftsson, 2013). In contrast with β-CD that presents limited water solubility and nephrotoxicity, their hydrophilic derivatives HP-βCD and SBE-βCD have been considered very safe for parenteral administration (Del Valle, 2004; Loftsson et al., 2005; Kurkov & Loftsson, 2013). The cyclodextrins are able to minimize not only the degradation, but also the isomerization of compounds mainly due to their ability for inclusion of the labile moiety of compound into hydrophobic cavity (Loftsson et al., 2005). Thus, the isomerization rate as well as the degradation of the astilbin, a dihydroflavonol found in *Hypericum perforatum*, was minimized after complexation with β-CD and γ-CD (Zhang et al., 2013). Moreover, the isomerization of the *trans*-resveratrol to *cis*-resveratrol induced by sunlight exposure also could be decreased after complexation with α-CD (Bertacche et al., 2006).

Several in vitro studies have been performed with the isolated oxindole alkaloids from cat's claw, mainly in relation to their antitumor properties (Stuppner et al., 1993; Muhammad et al., 2001; Bacher et al., 2006; Giménez et al., 2007; Prado et al., 2007; Rinner et al., 2009). However, these studies did not take into account the easy isomerization of the oxindole alkaloids that occurs under incubation conditions and it relationship with the biological activity (Kaiser et al., 2013a). In addition, molecular docking studies revealed that the mitraphylline had the best fitting in the binding site of the dihydrofolate reductase, a target site for anticancer and antimicrobial drugs, in comparison with isomitraphylline, speciophylline, uncarine F, pteropodine and isopteropodine (Kozielewicz et al., 2014).

Thus, taking account the importance of minimizing the isomerization of oxindole alkaloid mainly throughout the biological activity evaluation, the present study aims to evaluate the effect of cyclodextrins on the oxindole alkaloids isomerization under incubation conditions commonly used in the culture cells experiments.

EXPERIMENTAL

Materials

β-cyclodextrin (β-CD, Kleptose® standard) and hydroxypropyl β-cyclodextrin (HP-βCD, Kleptose® HPB) were supplied by Roquette Frères (Lestrem, France) while Sulfobutyl ether β-cyclodextrin (SBE-βCD, Captisol®) was kindly supplied by CyDex Inc. (CA, USA). Acetonitrile HPLC grade (Tedia, USA) and ultrapure water obtained from Milli-Q® system (Millipore, USA) were used in phase-solubility study and HPLC analyses. All other reagents used were of analytical grade.

Obtaining of the oxindole alkaloids purified fraction (OAPF)

An authentic cat's claw stem bark sample collected from the Peruvian Amazon (November 2012) was certified by J.R. Campos De la Cruz (Museo de Historia Natural de la Universidad Nacional Mayor de San Marcos, Lima, Peru) being the voucher of specimen (ICN157759) deposited at Herbarium of Universidade Federal do Rio Grande do Sul (Porto Alegre, Brazil). The sample after drying at 40 ºC in air-circulating convection oven (Memmert, Germany) was comminuted in cutter mill (SK1 Retsch, Germany) and extracted by 2-h dynamic maceration in magnetic stirrer at 300 rpm (IKA RH basic 1, Germany) with hydroethanolic solution 63% (v/v) in a plant:solvent ratio of 0.5:10 (w/v) (Kaiser et al., 2013c). The resulting solution was filtered through paper filter (Paper filter Whatman nº 2, UK) and submitted to ion exchange process using a strong anionic resin (Dowex Marathon; Sigma-Aldrich, USA) in accordance with previously described (Kaiser et al., 2013a). The OAPF

obtained was concentrated under vacuum at 40°C up to half of their original weight (Büchi R-114, Germany), and freeze-dried at once (Modulyo 4 L, Edwards, USA).

Phase-solubility study

A phase-solubility study was carried out according to the method of Higuchi and Connors (1965). An excess amount of OAPF (5 mg) was added to 1.5 mL of water (pH 5.5) containing increase concentrations of cyclodextrins: β-CD (1 – 10 mM), HP-βCD (2 – 20 mM) and SBE-βCD (2 – 20 mM). After 48h of magnetic stirring (300 rpm) at 37 ± 2 ºC in a water bath (HE4B, IKA, Germany), the resulting solution was filtered through a PVDF 0.45-μm membrane (Millipore, USA), properly diluted (25 times) in acetonitrile:water (50:50, v/v) and analyzed by HPLC-PDA method to oxindole alkaloids assay in accordance with previously validated method (Kaiser et al., 2013b) employing mitraphylline (PhytoLab, Germany) as external standard. The total oxindole alkaloid content was determined by the sum of individual alkaloid contents (speciophylline, uncarine F, pteropodine, isopteropodine, mitraphylline, isomitraphylline) for POA, and (rhyncophylline and isorhyncophylline) for TOA. All results were expressed by the mean of three determinations.

The apparent stability constant (*Ks*, M^{-1}) of oxindole alkaloids/cyclodextrins complexes were calculated based on the phase-solubility diagram according to the following equation (1):

$$Ks = \frac{slope}{So(1 - slope)} \quad \textbf{(1)}$$

where the *slope* was determined by regression analysis and *So* represents the intrinsic solubility of the oxindole alkaloids in water (oxindole alkaloids solubility in absence of cyclodextrins).

Evaluation of pH effect on the complexation of oxindole alkaloids/ SBE-βCD

Excess amounts of OAPF (5 mg) were added to 1.5 mL of water (pH 3.0, adjusted with formic acid), water (pH 5.5, adjusted with formic acid); water (pH 7.4 adjusted with NaOH solution 10% (w/v), and phosphate buffered saline (PBS) 10 mM (pH 7.4 adjusted with NaOH solution 10% (w/v)) in the presence or absence of SBE-βCD (10mM). The oxindole alkaloids assay was performed by HPLC-PDA (Kaiser et al., 2013b) such as described in the phase-solubility study. The solubility increasing of the oxindole alkaloids was evaluated by comparison between the solubility in the solution containing SBE-βCD and intrinsic solubility of the oxindole alkaloids in the medium.

Preparation of the oxindole alkaloids/SBE-βCD solid complex and physical mixture

The solid complex of oxindole alkaloids/SBE-βCD was prepared in the molar ratio 1:1 in water (pH 5.5, adjusted with formic acid). After 48h of magnetic stirring (300 rpm) at 37 ºC in a thermostatic water bath, the resulting solution was filtered through a PVDF 0.45-µm membrane and the filtrated was freeze-dried at once. The physical mixture of oxindole alkaloids/SBE-βCD was prepared by geometric mixing following the same molar ratio used in the solid complex preparation. Both preparations were stored in the dry conditions (25 ºC; moisture 65 %, w/w).

Characterization of oxindole alkaloids/SBE-βCD solid complex and physical mixture

The oxindole alkaloids/SBE-βCD solid complex and the corrresponding physical mixture were characterized by infrared spectroscopy analysis, differential scanning calorimetry analysis and assay of the oxindole alkaloids content by HPLC-PDA.

Assay of the oxindole alkaloid content by HPLC-PDA

Aliquots of oxindole alkaloids/SBE-βCD solid complex (6 mg) or physical mixture (6mg) were dissolved in 25.0 mL of acetonitrile:water (50:50, v/v) and analyzed by HPLC-PDA (Kaiser et al., 2013b).

Differential scanning calorimetry (DSC)

Thermal analysis of the samples was performed using a DSC-60 calorimeter (Shimadzu, Japan). The samples were accurately weighed (1 – 2 mg) in aluminum pans, crimped and analyzed at 10 °C/min of heating rate (25 °C – 300 °C) and 50 ml/min of nitrogen gas flow. The temperature was previously calibrated employing indium (mp 157 °C) and zinc (mp 420 °C) as standards.

FT-IR analysis

The solid samples were analyzed at FT-IR Spectrometer (Spectrum BX, Perkin Elmer, Germany) using the diamond ATR sensor. The spectra were recorded in the range 400 − 4400 cm^{-1} using a resolution of 4 cm^{-1} and twenty accumulations.

Scanning electron microscopy (SEM)

Photomicrographs were performed at a voltage of 10 kV in a JSM 6060 scanning electron microscope (Jeol, USA). Samples were deposited on aluminum stubs containing double-sided tape and coated under vacuum with a thin layer of gold.

Isomerization kinetic evaluation

Aliquots of OAPF (10 mg), oxindole alkaloids/SBE-βCD solid complex (100 mg) and physical mixture (100 mg) were dissolved in 100 mL of PBS 10 mM (pH 7.4 adjusted

with NaOH solution 10% (w/v)) and incubated at 37°C. Aliquot of 200μL were collected in the initial time and after 1, 2, 4, 6, 8 and 24 h of incubation, properly diluted (ten times) in acetonitrile:water (50:50, v/v) and analyzed by HPLC-PDA (Kaiser et al., 2013b).

Statistical analysis

The results were statistically evaluated by Snedecor *f*-test for variances followed by Student *t*-test (Microsoft Excel software, USA) and $p < 0.05$ values were considered significant.

RESULTS AND DISCUSSION

Phase-solubility study

The phase-solubility diagrams obtained from oxindole alkaloids/cyclodextrin complexes (**Figure 2**) showed distinct behaviors according to Higuchi and Connors (1965). From oxindole alkaloids/βCD phase-solubility diagram was verified a small increase in the both TOA and POA solubility at initial concentrations of βCD followed by decrease in oxindole alkaloids solubility after 2 mM of βCD (**Figure 2A**). This behavior, classified as B_S-type characteristic for complexes with limited solubility, can be explained by the poor hydrosolubility of the βCD (Del Valle; 2004; Loftsson et al., 2005).

Figure 2

From oxindole alkaloids/HP-βCD phase-solubility diagram could be verified an increase in the POA solubility with the increase in HP-βCD concentration, a characteristic behavior of the A_N-type curve (**Figure 2B**). The negative deviation from linearity may be associated with changes in the dielectric constant of the aqueous medium, changes in complex solubility or self-association of cyclodextrin molecules (Loftsson et al., 2005). On the other hand, the TOA solubility decreases linearly with

the increase in the HP-βCD concentration, behavior characteristic of the B_I-type curve (**Figure 2B**). The TOA solubility reduction occurred probably due to the formation of the insoluble complexes with HP-βCD in the medium (Del Valle; 2004; Loftsson et al., 2005).

From oxindole alkaloids/SBE-βCD phase-solubility diagram was verified a linear relationships between increases in the aqueous solubility of oxindole alkaloids (POA and TOA) and SBE-βCD concentration (**Figure 2C**), in contrast with the profile observed in βCD and HP-βCD phase-solubility diagrams (**Figures 2A** and **2B**). Thus, the curves obtained could be classified as A_L-type in accordance with Higuchi and Connors (1965). As the slopes obtained from linear regression analyses were less than unity for both POA and TOA, it can be assumed that the increases in solubility were due to formation of 1:1 complexes (**Table 1**). In addition, higher apparent stability constant (Ks) obtained for POA (122.47 M^{-1}) in relation to TOA (25.57 M^{-1}) demonstrated the preference of SBE-βCD by POA. Consequently, was obtained 2.92-fold increase in aqueous solubility of POA, while for TOA it was just about 1.33-fold (**Table 1**).

Table 1

The POA is composed by six diastomeric forms (speciophylline, uncarine F, pteropodine and isopteropodine with *cis* D/E ring junction; mitraphylline and isomitraphylline with *trans* D/E ring junction), while TOA is composed by a pair of diastomeric forms (rhyncophylline and isorhyncophylline). In solution, these diastomeric forms show distinct physicochemical properties and structural conformations, which confer individual parameters of complexation for each compound (**Table 1**). In a general mode, the affinity for SBE-βCD seems to be related to D/E ring junction conformation, since the POA with *cis* D/E ring junction (uncarine F > isopteropodine > pteropodine) showed higher apparent stability constant (*Ks*) in comparison to POA with *trans* D/E ring junction (isomitraphylline > mitraphylline), excepting for speciophylline. The last one is extremely unstable in aqueous solution, so that after few hours in solution its concentration decreases significantly due to the isomerization (Laus et al., 1996; Keplinger et al., 1999; Kaiser et al., 2013a). For this

reason, the speciophylline/SBE-βCD complexation was ineffective since its isomerization rate seems to be faster than kinetics of complex formation in aqueous solution. In relation to TOA, the rhyncophylline showed a higher affinity by SBE-βCD in relation to isorhyncophylline.

Evaluation of pH effect on the complexation of oxindole alkaloids/ SBE-βCD

As oxindole alkaloids are weak bases, their intrinsic solubility can be modulated by pH. From non-ionized compounds can be obtained more stable complexes in comparison to their ionic forms, but their ionization can increase the intrinsic solubility and consequently enhance the complexation efficiency (Del Valle; 2004; Loftsson et al., 2005; Kurkov & Loftsson; 2013). On the other hand, under basic conditions the isomerization rate of the oxindole alkaloids is higher than in under acid conditions (Laus et al., 1996). Thus, the pH modulation of the medium can modify the complexation efficiency and the isomerization rate of oxindole alkaloids.

Both POA and TOA concentration decreased with the increase in the pH of the medium (**Figure 3**). Mainly for POA, the SBE-βCD (10 mM) minimized the concentration decrease in relation to absence of cyclodextrins in the medium (intrinsic solubility). Moreover, significant increments in the oxindole alkaloids solubility were verified, mainly in buffered medium pH 7.4 in the presence of SBE-βCD. This behavior can be explained in part by the ionization of the oxindole alkaloids. The POA showed pKa values ranging from 4.05 to 5.5, while the TOA ranging from 5.3 to 6.4 (Finch & Taylor, 1962; Chan et al., 1966). Thus, under acid conditions the oxindole alkaloids are in the ionized form, mainly at pH 3.0. Consequently, the aqueous solubility of oxindole alkaloids increased, but their stability decreased as evidenced by non significant difference between the intrinsic solubility and the SBE-βCD ($p > 0.05$) (**Figure 3A** and **3B**). On the other hand, at pH 7.4 the oxindole alkaloids in the non-ionized form showed lower aqueous solubility than at pH 3.0, but the complex stability increased as verified from significant difference between the intrinsic solubility and SBE-βCD, mainly for POA ($p < 0.05$). Moreover in buffered medium at pH 7.4, the

aqueous solubility of oxindole alkaloids decreased significantly in relation to pH 7.4 unbuffered medium evidencing a salting out event. Under this condition, significant increases in the aqueous solubility were verified for both POA (2.78) and TOA (2.10) in the presence of SBE-βCD in relation to their intrinsic solubility ($p < 0.05$) (**Figure 3A** and **3B**). Although the aqueous solubility increment of indole alkaloids at pH 7.4 had been higher than that observed at pH 5.5, the isomerization rate at pH 7.4 is higher than that verified at pH 5.5 (Laus et al., 1996). Thus, the pH 5.5 seems to be better choice taking into account the equilibrium between isomerization rate of the oxindole alkaloids and their complexation efficiency with SBE-βCD.

Figure 3

Characterization of oxindole alkaloids/SBE-βCD solid complex and physical mixture (PM)

Assay of the oxindole alkaloid content by HPLC-PDA

The OAPF used for obtaining the solid complex and physical mixture showed a total oxindole alkaloids content of 87.9% (w/w). On the other hand, the oxindole alkaloids/SBE-βCD solid complex showed a total oxindole alkaloids content of 7.3 % (w/w), while the physical mixture showed a content of 11.1 %(w/w).

Differential scanning calorimetry (DSC)

The differential scanning calorimetry (DSC) curve obtained for OAPF (**Figure 4A**) showed three endothermic events: the first one at 62 °C corresponds to the loss of bounded water; the second at 172 °C related to the oxindole alkaloids melting point; and the third at 298 ºC, probably related with decomposition of the oxindole alkaloids. In the DSC curve obtained for SBE-βCD, the endothermic event at 84 ºC corresponds to the loss of bounded water while the second endothermic event at 263 ºC corresponds to its decomposition (Jain et al., 2011) (**Figure 4B**). From the oxindole

alkaloids/SBE-βCD solid complex analysis (**Figure 4C**), could be verified a shift in the endothermic event corresponds to loss of bounded water at 56 ºC, while the endothermic event related to decomposition of SBE-βCD was shifted to 274 ºC accompanied with a decrease of the enthalpy variation. Moreover, the absence of endothermic event correspondent to oxindole alkaloids melting point suggests an interaction between the oxindole alkaloids and SBE-βCD. Similar behavior could be verified in DSC curve from physical mixture (**Figure 4D**). Consequently, the interaction between the oxindole alkaloids and SBE-βCD occurs even in the solid phase.

Figure 4

FT-IR analysis

The FT-IR spectrum from OAPF (**Figure 5A**) showed followed characteristic absorption bands: 3,198 cm^{-1} (N−H stretching); 2,934 cm^{-1} (C−H stretching); 1,698 cm^{-1} (C=O stretching); 1,618 cm^{-1} (aromatic C=C stretching); 752 cm^{-1} (=C−H stretching) (Finch & Taylor, 1962; Chan et al., 1966). On the other hand, the FT-IR spectrum from SBE-βCD showed characteristic absorption bands at 3,374 cm^{-1} (−OH stretching), 2,931 cm^{-1} (C−H stretching) and 1,032 and 1,153 cm^{-1} (C−O stretching in alcohol and ether groups, respectively) (**Figure 5B**). The decrease in the intensity of absorption bands correspondent to C=O (stretching), C=C (stretching) and =C−H (stretching) of the oxindole alkaloids, associated to band shifts of 9 cm^{-1} and 3 cm^{-1} in the absorption bands related to −OH and C−O (alcohol and ether groups) in the SBE-βCD, suggest interaction between oxindole alkaloids and SBE-βCD (**Figure 5C**). The physical mixture showed a similar FT-IR spectrum (**Figure 5D**) when compared to solid complex (**Figure 5C**). These findings revealed an interaction between aromatic ring and carbonyl of lactam of oxindole alkaloids and hydroxyl groups of SBE-βCD, even in the solid phase, such as earlier verified from DSC curves.

Figure 5

Scanning electron microscopy (SEM)

The SEM photomicrographs of OAPF showed particles with amorphous characteristic (**Figure 6A**) while the SBE-βCD showed amorphous particles with shrunken spherical shape characteristic of spray dried powder (**Figure 6B**), such as verified previously from X-ray diffraction studies (Jain et al., 2011). Knownly, the SBE-βCD (Captisol ®) is currently isolated by spray drying process that explains the particle shape verified. In the oxindole alkaloids/SBE-βCD solid complex the particles maintained the shrunken spherical shape with small depositions onto surface suggesting a coating of SBE-βCD particles with OAPF particles (**Figure 6C**). The physical mixture (**Figure 6D**) showed a similar particle shape verified in the solid complex (**Figure 6C**), but the deposition of the OAPF particles onto surface of SBE-βCD particles was even more clear.

Figure 6

Isomerization kinetic evaluation

Although the complexation between oxindole alkaloids and SBE-βCD has been evidenced by the characterization of the oxindole alkaloids/SBE-βCD solid complex and physical mixture, the evaluation of the isomerization kinetic deserves attention since the oxindole alkaloids are susceptible to isomerization under incubation conditions similar those generally used in cell cultures for evaluation of biological activity (Kaiser et al., 2013a). Moreover, until now no system was purposed to inhibit or minimize the isomerization of oxindole alkaloids in aqueous medium in order to ensure an alkaloid fraction with the same composition along the biological evaluation, at least.

The isomerization profiles obtained are shown in the **Figure 7**. The isomerization rate of speciophylline, uncarine F and pteropodine to isopteropodine (POA with *cis* D/E ring junction) as well as the isomerization rate of mitraphylline to isomitraphylline

(POA with *trans* D/E ring junction), and isorhyncophylline to rhyncophylline (TOA), decreased in the oxindole alkaloids/SBE-βCD solid complex (**Figure 7B**) and physical mixture (**Figure 7C**) in comparison to OAPF (**Figure 7A**) although their individual proportions are equivalents after 24h of incubation. The oxindole alkaloids/SBE-βCD solid complex showed distinct initial proportion in relation to OAPF and physical mixture that could be associated to isomerization occurrence throughout the solid complex preparation. Previously to freeze drying process, the oxindole alkaloids were magnetically stirred with SBE-βCD in water (pH 5.5) for 48h which may have induced the isomerization of oxindole alkaloids. Therefore, the obtaining of complex in solid state such as in physical mixture was preferable for the complexation aiming to minimize the isomerization process.

Figure 7

The complexation of oxindole alkaloids with SBE-βCD is an equilibrium system between the complex (oxindole alkaloids/SBE-βCD) and its individual components (oxindole alkaloids and SBE-βCD). This dynamic system is susceptible to modifications in the equilibrium conditions, as occurs in the oxindole alkaloids isomerization system. Thus, the free-oxindole alkaloids in solution are isomerized to more stable forms (isopteropodine, POA with *cis* D/E ring junction; isomitraphylline, POA with *trans* D/E ring junction; and rhyncophylline for TOA) even that in lower isomerization rate when compared to verified in OAPF. While in the OAPF the new equilibrium condition was reached after 6 h for POA with *cis* D/E ring junction and after 4 h for POA with *trans* D/E ring junction and TOA (**Figure 7A**), in the physical mixture the new equilibrium condition was reached only after 8 h of incubation period (**Figure 7C**). Therefore, the complexation of oxindole alkaloids with SBE-βCD minimized the isomerization rate but without inhibiting it absolutely.

CONCLUSION

The complexation of oxindole alkaloids was more efficient with SBE-βCD in comparison with HP-βCD and βCD. The characterization of oxindole alkaloids/SBE-βCD solid complex and physical mixture by DSC and FT-IR analysis evidenced that complexation occurs even in solid state. Moreover, the complexation of oxindole alkaloids with SBE-βCD was able to minimize the isomerization rate under incubation conditions mainly in the complex obtained in solid state. On the other hand, in liquid medium the isomerization of oxindole alkaloids was induced even during the complexation process owing to their high susceptibility to isomerization. Therefore, the complexation of oxindole alkaloids with SBE-βCD in solid state can be a valuable alternative to reduce their isomerization under incubation conditions commonly used in cell culture experiments.

ACKNOWLEDGMENTS

The authors are grateful to Brazilian Conselho Nacional de Desenvolvimento Científico e Tecnológico (CNPq) and Coordenação de Aperfeiçoamento de Pessoal de Nível Superior (CAPES) for financial support to conduct this research and Roquette Frères and CyDex Inc. for kindly supplied the βCD; HP-βCD and SBE-βCD, respectively.

REFERENCES

Bacher N, Tiefenthaler M, Sturm S, Stuppner H, Ausserlechner MJ, Kofler R, Konwalinka G. 2006. Oxindole alkaloids from *Uncaria tomentosa* induce apoptosis in proliferating, G0/G1-arrested and bcl-2-expressing acute lymphoblastic leukaemia cells. *Br J Haematol* **132:** 615–622.

Bertacche V, Lorenzi N, Nava D, Pini E, Sinico C. 2006. Host–Guest Interaction Study of Resveratrol With Natural and Modified Cyclodextrins. *J Incl Phenom Macro* **55:** 279–287.

Chan KC, Morsingh F, Yeoh GB. 1966. Alkaloids of *Uncaria pteropoda*. Isolation and structures of pteropodine and isopteropodine. *J Chem Soc Perkin 1* **24:** 2245-2249.

Del Valle, EMM. 2004. Cyclodextrins and their uses: a review. *Proc Biochem* **39:** 1033–1046.

Finch N, Taylor WI. 1962. Oxidative Transformations of Indole Alkaloids. I. The Preparation of Oxindoles from Yohimbine; the Structures and Partial Syntheses of Mitraphylline, Rhyncophylline and Corynoxeine. *J Am Chem Soc*, **84:** 3871–3877.

Giménez DG, Prado EG, Rodríguez TS, Arche AF, De La Puerta R. 2007. Cytotoxic effect of the pentacyclic oxindole alkaloid mitraphylline isolated from *Uncaria tomentosa* bark on human Ewing's sarcoma and breast cancer cell lines. *Planta Med* **76:** 133–136.

Heitzman ME, Neto CC, Winiarz E, Vaisberg AJ, Hammond GB. 2005. Ethnobotany, phytochemistry and pharmacology of *Uncaria* (Rubiaceae). *Phytochemistry* **66:** 5–29.

Higuchi T, Connors KA. 1965. Phase-solubility techniques. *Adv Anal Chem Instrum* **4:** 117–212.

Jain AS, Date AA, Pissurlenkar RRS, Coutinho EC, Nagarsenker MS. 2011. Sulfobutyl Ether7 β-Cyclodextrin (SBE7 β-CD) Carbamazepine Complex: Preparation, Characterization, Molecular Modeling, and Evaluation of In Vivo Anti-epileptic Activity. *AAPS PharmSciTech* **12:** 1163:1175.

Kaiser S, Dietrich F, de Resende PE, Verza SG, Moraes RC, Morrone FB, Batasttini AMO, Ortega GG. 2013a. Cat's Claw Oxindole Alkaloid Isomerization Induced by Cell Incubation and Cytotoxic Activity against T24 and RT4 Human Bladder Cancer Cell Lines. *Planta Med* **79:** 1413–1420.

Kaiser S, Verza SG, Moraes RC, De Resende PE, Barreto F, Pavei C, Ortega GG. 2013b. Cat's claw oxindole alkaloid isomerization induced by common extraction methods. *Quim Nova* **36:** 808–814.

Kaiser S, Verza SG, Moraes RC, Pittol V, Peñaloza EMC, Pavei C, Ortega GG. 2013c. Extraction optimization of polyphenols, oxindole alkaloids and quinovic acid glycosides from cat's claw bark by Box–Behnken design. *Ind Crop Prod* **48:** 153–161.

Keplinger K, Laus G, Wurm M, Dierich MP, Teppner H. 1999. *Uncaria tomentosa* (Wild). Ethnomedicinal uses and new pharmacological, toxicological and botanical results. *J Ethnopharmacol* **64:** 23–34.

Kozielewicz P, Paradowska K, Eric´ S, Wawer I, Zloh M. 2014. Insights into mechanism of anticancer activity of pentacyclic oxindole alkaloids of *Uncaria tomentosa* by means of a computational reverse virtual screening and molecular docking approach. *Monatsh Chem* **145:**1201–1211.

Kurkov SV, Loftsson T. 2013. Cyclodextrins. *Int J Pharm* **453:** 167–180.

Laus G, Brössner D, Senn G, Wurst K. 1996. Analysis of the kinetics of isomerization of spiro oxindole alkaloids. *J Chem Soc Perkin Trans 2* 1931–1936.

Laus G. 1998. Kinetics of isomerization of tetracyclic spiro oxindole alkaloids. *J Chem Soc Perkin Trans 2* 315–331.

Loftsson T, Jarho P, Másson M, Järvinen T. 2005. Cyclodextrins in drug delivery. *Expert Opin Drug Deliv* **2:** 335–351.

Muhammad I, Dunbar DC, Khan RA, Ganzera M, Khan IA. 2001. Investigation of Uña De Gato I. 7-Deoxyloganic acid and 15 N NMR spectroscopic studies on pentacyclic oxindole alkaloids from *Uncaria tomentosa*. *Phytochemistry* **57:** 781–785.

Prado GE, Giménez GMD, Vázquez DR, Sánchez EJL, Rodríguez SMT. 2007. Antiproliferative effects of mitraphylline, a pentacyclic oxindole alkaloid of *Uncaria tomentosa* on human glioma and neuroblastoma cell lines. *Phytomedicine* **4:** 280–284.

Rinner B, Li ZX, Haas H, Siegl V, SturmS, Stuppner H, Pfragner R. 2009. Antiproliferative and pro-apoptotic effects of *Uncaria tomentosa* in human medullary thyroid carcinoma cells. *Anticancer Res* **29:** 4519– 4528.

Stuppner H, Sturm S, Geisen G, Zmian U, Konwalinka G. 1993. A differential sensitivity of oxindole alkaloids to normal and leukemic cell lines. *Planta Med* **59:** A583.

Zhang Q-F, Nie H-C, Shangguang X-C, Yin Z-P, Zheng G-D, Chen J-G. 2013. Aqueous Solubility and Stability Enhancement of Astilbin through Complexation with Cyclodextrins. *J Agric Food Chem* **61:** 151−156.

FIGURES

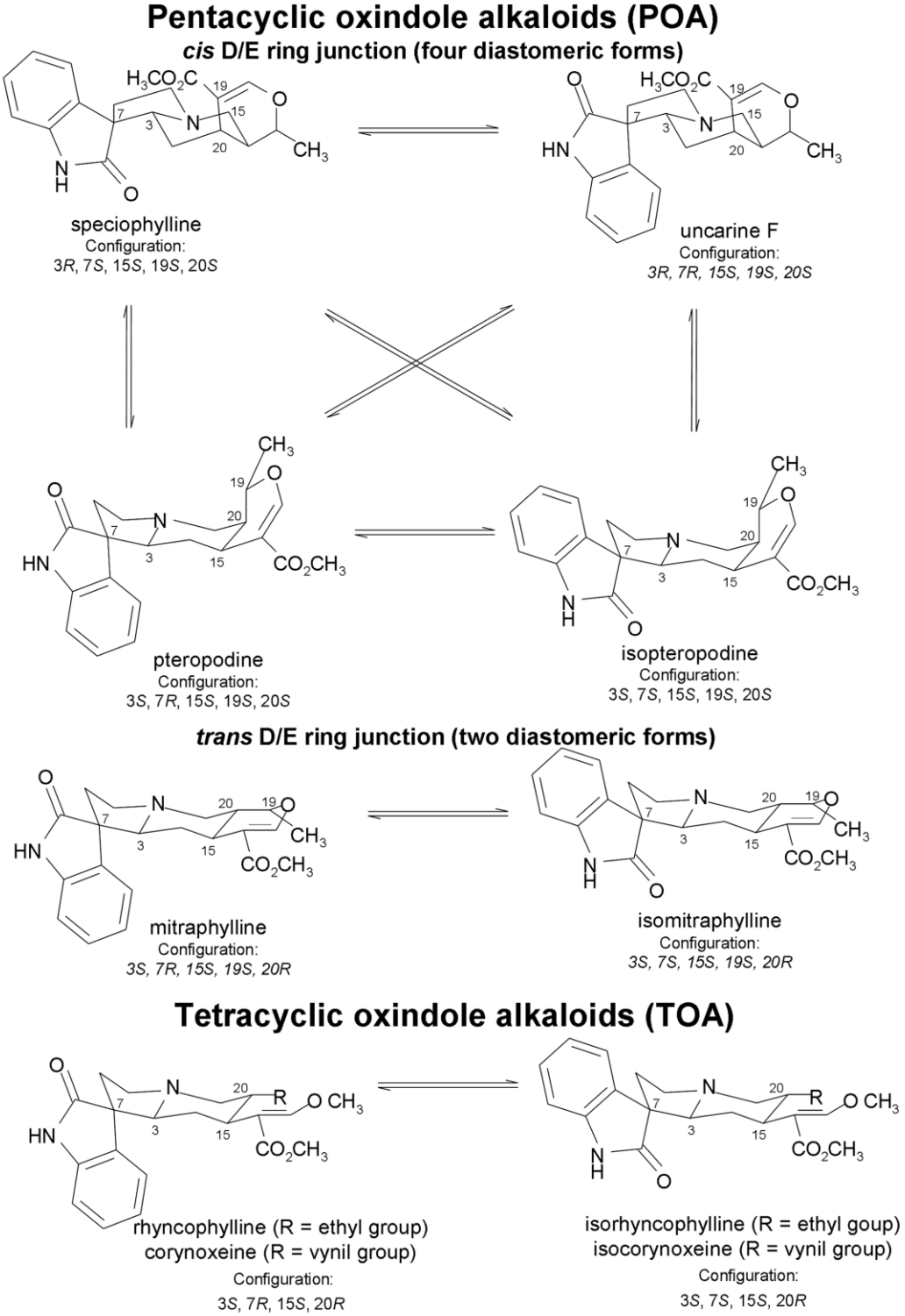

Figure 1. Schematic representation of main oxindole alkaloids reported in cat's claw and their isomerization process.

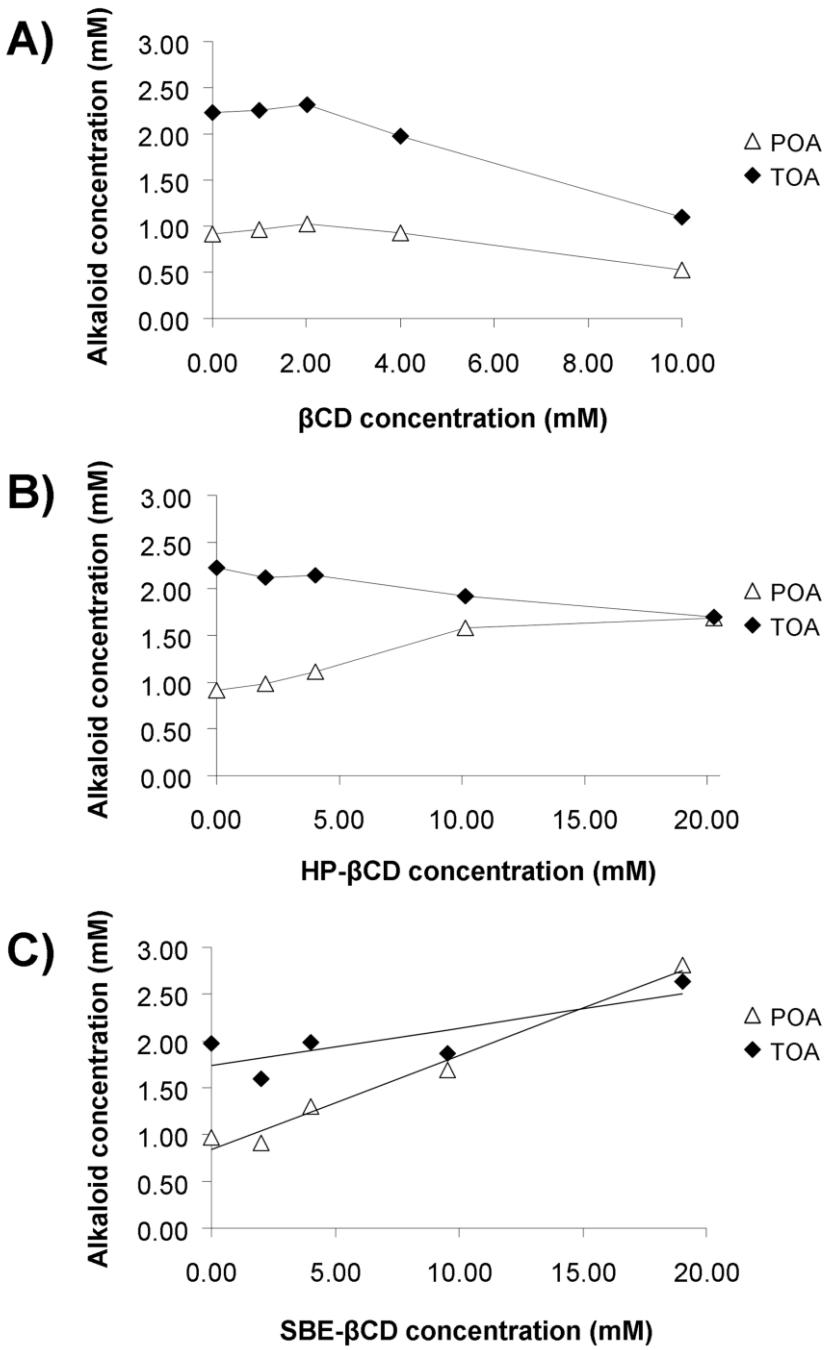

Figure 2. Phase-solubility studies of oxindole alkaloids from cat's claw in presence of βCD (1 – 10 mM) (**A**), HPβCD (2 – 20 mM) (**B**) and SBE-βCD (2 – 20 mM) (**C**). Pentacyclic oxindole alkaloids (POA) content was calculated from the sum of their individual contents (mitraphylline, isomitraphylline, speciophylline, uncarine F, pteropodine and isopteropodine); Tetracyclic oxindole alkaloids (TOA) content was calculated from the sum of their individual contents (rhyncophylline and isorhyncophylline).

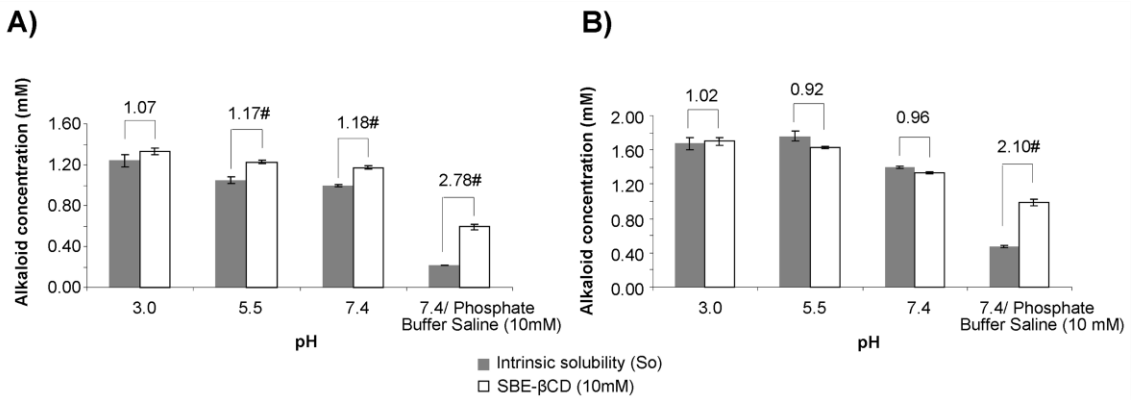

Figure 3. pH effect on the solubility of pentacyclic (POA) (**A**) and tetracyclic oxindole alkaloids (TOA) (**B**) in the absence (intrinsic solubility) and presence of SBE-βCD (10 mM). Upper values represent the solubility increase obtained by ratio between intrinsic solubility (*So*) and solubility in the presence of SBE-βCD 10mM; # significant statistical difference obtained from Snedecor *f*-test for variances followed by Student *t*-test ($p < 0.05$).

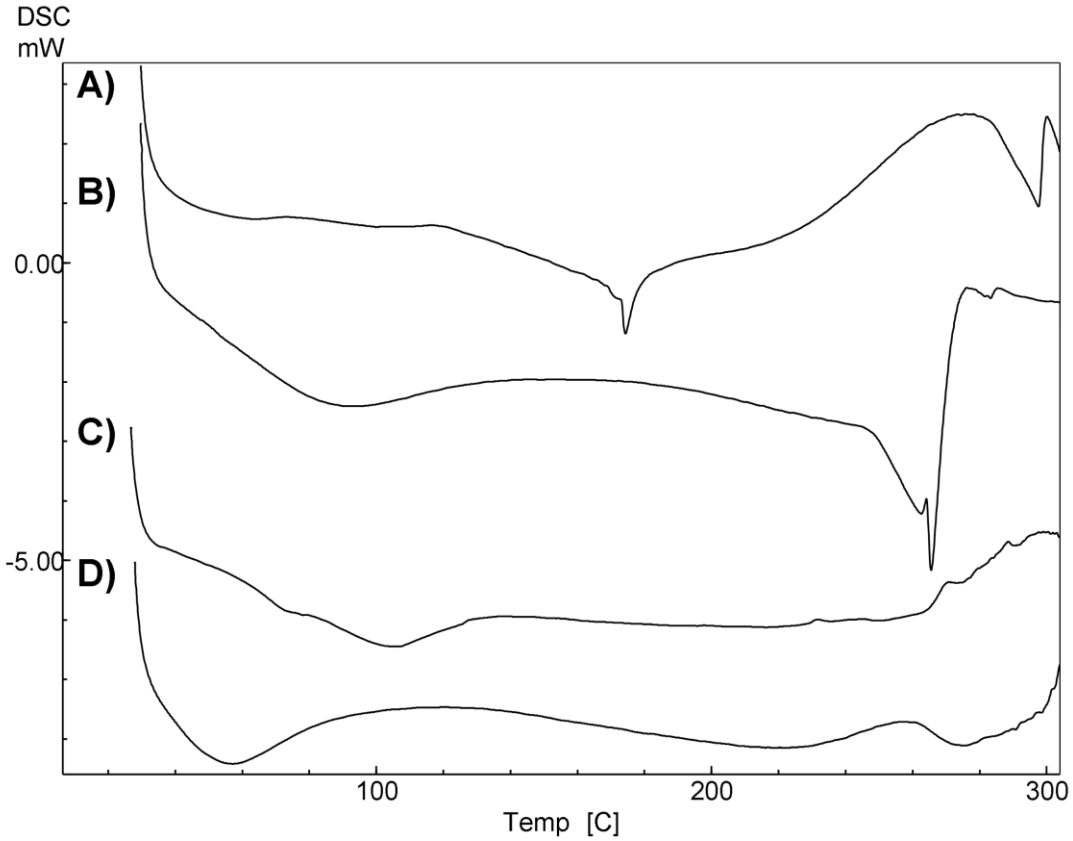

Figure 4. DSC thermograms of oxindole alkaloids purified fraction (OAPF) (**A**), SBE-βCD (**B**), oxindole alkaloids/SBE-βCD solid complex (**C**) and physical mixture (**D**).

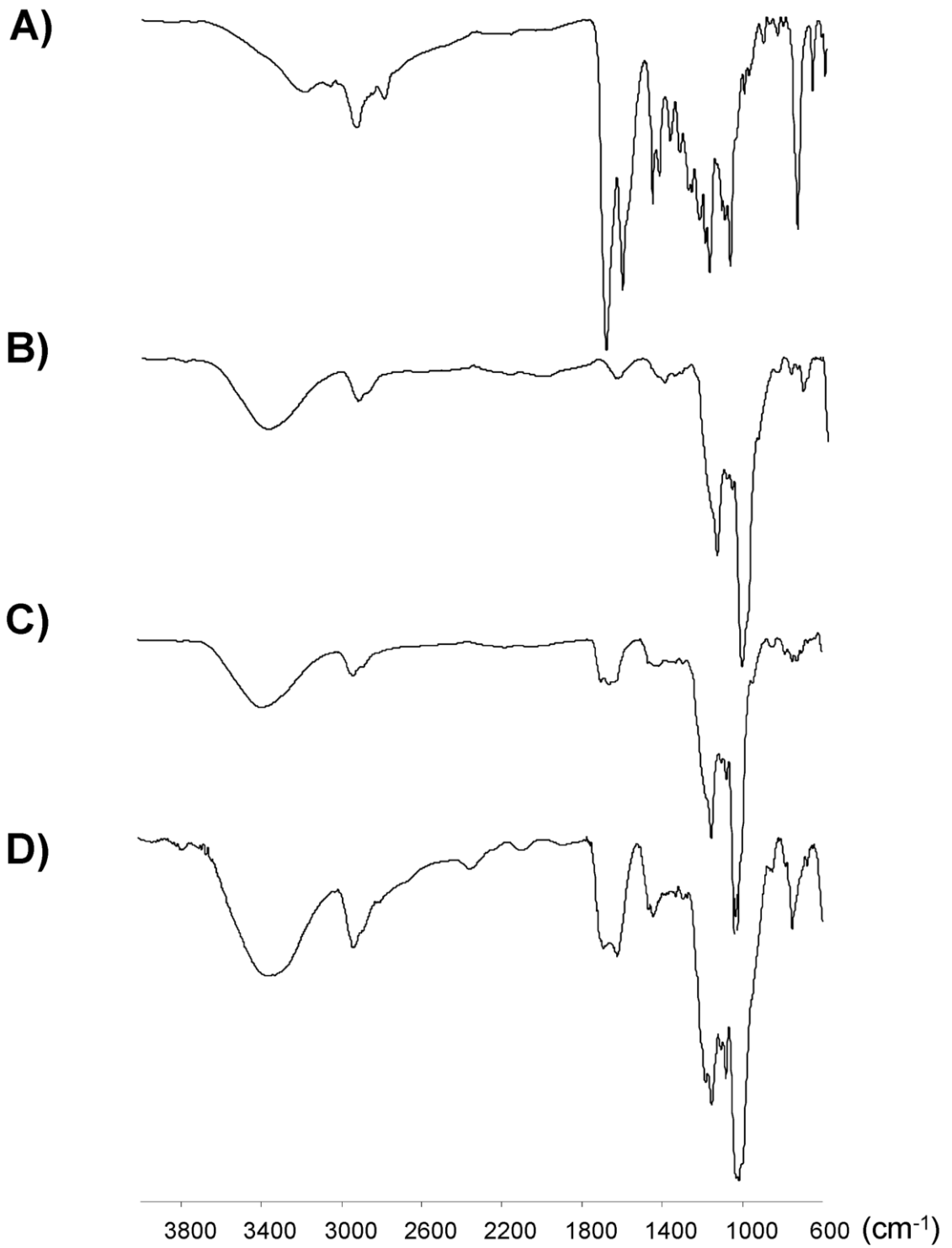

Figure 5. FT-IR spectra of oxindole alkaloids purified fraction (OAPF) (**A**), SBE-βCD (**B**), oxindole alkaloids/SBE-βCD solid complex (**C**) and physical mixture (**D**).

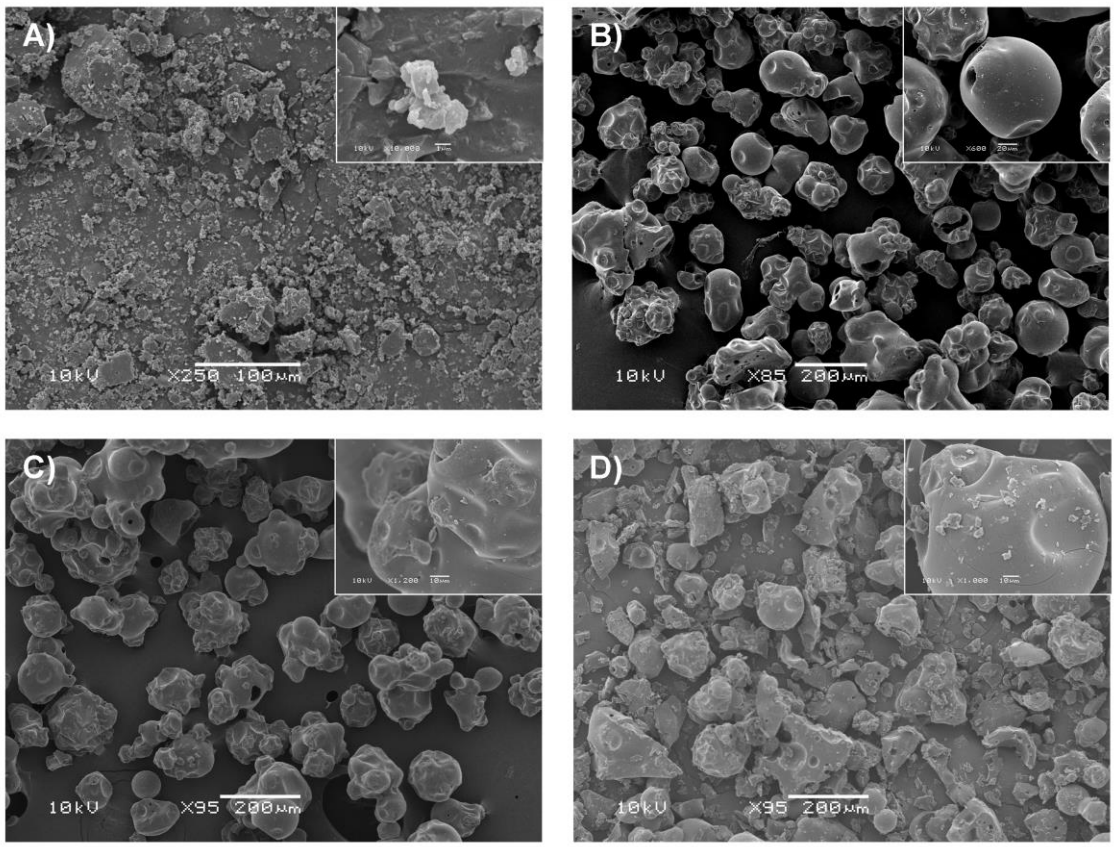

Figure 6. Photomicrographs obtained by scanning electron microscopy (SEM) of oxindole alkaloids purified fraction (OAPF) (**A**), SBE-βCD (**B**), oxindole alkaloids/SBE-βCD solid complex (**C**) and physical mixture (**D**). *Upper right*: higher magnification of the specific regions for more detail.

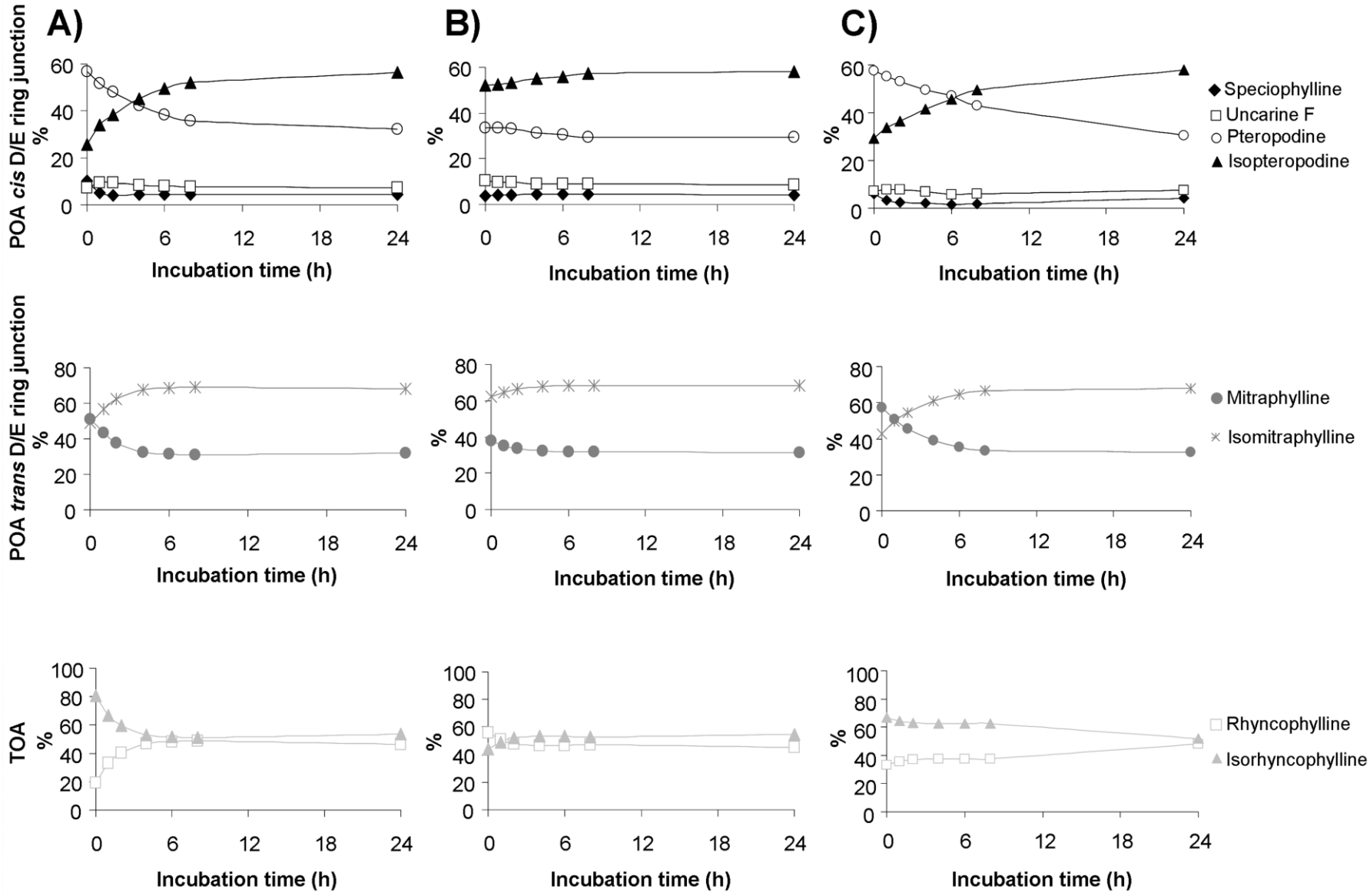

Figure 7. Evaluation of oxindole alkaloids isomerization kinetics in purified fraction (OAPF) (**A**), oxindole alkaloids/SBE-βCD solid complex (**B**) and physical mixture (**C**) throughout the incubation in phosphate buffered saline (pH 7.4) at 37 ºC.

TABLES

Table 1. Parameters of phase-solubility study obtained for oxindole alkaloids in presence of SBE-βCD.

Alkaloid	D/E ring junction	Regression equation	R^2	*So* (mM)	*Ks* (M^{-1})	Solubility increase[a]
mitraphylline	*trans*	y = 0.0084x + 0.214	0.70	0.27	31.05	1.46
isomitraphylline	*trans*	y = 0.0109x + 0.1501	0.99	0.15	73.85	2.42
speciophylline	*cis*	NA	NA	0.09	NA	NA
uncarine F	*cis*	y = 0.0248x + 0.0304	0.99	0.05	492.64	9.91
pteropodine	*cis*	y = 0.0183x + 0.2612	0.95	0.28	67.17	2.25
isopteropodine	*cis*	y = 0.0371x + 0.1299	0.99	0.12	311.54	6.77
Total POA[b]	*NA*	*y = 0.1055x + 0.7671*	*0.97*	*0.96*	*122.47*	*2.92*
rhyncophylline	NA	y = 0.0322x + 1.0369	0.77	1.20	27.62	1.43
isorhyncophylline	NA	y = 0.0084x + 0.6936	0.70	0.77	11.03	1.18
Total TOA[c]	*NA*	*y = 0.048x + 1.6233*	*0.71*	*1.97*	*25.57*	*1.33*

NA: not applied; R^2: determination coefficient; *So*: intrinsic solubility of the oxindole alkaloids in water; *Ks*: apparent stability constant; [a]Obtained by ratio between intrinsic solubility (*So*) and solubility in the presence of SBE-βCD 20mM; [b]Total content of pentacyclic oxindole alkaloids (POA) obtained by the sum of their individual contents (mitraphylline, isomitraphylline, speciophylline, uncarine F, pteropodine and isopteropodine); [c] Total content of tetracyclic oxindole alkaloids (TOA) obtained by the sum of their individual contents (rhyncophylline and isorhyncophylline).

DISCUSSÃO GERAL

A presente tese foi desenvolvida com o intuito de determinar a relevância dos alcaloides oxindólicos em *U. tomentosa* e sua relação com a adulteração empregando-se *U. guianensis*, a ocorrência de quimiotipos em função do perfil de alcaloides oxindólicos e a isomerização dos mesmos. Reconhecidamente, os alcaloides oxindólicos são protagonistas em *U. tomentosa*, tanto em relação aos aspectos analíticos, quanto em relação ao potencial biológico da espécie. Contudo, a elevada susceptibilidade dos mesmos à isomerização bem como a ocorrência de quimiotipos na espécie baseados em seus perfis de alcaloides oxindólicos podem levar a artefatos de processo e dificultar a generalização de resultados, respectivamente. Além disso, a espécie apresenta em sua constituição química, derivados triterpênicos e polifenóis, metabólitos secundários que também possuem elevado potencial biológico.

Os alcaloides oxindólicos são utilizados como marcadores químicos no controle de qualidade da matéria-prima vegetal e derivados de *U. tomentosa*, como extratos secos, cápsulas e comprimidos (USP, 2016). Assim, inicialmente foi avaliada a capacidade de reconhecimento de adulteração em *U. tomentosa* empregando-se *U. guianensis* de acordo com as especificações de qualidade estabelecidas na monografia farmacopêica de *U. tomentosa*, centradas nos alcaloides oxindólicos. Os resultados obtidos com amostras de cascas de caule de *U. tomentosa* adulteradas de forma proposital com cascas de caule de *U. guianensis* (10%, 30% e 50%, m/m), revelaram que mesmo as amostras adulteradas em até 50% atendem as especificações farmacopêicas. Portanto, metodologias alternativas via CLAE-PDA, IV e UV associadas à análise multivariada de dados foram aplicadas com o intuito de diferenciar *U. tomentosa* de *U. guianensis* e, consequentemente, reconhecer e quantificar o percentual de adulterante em amostras de cascas de caule de *U. tomentosa*. A análise de UV da solução extrativa propiciou tanto o reconhecimento de adulteração em *U. tomentosa* de forma satisfatória, quanto à quantificação da proporção de adulterante mediante emprego de modelos de regressão multivariada. Claramente os polifenóis, mais especificamente os flavonóides contribuíram para a diferenciação de ambas as espécies, devido a sua maior concentração nas cascas do caule em *U. guianensis* quando comparada a *U. tomentosa* como evidenciado mediante análise de polifenóis por CLAE-PDA. Dois flavonóides tri-O-glicosilados

derivados da quercitina e do camferol relacionados à diferenciação entre *U. tomentosa* e *U. guianensis* e, consequentemente, ao reconhecimento de aldulteração em *U. tomentosa*, foram devidamente caracterizados por CLAE-EM. Além disso, foi possível reconhecer a prática de adulteração ou substituição em duas amostras de casca de caule comercializadas no mercado popular Peruano como cascas de caule de *U. tomentosa*. Este fato demonstra que a adulteração e até mesmo a substituição parecem ser corriqueiras em cascas de caule de *U. tomentosa* e por isso merecem a devida atenção, considerando que grande parte da matéria-prima disponível para a comercialização e, consequente, produção de derivados é obtida via extrativismo. Portanto, a utilização dos alcaloides oxindólicos como marcadores químicos é no mínimo questionável se considerada à deficiência dos métodos analíticos focados nestes metabólitos em reconhecer a adulteração em *U. tomentosa* (Capítulo 1).

Outra particularidade em *U. tomentosa* é a existência de quimiotipos na espécie. Até o momento, três quimiotipos baseados nos perfis de alcaloides oxindólicos foram relatados: *quimiotipo I*, composto majoritariamente por alcaloides oxindólicos pentacíclicos com conformação dos anéis D/E em *cis* (especiofilina, uncarina F, pteropodina e isopteropodina); *quimiotipo II*, composto majoritariamente por alcaloides oxindólicos pentacíclicos com conformação dos anéis D/E em *trans* (mitrafilina e isomitrafilina); *quimiotipo III*, composto majoritariamente por alcaloides oxindólicos tetracíclicos (rincofilina e isorrincofilina). Assim, o presente trabalho também visou avaliar a influência dos diferentes quimiotipos sobre a atividade antitumoral reconhecidamente atribuída aos alcaloides oxindólicos, bem como a sua relevância em relação à genotoxicidade e citotoxidade frente a células não-malignas. Constatou-se que os três quimiotipos apresentavam atividade citotóxica equivalente frente às células tumorais de bexiga e glioblastoma humano (T24 e U-251-MG), mas diferenciadas em relação aos leucócitos humanos (células não-malignas) o que se refletiu no índice de seletividade. Apenas o *quimiotipo II* apresentou índice de seletividade superior à unidade (1.11−3.04) quando comparado aos *quimiotipos I* (0.10−0.19) e *III* (0.21−0.57). Isto significa que o *quimiotipo II* apresenta concentração efetiva menor frente às células tumorais se comparado as células não-malignas sendo, portanto, mais seletivo quando comparado aos demais quimiotipos. Em contrapartida,

nenhuma modificação significativa foi verificada em relação à genotoxicidade dos diferentes quimiotipos. Assim, pôde-se constatar que o perfil de alcaloides oxindólicos alterou a seletividade frente às células tumorais. Consequentemente, a definição do quimiotipo em *U. tomentosa* é de extrema importância e não permite generalizações em relação aos alcaloides oxindólicos e suas potencialidades biológicas, uma vez que os diferentes quimiotipos da espécie não são equivalentes (Capítulo 2).

A susceptibilidade dos alcaloides oxindólicos à isomerização é de extrema relevância, já que modificações no perfil de alcaloides podem alterar o potencial biológico das preparações a base de *U. tomentosa*. Consequentemente, minimizar a cinética de isomerização é relevante, principalmente, durante experimentos biológicos *in vitro* que necessitam de incubação em condições controladas de pH (7,4) e temperatura (37 ºC). As ciclodextrinas surgem como uma alternativa para minimizar a velocidade de isomerização dos alcaloides oxindólicos devido a sua capacidade de formar complexos estáveis com moléculas de interesse. Neste sentido, foi avaliada a complexação dos alcaloides oxindólicos de *U. tomentosa* com distintas ciclodextrinas, a saber, β-ciclodextrina (β-CD) e seus derivados hidrossolúveis, hidroxipropil-β-ciclodextrina (HP-βCD) e sulfobutil-éter-β-ciclodextrina (SBE-βCD). A complexação dos alcaloides oxindólicos foi mais efetiva com a SBE-βCD se comparada a β-CD e HP-βCD conforme verificado mediante diagramas de solubilidade de fases. Além disso, o complexo obtido em estado sólido via mistura física dos alcaloides oxindólicos com SBE-βCD manteve o perfil de alcaloides oxindólicos se comparado ao complexo obtido em solução. Embora a velocidade de isomerização tenha sido minimizada através da complexação com SBE-βCD em condições de incubação que mimetizam experimentos *in vitro*, a extensão do processo de isomerização foi equivalente em 24h ao verificado na ausência de SBE-βCD. Isso se deve basicamente a natureza dinâmica do sistema em equilíbrio, tanto no processo de isomerização, quanto no processo de complexação. Assim, a complexação dos alcaloides oxindólicos de *U. tomentosa* com SBE-βCD pode ser uma alternativa para reduzir a velocidade de isomerização dos mesmos (Capítulo 3).

Portanto, o presente trabalho abordou temas extremamente relevantes em relação ao protagonismo dos alcaloides oxindólicos em *U. tomentosa* e evidenciou muitas fragilidades decorrentes deste protagonismo, principalmente, em relação aos aspectos analíticos da espécie e sua incapacidade em relação ao reconhecimento de adulteração (Capítulo 1); os quimiotipos que dificultam a generalização das avaliações biológicas (Capítulo 2); e, para finalizar, a isomerização dos alcaloides oxindólicos, inclusive durante avaliações biológicas, que pode ser retardada mediante complexação com ciclodextrinas, por exemplo, mas que dificilmente será completamente inibida (Capítulo 3).

CONCLUSÕES

- Os modelos multivariados desenvolvidos com base nas análises de UV e CLAE-PDA de polifenóis permitiram a diferenciação entre as cascas do caule de *U. tomentosa* e *U. guianensis* em função de sua constituição química e, consequentemente, o reconhecimento e a quantificação do percentual de adulterante em *U. tomentosa*;

- A avaliação das amostras de cascas de caule provenientes do mercado popular Peruano evidenciou que a adulteração em *U. tomentosa* empregando-se *U. guianensis* ocorreu em duas das onze amostras avaliadas;

- A avaliação da atividade citotóxica *in vitro*, tanto em células tumorais de bexiga e glioblastoma humano (T24 e U-251-MG), quanto em leucócitos humanos, revelou que os diferentes quimiotipos em *U. tomentosa* apresentam atividade citotóxica equivalente frente às células tumorais mas possuem seletividade diferenciada sendo, portanto, a definição e a escolha do quimiotipo de extrema importância;

- Não foi evidenciada atividade genotóxica significativa dos diferentes quimiotipos de *U. tomentosa* mediante ensaio cometa e frequência de micronúcleos;

- A complexação dos alcaloides oxindólicos com sulfobutil-éter-β-ciclodextrina (SBE-βCD) ocorreu, mesmo em estado sólido, como caracterizado mediante análises de calorimetria exploratória diferencial e IV;

- Embora a complexação dos alcaloides oxindólicos com a sulfobutil-éter-β-ciclodextrina (SBE-βCD) seja capaz de reduzir a velocidade de isomerização dos alcaloides oxindólicos sob condições de incubação comumente utilizadas em experimentos *in vitro* (pH = 7,4; 37 ºC), não altera a extensão do processo de isomerização em decorrência da natureza dinâmica do sistema em equilíbrio.

PERSPECTIVAS

- Avaliar a atividade citotóxica comparativa entre o complexo alcaloides oxindolicos/SBE-βCD obtido em fase sólida e os alcaloides oxindólicos livres frente às células tumorais de bexiga (T24) e glioblastoma humano (U-251-MG);
- Caracterizar o complexo sólido dos alcaloides oxindólicos com sulfobutil-éter-β-ciclodextrina (SBE-βCD) e a mistura física por RMN ^{1}H.

REFERÊNCIAS

AGUILAR, J.L.; ROJAS, P.; ADOLFO, M.; PLAZA, A.; BAUER, R.; REININGER, E.; KLAAS, C.; MERFORD, I. Anti-inflammatory activity of two different extracts of *Uncaria tomentosa* (Rubiaceae). **Journal of Ethnopharmacology**, v.81, p.271–276, 2002.

AKESSON, C.; LINDGRENA, H.; PERO, R.W.; LEANDERSON, T.; IVARS, F. An extract of *Uncaria tomentosa* inhibiting cell division and NF-κB activity without inducing cell death. **International Immunopharmacology**, v.3, p.1889–1900, 2003.

ALLEN-HALL, L.; ARNASON, J.T.; CANO, P.; LAFRENIE, R.M. *Uncaria tomentosa* acts as a potent TNF-α inhibitor through NF-κB . **Journal of Ethnopharmacology**, v.127, p.685–693, 2010.

ALLEN-HALL, L.; CANO, P.; ARNASON, J.T.; ROJAS, R.; LOCK, O.; LAFRENIE, R.M. Treatment of THP-1 cells with *Uncaria tomentosa* extracts differentially regulates the expression if IL-1β and TNF-α. **Journal of Ethnopharmacology**, v.109, p.312–317, 2007.

AMARAL, S.; MIRA, L.; NOGUEIRA, J.M.F.; DA SILVA, A.P.; FLORENCIO, M.H. Plant extracts with anti-inflammatory properties—A new approach for characterization of their bioactive compounds and establishment of structure–antioxidant activity relationships. **Bioorganic & Medicinal Chemistry**, v.17, p.1876–1883, 2009.

AQUINO, R.; DE TOMMASI, N.; DE SIMONE F.; PIZZA, C. Triterpenes and quinovic acid glycosides from *Uncaria tomentosa*, **Phytochemistry**, v.45, p.1035-1040, 1997.

AQUINO, R.; VICENZO, F.; FRANCESCO, S. Plant Metabolites. New compounds and anti inflammatory activity of *Uncaria tomentosa.* **Journal of Natural Products**, v.54, p.453–459, 1991.

AQUINO, R.; VICENZO, F.; FRANCESCO, S. Plant Metabolites. structure and in vitro antiviral activity of quinovic acid glycosides from *Uncaria tomentosa* and *Guettarda platypoda*. **Journal of Natural Products**, v.52, p.679–685; 1990.

ARAÚJO, M.C.S.; FARIAS I.L.; GUTIERRES, J.; DALMORA, S.L.; FLORES, N.; FARIAS, J.; DE CRUZ, I.; CHIESA, J.; MORSCH, V.M.;SCHETINGER, M.R.C. *Uncaria tomentosa*—Adjuvant Treatment for Breast Cancer: Clinical Trial, **Evidence-Based Complementary and Alternative Medicine**, DOI:10.1155/2012/676984, 2012.

BACHER, N.; TIEFENTHALER, M.; STURM, S.; STUPPNER, H.; AUSSERLECHNER, M.J.; KOFLER, R.; KONWALINKA, G. Oxindole alkaloids from *Uncaria tomentosa* induce apoptosis in proliferating, G0/G1-arrested and bcl-2-

expressing acute lymphoblastic leukaemia cells. **British Journal of Haematology**, v.132, p.615–622, 2006.

BERTACCHE, V.; LORENZI, N.; NAVA, D.; PINI, E.; SINICO, C. Host–Guest Interaction Study of Resveratrol With Natural and Modified Cyclodextrins. **Journal of Inclusion Phenomena and Macrocyclic Chemistry**, v.55, p.279–287, 2006.

BERTOL, G.; FRANCO, L., OLIVEIRA, B.H. HPLC Analysis of Oxindole Alkaloids in *Uncaria tomentosa*: Sample Preparation and Analysis Optimization by Factorial Design. **Phytochemical Analysis**, v.23, p.143–151, 2012.

BRERETON RG. CHEMOMETRICS: DATA ANALYSIS FOR THE LABORATORY SYSTEMS AND CHEMICAL PLANTS. 1 ed. John Wiley & Sons Ltda: Chichester, 2003.

CAON, T.; KAISER, S.; FELTRIN, C.; CARVALHO, A.; SINCERO, T.C.M.; ORTEGA, G.G.; SIMÕES, C.M.O. Antimutagenic and antiherpetic activities of different preparations from *Uncaria tomentosa* (cat's claw), **Food and Chemical Toxicology**, v.66, p. 30-35, 2014.

CERRI, R.; AQUINO, R.; DE SIMONE, F.; PIZZA, C. New quinovic acid glycosides from *Uncaria tomentosa*. **Journal of Natural Produts**, v.51, p.257–261, 1988.

CHENG, A.; JIAN, C.; HUANG, Y.; LAI, C.; HSU, P.; PAN, M. Induction of apoptosis by *Uncaria tomentosa* through reactiveoxygen species production, cytochrome c release, and caspases activation in human leukemia cells. **Food and Chemical Toxicology**, v.45, p.2206–2218, 2007.

CISNEROS, F.J.; JAYO, M.; NIEDZIELA, L. An *Uncaria tomentosa* (cat's claw) extract protects mice against ozone-induced lung inflammation. **Journal of Ethnopharmacology**, v.96, n.3, p.355–364, 2005.

DE MARINO, L.; MARTINOT, J.L.S.; FRANCESCHELLI, S.; LEONE, A.; PIZZA, C.; DE FEO, V. Proapoptotic effect of *Uncaria tomentosa* extracts. **Journal of Ethnopharmacology**, v.107, p.91–94, 2006.

DEL VALLE, E.M.M. Cyclodextrins and their uses: a review. **Process Biochemistry**, v.39, p.1033–1046, 2004.

DIETRICH, F.; KAISER, S.; ROCKENBACH, L.; FIGUEIRÓ, F.;BERGAMIN, L.S.; DA CUNHA, F.M.; MORRONE, F.B.; ORTEGA, G.G.; BATTASTINI, A.M.O. Quinovic acid glycosides purified fraction from *Uncaria tomentosa* induces cell death by apoptosis in the T24 human bladder cancer cell line, **Food and Chemical Toxicology**, v.67, p. 222-229, 2014.

DIETRICH, F.; PIETROBON, M.J.; KAISER, S.; SILVA, R.B.M.; ROCKENBACH, L.; EDELWEISS M.I.A.; ORTEGA, G.G.; MORRONE, F.B.; CAMPOS M.M.; BATTASTINI, A.M.O. The Quinovic Acid Glycosides Purified Fraction from *Uncaria tomentosa* Protects against Hemorrhagic Cystitis Induced by Cyclophosphamide in Mice. **PLoS One**, DOI:10.1371/journal.pone.0131882, 2015.

DOMINGUES, A.; SARTORI, A.; GOLIM, M.A.; VALENTE L.M.M.; DA ROSA, L.C.; ISHIKAWA, L.L.W.; SIANI, A.C.; VIERO R.M. Prevention of experimental diabetes by *Uncaria tomentosa* extract: Th2 polarization, regulatory T cell preservation or both? **Journal of Ethnopharmacology**, v.137, p.635–642, 2011b.

DOMINGUES, A.; SARTORI, A.; VALENTE, L.M.M.; GOLIM, M.A.; SIANI, A.C.; VIERO, R.M. *Uncaria tomentosa* Aqueous-ethanol Extract Triggers an Immunomodulation toward a Th2 Cytokine Profile. **Phytotherapy Research**, v.25, p.1229–1235, 2011a.

DREIFUSS, A.A.; BASTOS-PEREIRA, A.L.; ÁVILA, T.V.; SOLEY, B.S.; RIVERO, A.J.; AGUILAR, J.L.; ACCO, A. Antitumoral and antioxidant effects of a hydroalcoholic extract of cat's claw (*Uncaria tomentosa*) (Willd. Ex Roem. & Schult) in an in vivo carcinosarcoma model. **Journal of Ethnopharmacology**, v.130, p.127–133, 2010.

DREIFUSS, A.A.; BASTOS-PEREIRA, A.L.; FABOSSI, I.A.; LÍVERO, F.A.; STOLF, A.M.; ALVES DE SOUZA, C.E.; GOMES, L.O.; CONSTANTIN, R.P.; FURMAN, A.E.; STRAPASSON, R.L.; TEIXEIRA, S.; ZAMPRONIO, A.R.; MUSCARÁ, M.N.; STEFANELLO, M.E.; ACCO A. *Uncaria tomentosa* exerts extensive anti-neoplastic effects against the Walker-256 tumour by modulating oxidative stress and not by alkaloid activity, **PLoS One**, DOI: 10.1371/journal.pone.0054618, 2013.

GAD, H.A.; EL-AHMADY, S.H.; ABOU-SHOER, M.I.; AL-AZIZI, M.M. Application of chemometrics in authentication of herbal medicines: a review, **Phytochemical Analysis**, v.24, p.1–24, 2013a.

GAD, H.A.; EL-AHMADY, S.H.; ABOU-SHOER, M.I.; AL-AZIZIA, M.M. A Modern Approach to the Authentication and Quality Assessment of Thyme Using UV Spectroscopy and Chemometric Analysis, **Phytochemical Analysis**, v.24, p.520–526, 2013b.

GANZERA, M.; MUHAMMAD, I.; KHAN, R.A.; KHAN, I. A. Improved method for the determination of oxindole alkaloids in *Uncaria tomentosa* by high performance liquid chromatography. **Planta Medica**, v.67, p.447–450, 2001.

GARCÍA PRADO, E.;, GIMENEZ M.D.G.; VAZQUEZ, R.D.P.; SANCHEZ, J.L.E.; RODRIGUEZ, M.T.S. Antiproliferative effects of mitraphylline, a pentacyclic

oxindole alkaloidof *Uncaria tomentosa* on human glioma and neuroblastoma cell lines. **Phytomedicine**, v.14 p.280–284, 2007.

GATTUSO, M.; DI SAPIO, O.; GATTUSO, S.; PEREYRA, E.L. Morphoanatomical studies of *Uncaria tomentosa* and *Uncaria guianensis* bark and leaves, **Phytomedicine**, v.11, p.213–223, 2004.

GIMÉNEZ, D.G.; GARCÍA PRADO, E.; RODRÍGUEZ, T.S.; ARCHE, A.F.; DE LA PUERTA, R. Cytotoxic Effect of the pentacyclic oxindole alkaloid mitraphylline isolated from *Uncaria tomentosa* bark on human Ewing's sarcoma and breast cancer cell lines. **Planta Medica**, v.76, p.133–136, 2010.

GONÇALVES, C.; DINIS, T.; BATISTA, M.T. Antioxidant properties of proanthocyanidins of *Uncaria tomentosa* bark decoction: a mechanism for anti-inflammatory activity. **Phytochemistry**, v.66, p.89–98, 2005.

GRIEBELER, S.A. **Validação de metodologia analítica para matéria-prima vegetal, extrato seco e cápsulas de gelatina dura contendo extrato seco de *Uncaria tomentosa* (Willd) DC.** Porto Alegre: Curso de Pós-Graduação em Ciências Farmacêuticas da Faculdade de Farmácia da UFRGS. 2006. Dissertação de Mestrado Profissionalizante.

GURROLA-DÍAZA, C.M.; GARCÍA-LÓPEZ, P.M.; GULEWICZ, K.; PILARSKI, R.; DIHLMANN, S. Inhibitory mechanisms of two *Uncaria tomentosa* extracts affecting the Wnt-signaling pathway. **Phytomedicine**, v.18, p.683–690, 2011.

HAIR, J.F.; BLACK, W.C.; BABIN, B.J.; ANDERSON, R.E.; TATHAM, R.L. ANÁLISE MULTIVARIADA DE DADOS. 6 ed. Bookman: Porto Alegre, 2009.

HEITZMAN, M.E.; NETO, C.C.; WINIARZ, E.; VAISBERG, A.J.; HAMMOND, G.B. Ethnobotany, phytochemistry and pharmacology of *Uncaria* (Rubiaceae). **Phytochemistry**, v.66, p.5–29, 2005.

HEMINGWAY, S.R.; PHILLIPSON, J.D. Alkaloids from South American species of *Uncaria* (Rubiaceae). **Journal of Pharmacy and Pharmacology**, v.26, p.113, 1974.

INTERNATIONAL UNION OF PURE AND APPLIED CHEMISTRY (IUPAC). Rules for the nomenclature of organic chemistry section E: Stereochemistry. **Pure and Applied Chemistry**, v.45, p.11–30, 1976.

KAISER, S. **Isomerização dos alcaloides oxindólicos de *Uncaria tomentosa* (Willd.) DC. (unha-de-gato) induzida por fatores tecnológicos e sua influência sobre a atividade citotóxica em linhagens de células tumorais de bexiga T24 e RT4.** Porto Alegre: Curso de Pós-Graduação em Ciências Farmacêuticas da Faculdade de Farmácia da UFRGS. 2012. Dissertação de Mestrado.

KAISER, S.; DIETRICH, F.; DE RESENDE P.E.; VERZA, S.G.; MORAES, R.C.; MORRONE, F.B.; BATASTTINI, A.M.O.; ORTEGA, G.G. Cat's Claw Oxindole Alkaloid Isomerization Induced by Cell Incubation and Cytotoxic Activity against T24 and RT4 Human Bladder Cancer Cell Lines, **Planta Medica**, v.79, p.1413–1420, 2013c.

KAISER, S.; VERZA, S.G.; MORAES, R.C.; DE RESENDE P.E.; BARRETO, F.; PAVEI, C.; ORTEGA, G.G. Cat's claw oxindole alkaloid isomerization induced by common extraction methods, **Quimica Nova**, v.36, p.808–814, 2013a.

KAISER, S.; VERZA, S.G.; MORAES, R.C.; PITTOL, V.; PEÑALOZA, E.M.C.; PAVEI, C.; ORTEGA, G.G. Extraction optimization of polyphenols, oxindole alkaloids and quinovic acid glycosides from cat's claw bark by Box–Behnken design, **Industrial Crops and Products**, v.48, p.153–161, 2013b.

KEPLINGER, K.; LAUS, G.; WURM, M.; DIERICH, M.P.; TEPPNER, H. *Uncaria tomentosa* (Wild). Ethnomedicinal uses and new pharmacological, toxicological and botanical results. **Journal of Ethnopharmacology**, v.64, p.23–34, 1999.

KITAJIMA, M.; HASHIMOTO, K.; YOKOYA, M.; TAKAYAMA, H.; AIMI, N. Two new 19-Hydroxyursolic acid-type triterpenes from peruvian 'Unã de Gato' (*Uncaria tomentosa*). **Tetrahedron**, v.56, p.547–552, 2000.

KITAJIMA, M.; HASHIMOTO, K.I.; YOKOYA, M.; TAKAYAMA, H.; SANDOVAL, M.; AIMI, N. Two new nor-triterpenes glycosides from Peruvian Una de gato (*Uncaria tomentosa*). **Journal of Natural Products**, v. 66, p.320–323, 2003.

KOZIELEWICZ, P.; PARADOWSKA, K.; ERIC´, S.; WAWER, I.; ZLOH, M. Insights into mechanism of anticancer activity of pentacyclic oxindole alkaloids of *Uncaria tomentosa* by means of a computational reverse virtual screening and molecular docking approach, **Monatshefte fuer Chemie**, v.145, p.1201–1211, 2014.

KRISHNAIAH, D.; SARBATLY, R.; NITHYANANDAM, R. A review of the antioxidant potential of medicinal plant species. **Food and Bioproducts Processing**, v.89, p. 217–233, 2011.

KURKOV, S.V.; LOFTSSON, T. Cyclodextrins, **International Journal of Pharmaceutics**, v.453, p.167–180, 2013.

LAUS, G. Advances in chemistry and bioactivity of the genus *Uncaria*. **Phytotherapy Research**, v.18, p.259–274, 2004.

LAUS, G. Kinetics of isomerization of tetracyclic spiro oxindole alkaloids. **Journal Chemistry Society Perkin Transactions 2**, p.315–317, 1998.

LAUS, G.; BRÖSSNER, D.; KEPLINGER K. Alkaloids of peruvian *Uncaria tomentosa*. **Phytochemistry**, v.45, n.4, p.855–860, 1997.

LAUS, G.; BRÖSSNER, D.; SENN, G.; WURST, K. Analysis of the kinetics of isomerization of spiro oxindole alkaloids. **Journal Chemistry Society Perkin Transactions 2**, p.1931–1936, 1996.

LAUS, G.; KEPLINGER, D. Separation of stereoisomer oxindole alkaloids from *Uncaria tomentosa* by high performance liquid chromatography. **Journal of Chromatography**, v.662, n.2, p.243–249, 1994.

LEMAIRE, I.; ASSINEWE, V.; CANO, P.; AWANG, D.V.; ARNASON, J.T. Stimulation of interleukin-1 and -6 production in alveolar macrophages by the neotropical liana, *Uncaria tomentosa* (uña de gato), **Journal of Ethopharmacology**, v.64, p.109-115, 1999.

LIMA, V.L.E. Os fármacos e a quiralidade: uma breve abordagem. **Química Nova**, v.20, n.6, p.657–663, 1997.

LIU, Y.; LI, L.; XIAO, Y.Q.; YAO, J.Q.; LI, P.Y.; YU, D.R.; MA, Y.L. Global metabolite profiling and diagnostic ion filtering strategy by LC-QTOF MS for rapid identification of raw and processed pieces of *Rheum palmatum* L., **Food Chemistry**, v. 192, p. 531-540, 2016.

LOFTSSON, T.; JARHO, P.; MÁSSON, M.; JÄRVINEN, T. Cyclodextrins in drug delivery. **Expert Opinion Drug Delivery**, v.2, p.335–351, 2005.

LUNA-PALENCIA, G.R.; HUERTA-HEREDIA, A.A.; CERDA-GARCÍA-ROJAS, C.M.; RAMOS-VALDIVIA, A.C. Differential alkaloid profile in *Uncaria tomentosa* micropropagated plantlets and root cultures, **Biotechnology Letters**, v.35, p.791-797, 2013.

MAMMONE, T.; AKESSON, C.; GAN, D.; GIAMPAPA, V.; PERO, R.W. A Water Soluble Extract from *Uncaria tomentosa* (Cat's Claw) is a potent enhancer of DNA repair in primary organ cultures of human skin. **Phytotheraphy Research**, v.20, p.178–183, 2006.

MONTENEGRO DE MATTA, S.; DELLE MONACHE, F.; MONACHE, F.; FERRARI, F.; MARINI-BETTOLO, G.B. Alkaloids and procyanidins of an *Uncaria sp.* from Peru. **Farmaco**, v.31, p.527–535, 1976.

MONTORO, P.; CARBONE, V.; QUIROZ, J.D.Z.; DE SIMONE, F.; PIZZA, C. Identification and quantification of components in extracts of *Uncaria tomentosa* by HPLC-ES/MS. **Phytochemical Analysis**, v.15, p.55–64, 2004.

MONTSERRAT-DE LA PAZ, S.; DE LA PUERTA, R.; FERNANDEZ-ARCHE A.; QUILEZ, A.M.; MURIANA, F.J.; GARCIA-GIMENEZ, M.D.; BERMUDEZ, B. Pharmacological effects of mitraphylline from *Uncaria tomentosa* in primary human monocytes: Skew toward M2 macrophages, **Journal of Ethnopharmacology,** v.170, p.128–135, 2015.

MUHAMMAD, I.; DUNBAR, D.C.; KHAN, R.A.; GANZERA, M.; KHAN, I.A. Investigation of Unã De Gato I. 7-Deoxyloganic acid and ^{15}N NMR spectroscopic studies on pentacyclic oxindole alkaloids from *Uncaria tomentosa***. Phytochemistry**, v. 57, p.781–785, 2001.

MUR, E.; HARTIG, F.; EIBL, G.; SCHIRMER, M. Randomized double blind trial of an extract from the pentacyclic alkaloid-chemotype of *Uncaria tomentosa* for the treatment of rheumatoid arthritis. **Journal of Rheumatology**, v.29, p.678–681, 2002.

PAVEI, C. **Obtenção e avaliação de frações purificadas e farmacologicamente ativas presentes em *Uncaria tomentosa* (WILLD) DC. (unha-de-gato).** Porto Alegre: Curso de Pós-Graduação em Ciências Farmacêuticas da Faculdade de Farmácia da UFRGS. 2010. Tese de Doutorado.

PAVEI, C.; BORRÉ, G.L.; KAISER, S.; ORTEGA, G.G. Alkaloid isomerization induced by spray drying of *Uncaria tomentosa* bark extracts. **Latin American Journal of Pharmacy**, v.30, p.608–612, 2011.

PAVEI, C.; KAISER, S.; VERZA, S.G.; BORRÉ, G.L.; ORTEGA, G.G. HPLC-PDA method for quinovic acid glycosides assay in Cat´s Claw (Uncaria tomentosa) associated with UPLC/Q-TOF-MS analysis. **Journal of Pharmaceutical and Biomedical Analysis**, v.52, p.250–257, 2012.

PAVEI, C.; KAISER, S.; BORRE´, G.L.; ORTEGA, G.G. Validation of a LC method for polyphenols assay in cat's claw (*Uncaria tomentosa*). **Journal of Liquid Chromatography & Related Technologies**, v.33, p.1551–1561, 2010.

PEÑALOZA, E.M.C.; KAISER, S.; DE RESENDE, P.E.; PITTOL, V.; CARVALHO, A.R.; ORTEGA, G.G. Chemical composition variability in the *Uncaria tomentosa* (cat's claw) wild population, **Quimica Nova**, v.38, p.378-386, 2015.

PILARSKI, P.; GURROLA-DÍAZ, C.M.; GARCÍA-LÓPEZ, P.M.; SOLDEVILA, G.; OLEJNIKE, A.; GRAJEK, W.; GULEWICZ, K. Enhanced proapoptotic response of the promyelocytic leukemia HL-60 cells treated with an *Uncaria tomentosa* alkaloid preparation, **Journal of Herbal Medicine**, v.3, p.149-156, 2013.

PILARSKI, R.; FILIP, B.; WIETRZYK, J.; KURA´S, M.; GULEWICZ K. Anticancer activity of the *Uncaria tomentosa* (Willd.) DC. preparations with different oxindole alkaloid composition. **Phytomedicine**, v.17, p.1133–1139, 2010.

PILARSKI, R.; POCZEKAJ-KOSTRZEWSKA, M.; CIESIOLKA, D.; SZYFTER, K.; GULEWICZ, K. Antiproliferative activity of various *Uncaria tomentosa* preparations on HL-60 promyelocytic leukemia cells. **Pharmacological reports**, v.59, p.565–572, 2007.

PILARSKI, R.; ZIELINSKI, H.; CIESIOLKA, D.; GULEWICZ, K. Antioxidant activity of ethanolic and aqueous extracts of *Uncaria tomentosa* (Willd.) DC. **Journal of Ethnopharmacology**, v.104, p.18–23, 2006.

POLLITO, P.A.Z. **Dendrologia, anatomia do lenho e status de conservação das espécies lenhosas dos gêneros *Cinchona, Cróton* e *Uncaria* no estado do Acre, Brasil**. São Paulo: Escola superior de Agricultura Luiz de Queiroz. 2004. Tese de Doutorado.

POLLITO, P.A.Z.; TOMAZELLO, M. Anatomia do lenho de *Uncaria guianensis* e *U. tomentosa* (Rubiaceae) do estado do Acre, Brasil. **Acta Amazônica**, v.36, n.2, p.1–21, 2006.

QUINTERA, J.C.; UGAZ, O. L. Uña de gato – *Uncaria tomentosa* (Willd) DC. **Revista de Fitoterapia**, v.3, p.5–16, 2003.

REINHARD, K. H. *Uncaria tomentosa* (Willd.) D.C.: Cat's Claw, *Uña de Gato*, or Saventaro. **The Journal of Alternative Complementary Medicine**, v.5, p.143–151, 1999.

REIS, S.R.I.N.; VALENTE, L.M.M.; SAMPAIO, A.L.; SIANI, A.C.; GANDINI M.; AZEREDO E.L.; MAZZEI, J.L.; D'AVILA, L.A.; KUBELKA, C.F.; HENRIQUES M.G.M. Immunomodulating and antiviral activities of *Uncaria tomentosa* on human monocytes infected with Dengue Virus-2. **International Immunopharmacology**, v.8, p.468–476, 2008.

RINNER, B.; LI, Z.X.; HAAS, H.; SIEGL, V.; STURM, S.; STUPPNER, H.; PFRAGNER, R. Antiproliferative and pro-apoptotic effects of *Uncaria tomentosa* in human medullary thyroid carcinoma cells. **Anticancer Research,** v.29, p.4519–4528, 2009.

RIVA, L.; CORADINI, D.; DI FRONZO, G.; DE FEO, V.; DE TOMAASI, N.; DE SIMONE, F.; PIZZA. C. The antiproliferative effects of *Uncaria tomentosa* extracts and fractions on the growth of breast cancer cell line. **Anticancer Research**, v.21, p.2457–2462, 2001.

RIZZI, R.; RE, F.; BIANCHI, A.; DE FEO, V.; DE SIMONE, F.; BIANCHI, L.; STIVALA, L.A. Mutagenic and antimutagenic activities of *Uncaria tomentosa* and its extracts. **Journal of Ethnopharmacology**, v.38, p.63–77, 1993.

ROMERO-JIMÉNEZ, M.; CAMPOS-SÁNCHEZ, J.; ANALLA, M.; MUÑOZ-SERRANO, A.; ALONSO-MORAGA, A. Genotoxicity and anti-genotoxicity of some traditional medicinal herbs, **Mutation Research**, v.585, p.147–155, 2005.

SANDOVAL, M.; CHARBONNET, R.M.; OKUHAMA, N.N.; ROBERTS, J.; KRENOVA, Z.; TRENTACOSTI, A.M.; MILLER, M.J.S. Cat's Claw inhibits TNF-α production and scavenges free radicals: role in cytoprotection. **Free Radical Biology & Medicine**, v.29, n.1, p.71–78, 2000.

SANDOVAL, M.; OKUHAMA, N.N.; ZHANG, X.J.; CONDEZO, L.A.; LAO, J.; ANGELES, F.M.; MUSAH, R.A.; BOBROWSKI, P.; MILLER, M.J.S. Anti-inflammatory and antioxidant activities of cat's claw (*Uncaria tomentosa* and *Uncaria guianensis*) are independent of their alkaloid content. **Phytomedicine**, v.9, p.325–337, 2002.

SANDOVAL-CHACON, M.; THOMPSON, J.H.; ZHANG, X.J.; LIU, X.; MANNICK, E.E.; SANDOWSKA-KROWICKA, H.; CHARBONNET, R.M.; CLARK, D.A.; MILLER, M.S.J. Anti-inflammatory actions of Cat's Claw : The role of NF-κB. **Alimentary Pharmacology & Therapeutics**, v.12, p.1279–1289, 1998.

SETTY, A.R.; SIGAL, L.H. Herbal medications commonly used in the practice of rheumatology: mechanisms of action, efficacy, and side effects. **Seminars in Arthritis and Rheumatism**, 2005.

SHENG, Y.; BRYNGELSSON, C.; PERO, R.W. Enhanced DNA repair, immune function and reduced toxicity of C-MED-100™, a novel aqueous extract from *Uncaria tomentosa.* **Journal of Ethnopharmacology**, v.69, p.115–126, 2000.

SHENG, Y.; PERO, R.W.; AMIRI, A.; BRYNGELSSON, C. Induction of apoptosis and inhibition of proliferation in human tumor cells treated with extracts of *Uncaria tomentosa***. Anticancer Research**, v.18, p.3363–3368, 1998.

STUPPNER, H.; STURM, S.; GEISEN, G.; ZMIAN, U.; KONWALINKA, G. A differential sensitivity of oxindole alkaloids to normal and leukemic cell lines. **Planta Medica**, v.59, p.A583, 1993.
STUPPNER, H.; STURM, S.; KONWALINKA, G. HPLC analysis of main oxindole alkaloids from *Uncaria tomentosa*. **Chromatographia**, v.34, n.11/12, p.597–600, 1992.

UNITED STATES PHARMACOPEIA (USP). 39 ed. U.S. Pharmacopeia: Rockville, 2016.

VALENTE, L.M.M. Unha-de-gato [*Uncaria tomentosa*] (Willd.) DC. e *Uncaria guianensis* (Aubl.) Gmel.]: Um panorama sobre seus aspectos mais relevantes. **Revista Fitos**, v.2, n.1, p. 48–48, 2006.

VALENTE, L.M.M.; BIZARRI, C.H.B.; LIECHOCKI, S.; BARBOZA, R.S.; DA PAIXÃO, D.; ALMEIDA, M.B.S.; BENEVIDES, P.J.C.; MAGALHÃES, A.; SIANI, A.C. Kaempferitrin from *Uncaria guianensis* (Rubiaceae) and its potential as a chemical marker for the species. **Journal of Brazilian and Chemical Society**, v. 20, n. 6, p. 1041–1045, 2009.

VALERIO JR, L.G.; GONZALES, G.F. Toxicological Aspects of the South American Herbs Cat's Claw (*Uncaria tomentosa*) and Maca (*Lepidium meyenii*), **Toxicological Reviews**, v.24, p.11–35, 2005.

VAN GINKEL, A. Identification of the alkaloids and flavonoids from *Uncaria tomentosa* bark by TLC in quality control. **Phytotherapy Research**, v.10, p.9–18, 1997.

WAGNER, H.; KREUTZKAMP, B.; JURCIC, K. Die Alkaloide von *Uncaria tomentosa* und ihre Phagozytose-steigernde Wirkung. **Planta Medica**, v.51, n.5, p.419–423, 1985.

WINKLER, C.; WIRLEITNER, B.; SCHROECKSNADEL, K.; MUR, E.; FUCHS, D. *In vitro* effects of two extracts and two pure alkaloids preparations of *Uncaria tomentosa* on peripheral blood mononuclear cells, **Planta Medica**, v. 70, p.205–210, 2004.

WURM, M.; KACANI, I.; LAUS, G.; KEPLINGER, K.; DIERICH, M. P. Pentacyclic oxindole alkaloids from *Uncaria tomentosa* induce human endothelial cells to release a lymphocyte – proliferation – regulation factor. **Planta Medica**, v.64, p.701–704, 1998.

ZHANG, Q.; ZHAO, J.J.; XU, J.; FENG, F.; QU, W. Medicinal uses, phytochemistry and pharmacology of the genus *Uncaria*. **Journal of Ethnopharmacology**, v.173, p.48–80, 2015.

ZHANG, Q-F.; NIE, H-C.; SHANGGUANG, X-C.; YIN, Z-P.; ZHENG, G-D.; CHEN, J-G. Aqueous Solubility and Stability Enhancement of Astilbin through Complexation with Cyclodextrins, **Journal of Agricultural and Food Chemistry**, v. 61, p.151−156, 2013.

AGRADECIMENTO BOLSA DE ESTUDOS

Agradecemos o apoio financeiro do Conselho Nacional de Desenvolvimento Científico e Tecnológico (CNPq) mediante conceção de bolsa de estudos (Processo nº 159461/2012-0).